

PERFORMANCE INVESTIGATION OF A MICROPROCESSOR BASED CHOPPER FED CLOSED LOOP DC DRIVE

A DISSERTATION

submitted in partial fulfilment of
the requirements for the award of the degree
of
MASTER OF ENGINEERING
in
ELECTRICAL ENGINEERING
(Power Apparatus and Electric Drives)

By

R. SRIVATSA



**DEPARTMENT OF ELECTRICAL ENGINEERING
UNIVERSITY OF ROORKEE
ROORKEE-247667 (INDIA)**

February, 1988

TO MY PARENTS

ACKNOWLEDGEMENTS

I wish to place on record my profound sense of gratitude and deep sense of indebtedness to my guides, Dr. V.K.Verma, Professor, Electrical Engineering Department, University of Roorkee, Roorkee and Mr. Pramod Agarwal, Lecturer, Electrical Engineering Department, University of Roorkee, Roorkee. I consider myself privileged to have worked under their supervision and guidance during the term of this work.

I am highly thankful to Mr. Y.P.Singh, Lecturer, Electrical Engineering Department, University of Roorkee, Roorkee and Mr. D.M.Deshpande, Research Scholar in the Department for their kind help.

I am highly thankful to my friends Mr. B.Sailesh Kumar and Mr. Kishore Murthy for their help.

I am highly grateful to all the laboratory staff for their cooperation during the course of this work.

Thanks are also due to Mr. R.P.Singh, Steno, Office of the Dean Dev. & Plng, for typing this report neatly.

Thanks are also for those who have helped me directly or indirectly in preparing this report.

R. SRIVATSA

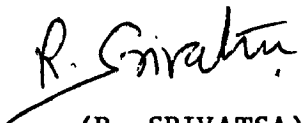
1

CANDIDATE'S DECLARATION

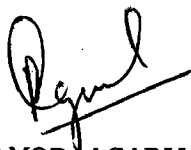
I hereby declare that the work which is being presented in the dissertation entitled **PERFORMANCE INVESTIGATION OF A MICROPROCESSOR BASED CHOPPER FED CLOSED LOOP DC DRIVE** in partial fulfilment of the requirements for the award of the Degree of **Master of Engineering in Electrical Engineering** with specialization in **Power Apparatus and Electric Drives**, submitted in the **DEPARTMENT OF ELECTRICAL ENGINEERING, UNIVERSITY OF ROORKEE, ROORKEE (INDIA)**, is an authentic record of my own work carried for a period of about six months, from August 1987 to January 1988 under the supervision of **DR. V.K. VERMA, Professor** and **Mr. PRAMOD AGARWAL, Lecturer, Department of Electrical Engineering, University of Roorkee, Roorkee, India.**

The matter embodied in this dissertation has not been submitted by me for the award of any other degree or diploma.

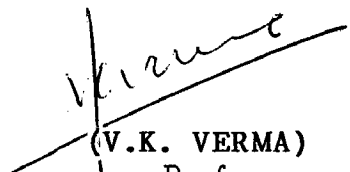
Dated : Feb. 25 , 1988


(R. SRIVATSA)

This is to certify that the above statement made by the candidate is correct to the best of our knowledge.



(PRAMOD AGARWAL)
Lecturer
Electrical Engg. Deptt.
University of Roorkee
ROORKEE - 247 667, INDIA


(V.K. VERMA)
Professor
Electrical Engg. Deptt.
University of Roorkee
ROORKEE - 247 667, INDIA

ABSTRACT

This dissertation deals with the experimental and theoretical studies on a Microprocessor based Chopper fed Closed Loop DC Drive system.

The separately excited DC Motor is fed by a single quadrant current commutated chopper. The closed loop control is achieved by incorporating an inner current loop and an outer speed loop. The control scheme is based on INTEL 8085 Microprocessor. The theoretical studies are conducted by simulating the drive system on a DEC 2050 Computer and the results obtained are verified experimentally.

Chapter 1 consists of Introduction, Chapter 2 the literature review. Chapter 3 bring out the analysis and design of power circuit along with waveforms. Chapter 4 deals with the control scheme implementation by the microprocessor. Chapter 5 consists of Simulation studies to design the controllers. Chapter 6 gives the experimental results of the drive system and Chapter 7 gives the conclusions together with the suggestions to improve the performance. .

CONTENTS

Page No.

	CANDIDATE'S DECLARATION	i
	ACKNOWLEDGEMENTS	ii
	ABSTRACT	iii
CHAPTER-1	INTRODUCTION	
1.1	Necessity of variable speed drive in Industry	1
1.2	Choice of d.c. machine as a variable speed Drive	1
1.3	Source of variable d.c. voltage for the Drive	2
1.4	Principle of operation of Chopper circuit	3
1.5	Classification of Chopper Circuits	5
1.6	Digital Control and its Advantages	6
CHAPTER-2		
2.1	Literature Review	8
2.2	Author's Contribution	17
CHAPTER-3	ANALYSIS AND DESIGN OF POWER CIRCUIT	
3.1	Introduction	18
3.2	Analysis of the waveforms	20
3.3	Design of circuit components L and C	22
3.4	Conclusion	24
CHAPTER-4	CLOSED LOOP CONTROL	
4.1	Introduction	26
4.2	Type of Controllers	28
4.3	Microprocessor Implementation	30
4.4	System Hardware	30
4.3.2	System Software	32

4.4	Conclusion	48
CHAPTER-5	MATHEMATICAL MODELLING AND COMPUTER SIMULATION OF THE DRIVE SYSTEM	
5.1	Introduction	49
5.2	Transfer function of various elements	50
5.3	System State Model	55
5.4	Design of Controllers	58
5.4.1	Current Controller	58
5.4.2	Speed Controller	67
5.5	up Translation of the Controller parameters	72
5.5.1	Speed Controller	72
5.5.2	Current Controller	72
5.6	Conclusion	80
CHAPTER-6	PERFORMANCE OF THE DRIVE SYSTEM	
6.1	Introduction	81
6.2	Load test on the up controlled drive system	81
6.3	Performance oscillograms	88
6.4	Conclusion	93
CHAPTER-7	CONCLUSIONS	94
	Scope for future work	96
	REFERENCES	97
	APPENDIX A	
	APPENDIX B	
	APPENDIX C	
	APPENDIX D	

CHAPTER - 1

INTRODUCTION

1.1 Necessity of Variable Speed Drives in Industry [1]

Many industrial drives and processes need to be run at different speeds to suit different application needs e.g. subway cars, trolley buses or battery driven vehicles, printing press etc. The variation of speed of these drives means variation of either input voltage or current.

1.2 Choice of d.c. machine as a Variable Speed Drive [2]

A d.c. machine has the following advantages over that of an a.c. machine. They are:-

1. D.C. machine is most versatile in speed control, i.e. both speed control upto base speed (by armature control) and above the base speed (by field control) are possible with relative ease.

2. Operation in all the four quadrants is possible with relatively simple solid state control.

3. Variation of torque-speed characteristics for both motoring and regenerative modes in either forward or reverse direction is possible.

4. Relatively easy methods are available for braking (both dynamic and regenerative) to stop the machine quickly.

However, it has some disadvantages, namely:-

1. Less power/weight ratio, and
2. Commutation difficulties at higher voltages and currents.

1.3 Source of Variable d.c. Voltage for the Drive

Owing to their various advantages such as minimum maintenance, less bulk and weight, higher efficiency, faster time response etc. the solid state devices have almost replaced the conventional ones (MG set and Mercury arc rectifier) to obtain variable d.c. either from fixed d.c voltage source (Choppers) or from a.c. source (phase controlled converters).

The dc to dc converter or chopper as it is popularly known has certain distinct advantages over phase controlled converters namely:-

1. The region of discontinuous operation can be reduced with a chopper control by increasing the frequency of chopper.

2. The ratio of peak to average and RMS to average motor currents as a function of speed is less in a chopper circuit than in phase controlled converter circuit. Also that the reduction in peak value of current increases commutation capability and decrease in RMS motor current decreases the heating of motor.

3. Associated components for firing circuit are fewer for chopper than for phase control.

4. Phase controlled converters have poor supply p.f. especially at large delay angles together with generation of considerable amount of harmonics in the line.

5. With higher chopping frequency the response time of drive is smaller.

However, choppers have some disadvantages, such as:-

1. Additional forced commutation circuits are to be used.

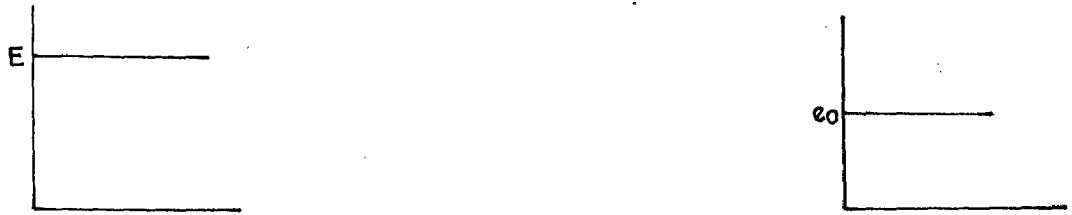
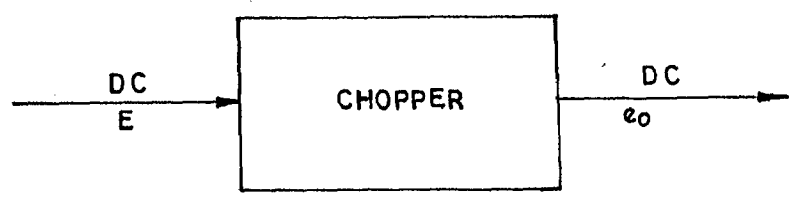
2. Special thyristors (inverter grade), have to be used at high frequency operation.

1.4 Principle of Operation of Chopper Circuit

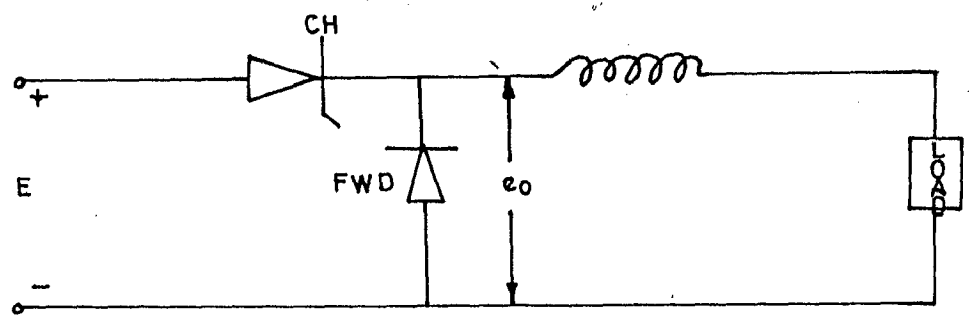
Thyristorised chopper in dc circuits work analogously as continuously variable turn transformer in ac circuits. The average voltage applied to a load can be varied by introduction of one or more chopper in between load and a constant dc source. Basically it is an electronic switch that connects to and disconnects the load from a constant input supply voltage as illustrated in Fig. 1. During the period T_{ON} , the chopper is ON and hence the supply terminals are connected to load. During OFF period, the chopper is turned off and current free wheels through the diode FWD and hence the load terminals are virtually short circuited.

The average or chopped dc voltage thus produced is given as:-

$$\begin{aligned} E_0 &= E \frac{T_{ON}}{T_{ON} + T_{OFF}} \\ &= E \frac{T_{ON}}{T_{CH}} \\ &= E \cdot \alpha \end{aligned}$$



(a) A DC TO DC THYRISTOR CONVERTER



(b) A BASIC CHOPPER CIRCUIT CONFIGURATION AND OPERATION

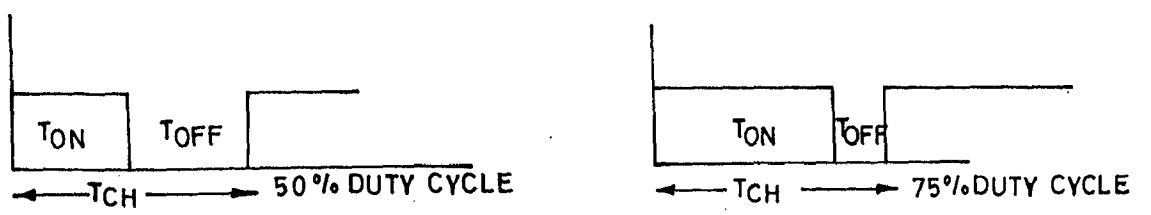


FIG. 1

where,

$$T_{CH} = T_{ON} + T_{OFF} = \text{Chopper period}$$

$$\alpha = T_{ON}/T_{CH} = \text{Duty cycle}$$

The output is usually controlled [3] either by using Time Ratio Control (TRC) or by using current limit control (CLC). In TRC the T_{ON} or T_{OFF} is adjusted. The chopper may then be operated either in fixed frequency (PWM) or as variable frequency (FM) mode. In CLC, the load current is restricted between certain specified maximum and minimum values. Although both the schemes have relative merits and demerits, PWM method is preferred since FM has following disadvantages:-

1. The frequency has to be varied over a wide range to provide the full output voltage range.
2. Filter design for FM is complex.
3. The possibility of interference with communication lines.
4. The large OFF time at low output voltage may result in discontinuous armature current.

1.5 Classification of Chopper Circuits

The classification is based upon:-

- a) The output voltage waveform and
- b) The quadrant of operation.

a) According to the output voltage waveform, the chopper circuits are classified as [4]

(i) Load independent chopper in which the output voltage waveform is approximately rectangular and the charging current of commutating capacitor is independent of the load and

(ii) The load dependent chopper in which the commutating capacitor is charged by the load current. In this case the current is approximated as Trapezoidal in waveform. This type is widely used in industry due to their significant advantage of increasing commutation capability with increase in load current in presence of source inductance.

b) The choppers classified on the basis of their operation in a particular quadrant, e.g. single, Two or Four quadrant chopper.

Although each circuit is meant for specific purpose, the 1st quadrant chopper is simpler and satisfy wide variety of application and hence is used here.

1.6 Digital Control and its Advantages

The drive control in closed loop is generally used to match certain drive-load characteristics. Such a control could be either analog or digital. With the capability of semi-conductor industry to produce chips that could perform complex functions [5] and at the same time flexible enough to be adopted to several applications have brought tremendous change in power and control industry. Microprocesor-INTEL 8085 is one such chip and is used here for our purpose. Such a digital control has numerous advantages over the analog control and they are [6].

1. There is no inherent nonlinearity in the speed transducer and the response is fast.

2. The digital signal (representing either speed or current) could be transmitted over a long distance without any degeneration.

3. The accuracy of digital system is not affected by aging, temperature variation and extraneous disturbances.

4. Suitable circuit design eliminates noise.

5. Very high accuracy such as ± 0.003 percent of steady state value could be achieved compared to ± 0.5 percent as achieved in analog systems.

In lieu of the points mentioned above, a Microprocessor based system is expected to give superior performance such as high accuracy, quick response etc.

CHAPTER - 2

2.1 Literature Review

When a Microprocessor based chopper fed closed loop dc drive system is to be designed, analysed and tested, it is essential to know the facts from the experience of the past research work. The various investigators have in detail, studied, analysed, designed and simulated such a drive system and the view points of some of them are given below.

Irie et al [7] while studying the operating characteristics of a separately excited dc motor fed by a rectangular wave chopper, have shown the possibility of discontinuous conduction of armature current. Hence in order to analyse such a system, it is essential to accurately represent the system and then derive its transfer function.

E A Parrish et al [8] have represented the thyristorised power source by a sample and hold circuit and there after have analysed it using z transforms. Nevertheless z transforms requires greatly complicated mathematical processing and not suitable for interrupted armature current.

Nitta et al [9] have represented the thyristorised power source by a continuous equivalent system assuming that the input disturbance is small. While their methods have many advantages, the electrical time constant is neglected and the physical meaning of the equivalent system is not so clear.

When the system has very small mechanical time constant of the order of 10 msec, as it is in the case of dc servo motor, electrical time constants cannot be neglected. N Matsui et al [10] have analysed the behaviour of the machine taking into account electrical time constant and the case of interrupted armature current. They have suggested that it is absolutely necessary to keep the armature current uninterrupted and this could be achieved by:-

1. inserting a reactor in the armature circuit or
2. increasing the frequency of chopper.

For the first case of increasing the inductance of armature circuit, Naik et al [11] have investigated the effect of inductance on the performance of the chopper fed motor and have shown that the large value of inductance deteriorates the transient response of the motor. Therefore, it is desirable that the value of inductance should be just sufficient to eliminate discontinuous current and keep the ripple current within limits. They have estimated its critical value to eliminate discontinuous operation for a load dependent chopper which has become very significant category of dc choppers with their ability to improve commutation with increase of load current.

While considering the case of increasing the frequency of chopper, it is to be remembered that, such a system is extensively used for electric traction work and wherein the electric rail road signalling are operated by sharing the traction control systems with the track circuit. Hence it is very essential to provide coordinating means to prevent ac current compo-

nents generated by dc chopper interfering telecommunication or causing safety device malfunction. T. Jinzenji et al [12] have developed a polyphase multi superimposed connection in which several switching thyristors are connected in parallel and this type sufficiently compensates for increasing the frequency and increase in power demand. They have also shown that such a two phase double superimposed auxiliary impulse commutated chopper has fascinating characteristics for electric traction. As the prior charge turn over in the commutating capacitor could be precluded, the commutation energy consumption could be minimized. This also reduces the bulk of commutating components, noise level. In such a chopper the main thyristor could be turned off immediately after the turn on, thus achieving low voltage levels.

William Mc Murray [13] has carried out a comparative study of different commutation circuits in DC choppers and has shown that the major art in circuit design is selecting the most suitable configuration for the given application, particularly the location of inductances. He has carried out computer aided analysis and optimization techniques to several chopper circuits and has shown that the best arrangement has the inductances in the path common to both the thyristors. When one of the thyristors has an antiparallel diode, there is generally an optimum value of inductance which yields maximum turn off time and if no such diode is used, the maximum turn off time is achieved when the inductance is zero.

In a conventional current commutated chopper circuit having an antiparallel diode the commutation is achieved by applying reverse voltage across the thyristor whenever the capacitor charges or discharges resulting in very high commutating current pulse through the capacitor and as the frequency of operation of chopper increases, the size of the commutating elements L&C also increases and commutation becomes difficult, commutation loss increases and efficiency becomes low. Keiju et al [14] have developed new scheme known as the time division commutation in which the commutating thyristor works alternately and the commutating current is suppressed by a saturable reactor. The new circuit has the advantages such as reduction in the capacity of commutating condenser, thyristors and to less than 27%, reduction in the commutating period of around 25 KHz as against 13 KHz in the conventional increase in the number of diodes and thyristors, high capacity saturable commutating transformer and reduction in the period or frequency at light loads.

The drive system is often operated in closed loop to achieve superior performance. T Krishnan and B Ramaswamy [15] have described the design, construction and testing of a thyristorised speed control unit for a separately excited dc motor fed by a six pulse fully controlled thyristor bridge. A speed loop with a PI controller maintains the desired speed irrespective of the variation in load on the motor. An inner current loop protects the thyristors from over currents. This loop also provides fast response over-coming

the effects of disturbances such as variations in supply voltage. The design aspects of the control loops are discussed and the experimental results are given.

The microprocessor (μp) control is basically used to achieve highest possible accuracy of the drive system. Due to their limitations, the maximum steady state accuracy realized in analog system for rated load, temperature variation and speed range is about $\pm 0.5\%$ of the top speed. When there is a demand for very high accuracy of the order of $\pm 0.03\%$ of the top speed with a good dynamic performance (as it is in the case of paper mill application), digital system is the only alternative. Many researchers have aimed at achieving this task. Finally the problem reduces to how accurately the actual speed is measured and how fast the error in speed is compensated in closed loop. Some of the methods for accurate measurement of speed are:-

(a) by calculating the reciprocal of the time between two consecutive speed encoder (digital Tacho) pulses - which means slow measurement time at low speeds,

(b) to count tacho pulses over a fixed sampling interval, which means that sampling time has to be large enough to measure speed accurately, and

(c) by means of Phase Locked Loops - which have limited stable operating range.

R.R. Sule et al [16] have developed a system for very high accuracy drives using a 280 microprocessor achieving

an accuracy of $\pm 0.025\%$ of the top speed. In this drive an optical pulse tachogenerator coupled to the dc motor with an inbuilt amplifier provides a pulse train output, the frequency (f_T) being proportional to the actual speed of the motor. The actual speed is computed from the speed feed back f_T accurately and updated with a time constant of 8 ms throughout the speed range. The reference speed was set by means of thumb wheel switches.

In another study of high speed accuracy drive system, the paper authored by E.S.N. Prasad et al [17] presents a Dual mode system for a chopper fed D.C. drive system with Phase Locked Loop (PLL) regulation and have shown that such a system combined the fast transient response and unlimited lock range capabilities of proportional system with the high speed accuracy of PLL.

W.G. Dunford and S.B. Dewan [18] have devised a procedure for writing program to produce control signals for a two quadrant chopper based on M6800 μ p. They have shown that minimum hardware is required in addition to the basic μ p system for implementation of the program. The listing of flow chart and program are given.

Kenneth et al [19] have derived a new method of current control called Interventionalist one which normally operates in speed control mode, the current limiter taking control only after the current has exceeded a threshold value. The speed response is high. This technique can be easily applied

to small hp motors where current overshoot is not of serious concern. It reduces the complexity of two loop system and avoids any possible restriction of speed controller due to current controller.

A.K. Lin and W.W. Koepsel [20] have discussed an approach to control the speed of a chopper fed d.c. motor using digital techniques. They have devised a control technique using Intel 8080 Microprocessor involving a speed loop. An elementary speed measurement routine is given. They have suggested improvements in the method of implementation such as using a high performance CPU, fast access memory and increasing the bit length of counter to achieve higher resolution for measurement of speed etc.

Pradeep K. Nandam and P.C. Sen [21] have developed a new IP control technique for the analog and digital speed control of dc drives. They have carried out comparative study of PI and IP schemes on the basis of the speed response for a step change in both reference speed and load torque. Analytical and experimental results show that the IP scheme has certain distinct advantages over PI scheme like eliminating the current over shoot and minimizing speed over shoot. The same result could be achieved with PI control but the speed response would be sluggish.

Tsutomu et al [22] have proposed a new method to regulate the speed of a dc motor driven by antiparallel connected

three phase dual thyristor convertor using a μ p. A fast response current controller is obtained by employing a nonlinear compensation subloop and a PI compensation subloop. The nonlinear compensation is used to linearise the nonlinear characteristics of the thyristor converter which is encountered in discontinuous mode of current. The PI compensation subloop reduces the deviation of detected current from the current reference. With these two current control subloops a fast motor speed response is achieved under both discontinuous and continuous modes and hence the steady state accuracy of speed is improved, a speed regulator using a μ p was trial manufactured, tested and it was shown that an extremely fast controlled current response can be obtained even with a long sampling period.

Microprocessors have also been effectively used in developing control schemes for four quadrant choppers which have wide range of applications such as dc cranes, dc servos, magnet power supplies and so on. S.B. DEWAN and ALI MIRBOD [23] have developed an optimum control strategy for a class B current commutated four quadrant chopper using an M6800 Microprocessor. They have shown that with this control strategy, the system provides special characteristics such as low input current ripple, low output voltage ripple and fast response. The experimental results of a 10 KW chopper on a RL load have been given.

After the design and fabrication of the drive system, computer simulation of the drive system is one of the effective

methods to know the performance of the drive before hand and in designing it for different specifications.

The paper authored by P.C. Sen [24] investigates the various control schemes in addition to the phase angle control (PAC), such as symmetrical angle control (SAC), extinction angle control (EAC), current limit control (CLC) and time ratio control (TRC). The drive system with these schemes is simulated on a digital computer and an efficient time saving method is used for computation. The performance characteristics such as torque-speed, input power factor, fundamental power factor, harmonic content and peak motor current are obtained and compared for different schemes.

C. Chellamattu and V.V. Sastry [25] have developed an efficient simulation program for the steady state performance of a chopper fed separately excited dc motor system by formulating an initial state vector without passing through the transient solution.

Pramod Agarwal and V.K. Verma [26] have described a new synthesis approach considering rigorous mathematical modelling for a dual converter system. The dual converter system is operated in circulating current mode and incorporates cosine firing technique. The speed and current loops are realised using PI controllers. They have simulated the system on a computer and have obtained the region of stability, using the parameter plane synthesis method (D composition). The stability region was checked by frequency scanning method.

2.2 Author's Contribution

The present work describes the design, analysis and performance evaluation of a Microprocessor based single quadrant current commutated chopper fed separately excited variable speed d.c. drive system.

A closed loop control scheme incorporating both speed and current loops based on Intel 8085 microprocessor is devised and the relevant software is developed. The flow charts of the software are given.

The drive system is simulated on a digital computer (DEC 2050 main frame) for parameter coordination using the parameter plane technique and transient studies are carried out to determine the most appropriate parameters of the controllers. The experimental results and the computer programs are given.

CHAPTER 3

ANALYSIS AND DESIGN OF POWER CIRCUIT

3.1 INTRODUCTION

The classification of chopper circuits are already given in section 1.4. The current commutated single quadrant chopper circuit used is as shown in Fig. 3.1. Such circuits characterised by an antiparallel diode across the main thyristor [27] have certain advantages over voltage commutated circuits. They do not subject the load to peak voltages in excess of the supply voltage, the turn off interval does not increase in inverse proportion to the load current and the effect of the commutation circuit on the minimum output voltage obtainable is much less significant.

The circuit has serious limitations that, the dc source should be of low impedance and be able to receive energy since it forms a part of the commutation circuit. This was perhaps true for our case also, with diode rectified dc supply, as there was commutation failure at certain operating conditions. Such limitation was over come by substituting alternative connection as shown in broken lines (Fig. 3.1). The difference between the two configurations is that, the main thyristor is fired first in the earlier one and the auxiliary thyristor in the later. The waveforms and the analysis of the configuration (with broken lines) is given.

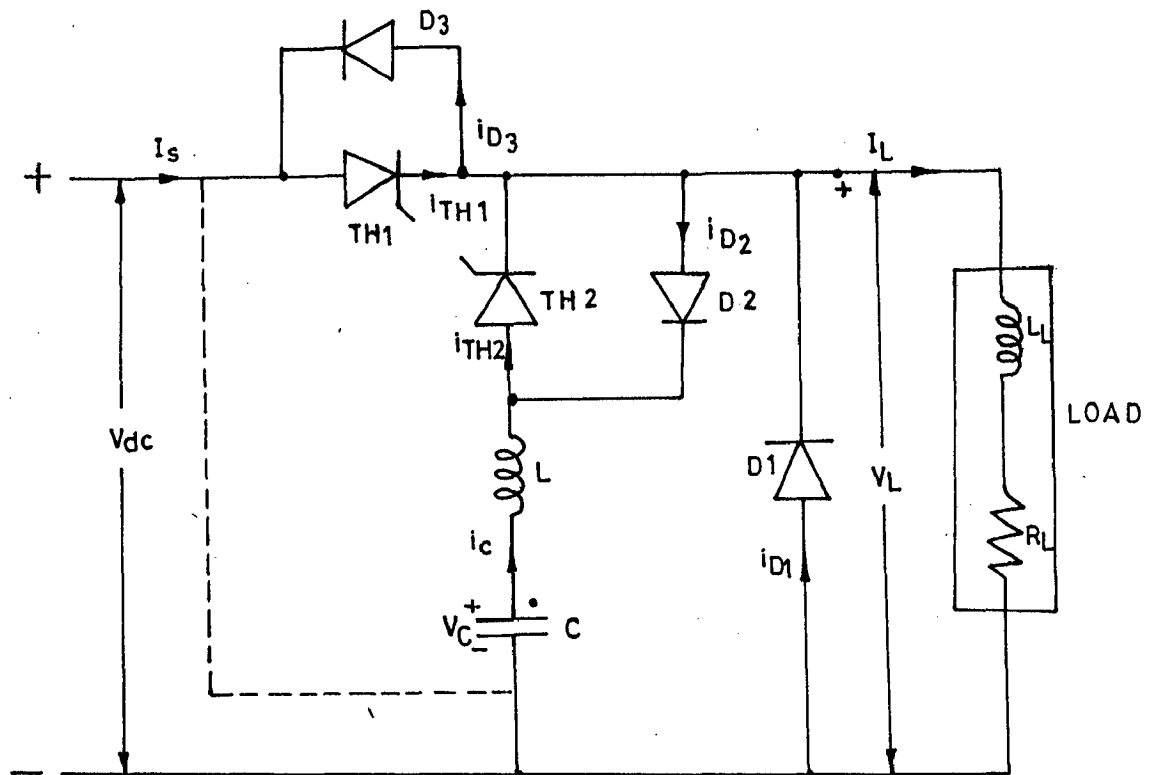


FIG.3-1-POWER CIRCUIT CONFIGURATION

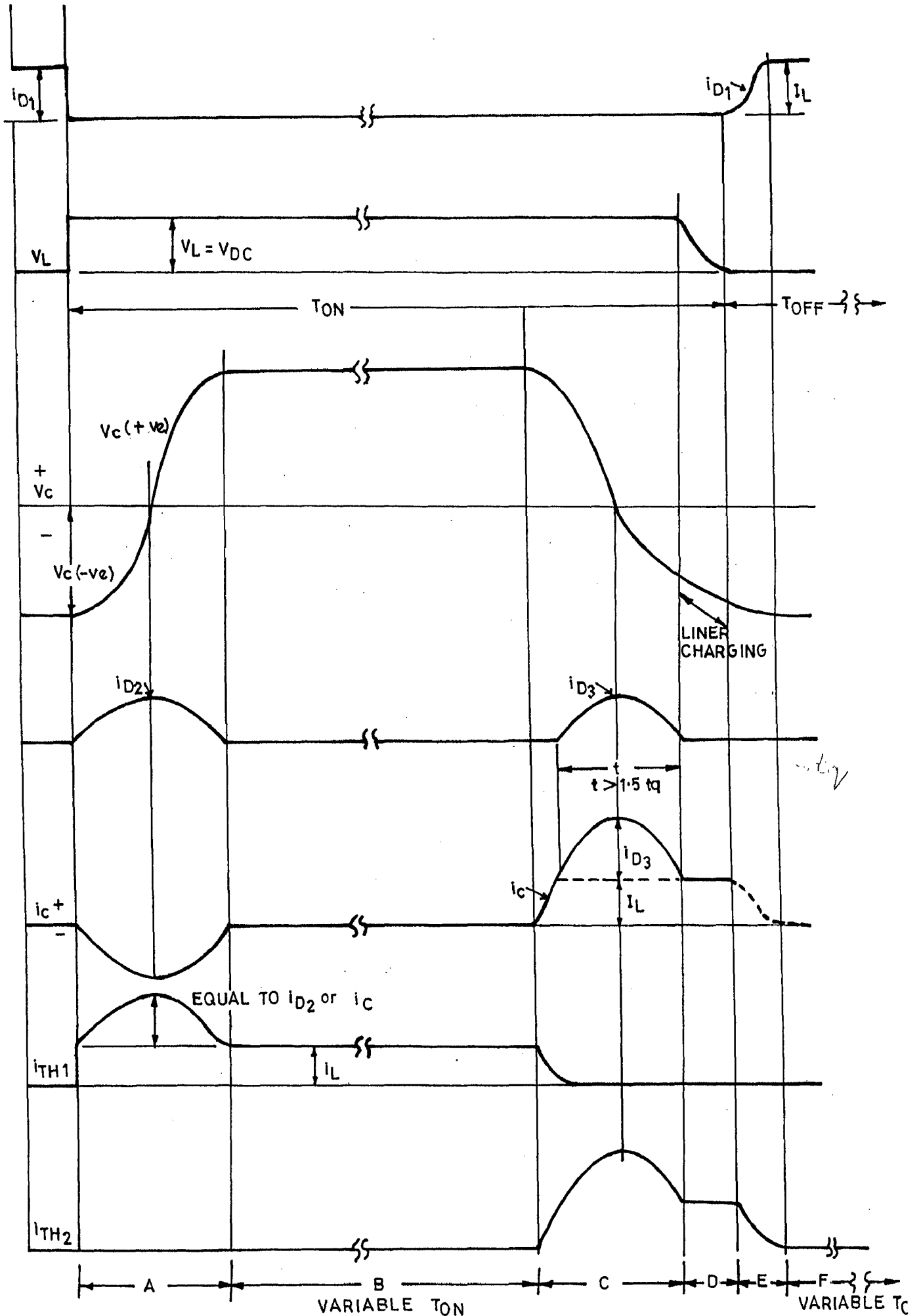


FIG.3-2—WAVE FORMS OF POWER CIRCUIT

3.2 Analysis of the waveforms (Fig. 3.2)

The capacitor C is not charged initially [28]. Firing of TH2 charges C to get charged with dot point as -ve i.e. $V_C = -V$.

Period A : The firing of TH1 immediately transfers the load current into it and the supply system. It also causes discharging and reversal of voltage of C via D2 and L. The presence of L makes the capacitor charge well above the supply voltage. Now V_C is charged with +ve polarity (dot point +ve). It can not discharge via D3 since it is reverse biased due to TH1 being ON.

Period B : This capacitor charge is maintained during the variable period ON time. The load current will generally increase under the influence of the supply voltage and the load inductance.

Period C : When TH2 is fired, the load current is taken over by C and TH1 turns off. The capacitor partially discharges via D3. Thus making TH1 reverse biased for a time larger than its turn off time (t_q).

Period D : When the current in D3 reaches zero, the capacitor carries only the load current and continues to charge linearly in the reverse polarity through

supply and load.

Period E : As the current through capacitor falls below the load current, the diode D1 gradually picks up the load current from TH2.

Period F : In variable T_{OFF} period, the diode D1 carries the full load current under the influence of load inductance. In case of larger T_{OFF} periods, and loads the load current may fall to zero and the diode current D1 also then drops to zero value.

3,3 Design of circuit components L and C [29]

Ratings : DC Motor - 2 HP, 230 V, 1050 RPM

Assuming 76% efficiency at full load, the motor line current can be calculated approximately as,

$$I_L = \frac{2 \times 736}{0.76 \times 230} = 8.5 \text{ A}$$

Assuming 100% sustained over load, the rms value of the current through thyristor $I_{rms} = 17\text{A}$.

Taking the commutation interval, it has to carry a surge or a peak current of $I_{peak} = 2 \times 20 = 40\text{A}$.

Now the value of $X = 2$ (fixed)

Commutating capacitor C and Inductor L

If T_q = Turn off time available for thyristor TH1 and

$W_r = \left(\frac{1}{LC}\right)^{\frac{1}{2}}$ ringing frequency of L - C circuit in rad/sec

then defining a function,

$$\begin{aligned} \text{But } G(X) &= W_r T_q \\ &= \pi - 2 \sin^{-1}(1/x) \text{ rad} \\ &= \pi - 2 \sin^{-1}\left(\frac{1}{2}\right) = 2\pi/3 \\ T_q &= \frac{2\pi/3}{\left(\frac{1}{LC}\right)^{\frac{1}{2}}} \end{aligned} \quad (3.1)$$

and the circuit turn off time T_q should be greater than the thyristor turn off time to ensure proper commutation

$$\begin{aligned} \therefore T_q &= t_{\text{off}} + \Delta t \\ \therefore \frac{2\pi}{3} (LC)^{\frac{1}{2}} &= t_{\text{off}} + \Delta T \end{aligned} \quad (3.2)$$

During this turn off time, assuming a constant load current, the capacitor voltage changes from $+V_{dc}$ to $-V_{dc}$

$$\begin{aligned} (2V_{dc})C &= X I_{\text{on}} T_q \quad \text{or} \\ \therefore V_{dc} (C/L)^{\frac{1}{2}} &= I_{\text{on}} \end{aligned} \quad (3.3)$$

from the equations (3.2) and (3.3),

$$C = \frac{3 I_{\text{on}} (t_{\text{off}} + \Delta t)}{2 E} \quad (3.4)$$

$$\text{and } L = \frac{3E (t_{\text{off}} + \Delta t)}{2 I_{\text{on}}} \quad (3.5)$$

In order to vary the load voltage E over a wide range, the minimum value of E_0 should be equal to or less than 10 percent of the supply voltage V_{dc}

$$\therefore T_{\text{ON}} : T_{\text{OFF}} = 10 : 1$$

As the frequency of operation of chopper is, 200 Hz,

$$T = \frac{1}{200} = 5 \text{ msec}$$

i.e. $T_{\text{ON}} + T_{\text{OFF}} = 5 \text{ msec}$

11 $T_{\text{OFF}} = 5 \text{ msec}$

.. $T_{\text{OFF}} = 400 \text{ usec}$ and

$T_{\text{ON}} = 4.6 \text{ msec}$ (maximum)

Substituting in (3.4) and (3.5),

$C = 16 \mu\text{f}$ and

$L = 2.196 \text{ mH}$

Thus the ratings of the main and auxiliary thyristor are,

Name : SS1012 R, 8439

$I_{\text{T rms}}$: 16 Amps, $I_{\text{TAV}} = 10 \text{ Amps}$

Voltage V_{DRM} : 1200 volts

The power diode ratings are,

Name : SR1612, SSE

Current : 16 Amps

Voltage : 1200 volts

The ratings of the DC generator is same as that of the motor.

3.4 Conclusion

The operating principle of the power circuit employing the current commutated single quadrant chopper is discussed and the waveforms are given. The ratings of the thyristors, diodes and the commutating components L and C are given.

The practical values of L and C used, slightly differ from the designed values. Actually they were varied over a range to get an undistorted waveforms and also to ensure that Commutation failure does not occur. The actual waveforms are shown with the help of photographs given in Chapter 6.

CHAPTER 4

CLOSED LOOP CONTROL

4.1 Introduction

Open loop operation of a DC Motor may not be satisfactory in [30] many applications. The Torque Speed characteristics shows that, any change in load torque keeping the firing angle constant, is accompanied by a change in speed also. However if the drive requires constant speed operation, the firing angle has to be changed in order to maintain a constant speed. This could be achieved in closed loop operation which is shown schematically in Fig. 4.1.

Here an inner current loop and an outer speed loop are incorporated to achieve the desired performance. The actual speed N^* is sensed and compared with the reference speed N_R . The resulting speed error e_N is compensated in speed controller and fed as current reference I_R to the current loop. In the current loop, the actual current I^* and I_R are compared. The resulting current error e_I is compensated in current controller and fed as a controlling signal to the chopper circuit to vary T_{on} and T_{off} , as desired to maintain a constant speed irrespective of the variations in the supply voltage, field current and the load Torque.

The advantages of incorporating current loop are

- 1) The speed controller automatically sets the I_R and

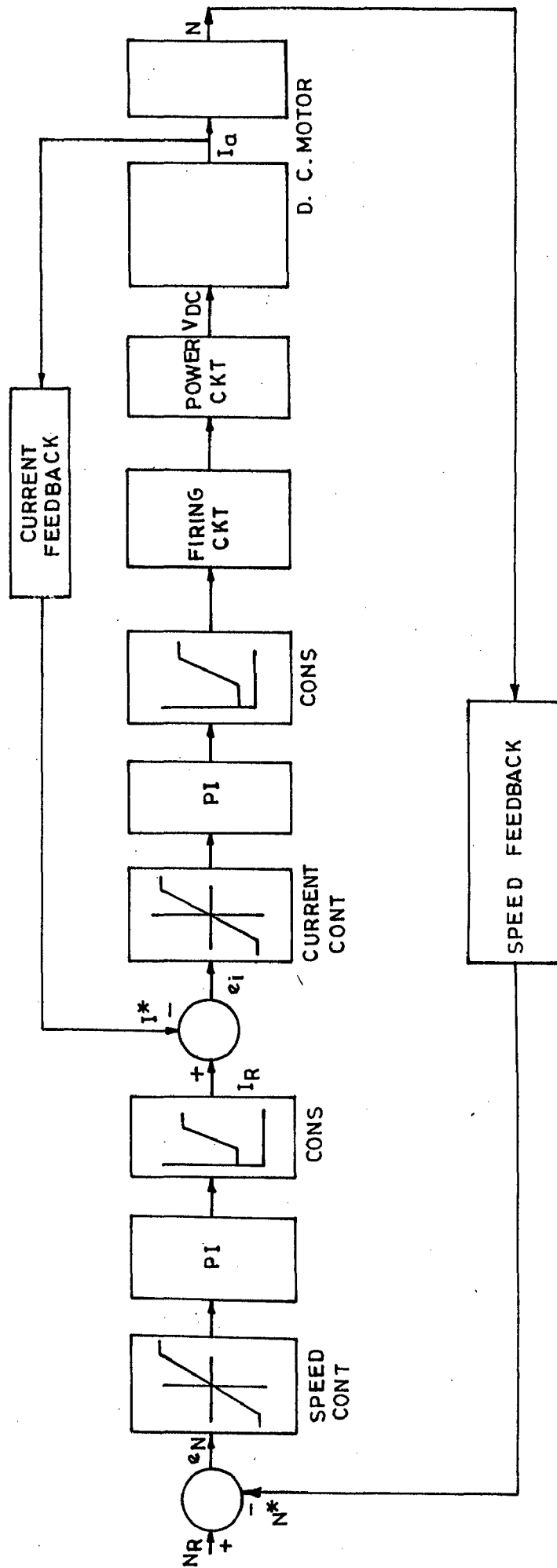


FIG. 4.1—BASIC BLOCK DIAGRAM OF CLOSED LOOP SPEED CONTROL

hence the normal large starting current and transient current which can damage the chopper and possibly the motor could be eliminated.

- 2) Since the electrical time constant of armature circuit is small compared to the mechanical time constant, the armature current, rather than speed drops almost instantaneously, whenever the supply voltage drops. The speed comes to the original value only after the drop in speed is integrated out by the speed controller to give a new T_{on} time. But with a current loop, the fall in current itself sets a new value of T_{on} at a very fast rate. Hence the current loop provides a fast dynamic response.

4.2 Type of Controllers:

The overall performance of the drive in closed loop is dependent mainly upon the nature of the controllers used for both the loops. From a consideration of steady state operation only [31], Integral Control (I) seems preferable to proportional (P) control. Normally with a controller generating a signal proportional to error only, the steady state error or offset remains as a result of sustained distance. But a controller which generates integral control in addition, is able to regulate without leaving any steady state error. Thus PI controller when used, combines the

desirable transient characteristics of a P controller and the feature of no steady state error of an I controller and in addition provides quick response.

In the present work a Proportional plus Integral (PI) controller has been designed and implemented through micro-processor software (Section 5.4) for both speed and current control. However, the general mathematical representation of PI controller is given below: (Fig. 4.1)

$$\text{The output from the controller } V = K_P \left(1 + \frac{1}{T_C s}\right) (N_{\text{ref}} - N^*)$$

where K_P = Proportional controller constant,

K_I = Integral controller constant,

N_R = Reference speed in Hex

N^* = Actual feedback speed in Hex

$$s = \frac{d}{dt} \text{ sec}^{-1}$$

$$V_n = K_P \cdot e_n + K_I \int_{-\infty}^{nT} e_n dt - \text{at the } n^{\text{th}} \text{ sampling instant (t=nT)}$$

e_n = error in reference speed and actual speed in n^{th} instant

$$= (N_{R_n} - N_n^*) \text{ in Hex}$$

$$V_{n-1} = K_P \cdot e_{n-1} + K_I \int_{-\infty}^{(n-1)T} e_{(n-1)} dt \text{ at the } (n-1)^{\text{th}} \text{ sampling instant}$$

$$e_{n-1} = (N_{R_{n-1}} - N_{n-1}^*)$$

$$\therefore V_n - V_{n-1} = K_P (e_n - e_{n-1}) + K_I \int_{(n-1)T}^{nT} e_n dt$$

$$\Delta V_n = K_P \cdot e_n + K_I T e_n \quad (4.1)$$

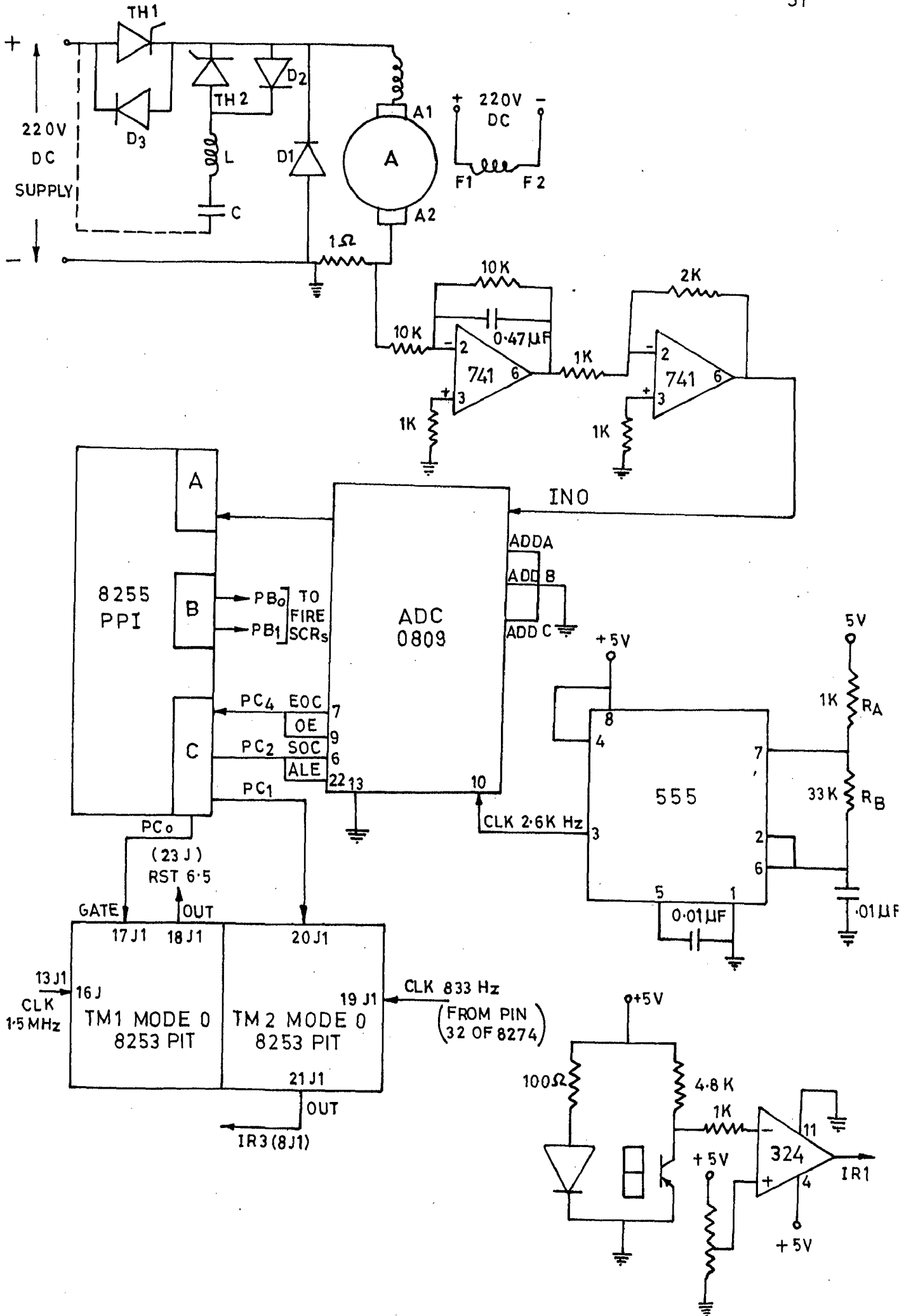
4.3 Microprocessor Implementation

The closed loop speed control scheme discussed so far, could be implemented and made conventional (Analog) by hard wired means, wherein the different analog and digital devices are soldered together. It could also be implemented by means of Instructions (software) using a Microprocessor. In view of the advantages of the digital systems as discussed before (Section 1.6), and also when the drive system becomes complex such as battery powered vehicle, rolling mills, paper mills etc., which require very high accuracy, a microcomputer based control system performs better than hard wired circuitary.

The μ p implementation of our system is explained in the next two sections.

4.3.1 System Hardware

The interfacing circuitary for the μ p control closed loop scheme is as shown in fig. 4.2. Port A, Port C Higher of 8255 (PPI) are programmed as input Ports and Port B, Port C Lower are used as output ports. Specifically, PB_0 and PB_1 are used for firing the thyristors using RST 6.5 interrupt. PC_0 and PC_4 bits are used to provide controlling signals for 8253 (PIT) and ADC. An optical shaft encoder is fitted on to the shaft of the machine. A photo transistor circuit is used to generate speeder pulses which are counted



by using IR1 and IR3 interrupts of 8259 (PIC). Actual current is sampled and input to μp via Port A of 8255. The speed sampling is done once in 200 ms and that of current once in 10 ms. The software written provides control over a range of 15% to 85% of the top speed. The flow charts given in the next section describe the implementation of the system through software.

4.3.2 System Software

a) Main program:

- 1) The various peripheral chips such as 8255, 8253, 8259 are initialised.
- 2) The memory area is initialised with constants.
- 3) The interrupts RST 5.5, 6.5 and 7.5 are unmasked.
- 4) Reference speed N_R is given via keyboard.
- 5) The desired ON and OFF periods namely $T_{ON\ DES}$ and $T_{OFF} = T_{CH} - T_{ON\ DES}$ (In Hex) are calculated and stored.
- 6) Smooth start S.R. is executed where in the main thyristor is fired (RST 6.5 ISS) for T_{ON} period and the machine starts at a very slow speed. The T_{ON} is increased in steps of ΔT till T_{ON} desired is reached. At this instant the machine would have attained a speed close to N_R and now it enters into

closed loop mode.

- 7) In closed loop, N^* the actual speed is calculated and the error in speed e_N is constrained to $\pm 5\%$ of maximum speed (i.e. 5% of $1050 = 50$ rpm) and this constrained speed error is PI processed. The resulting reference current I_R value constrained between I_{RY} maximum and I_{RY} minimum. All this is achieved entirely through software.
- 8) Actual value of current I^* is measured using ADC and is compared with I_R and the resulting error e_I is again constrained between $\pm 10\%$ of the maximum permissible reference value. The constrained current error is PI processed and the resulting quantity itself decides T_{ON} and T_{OFF} values. It is obvious that if the actual speed of the machine is less than the reference value, then T_{ON_n} calculated from the PI processing of speed and current is more than the previous (old) $T_{ON_{n-1}}$ so that, armature impressed voltage increases and the machine speeds up and vice versa. Thus the above procedure is repeatedly executed once in every 250 msec. and the machine tries to maintain the speed constant as commanded by the reference speed setting irrespective of, the variation in load torque or marginal fluctuations in supply voltage or the field flux. The flow chart of the main program is given in the next page.

ENTER

INITIALISATION
 I/O PORTS OF PPI'S, TIMERS(MODES), ALL GATES LOW, UNMASK RST
 6.5 INT, RST 5.5 KBD INT,
 VARIABLES - SPEED PI e_{sn} , e_{sn-1} , KP_s , KI_s
 - CURRENT PI e_{in} , e_{in-1} , KP_I , KI_I
 MIN, T_{ON} , MAX T_{ON} , T_{OFF} , T_{CH} (ALL 2 BYTES)

 STORE VALUES I_{REF} , $I_{REF_{MIN}}$
 REF SPEED 0000 H MAX
 EI

DE = 0000 CALL DELAY
 READ REF SPEED VIA KEY BOARD (IN BCD)

IS
 REF SPEED
 0000

YES

LPI

NO REF SPEED ACCEPTED
 BIT = 1RPM

STORE REF SPEED, CONVERT BCD TO HEX

SMOOTH START INDEX = 00, CYCLE = 00

$$T_{ON\ DES} = 8 \times T_{CH} \times \left\{ \frac{\text{REF SPEED (HEX) / 8}}{\text{MAX SPEED (HEX)}} \right\}$$
 CALL SMOOTH START SR

B

(E)

K = 01 SMOOTH START IS OVER

- INITIATE ACTUAL SPEED MEASUREMENT UNMASK PIC
- COUNT = 00, FI = 00, SMT = 00,
- LOAD SPEED TIMER TM2 WITH 200MSEC COUNT
- UNMASK IR1 AND IR3 FOR SPEED MEAS AND EI

HALT 2

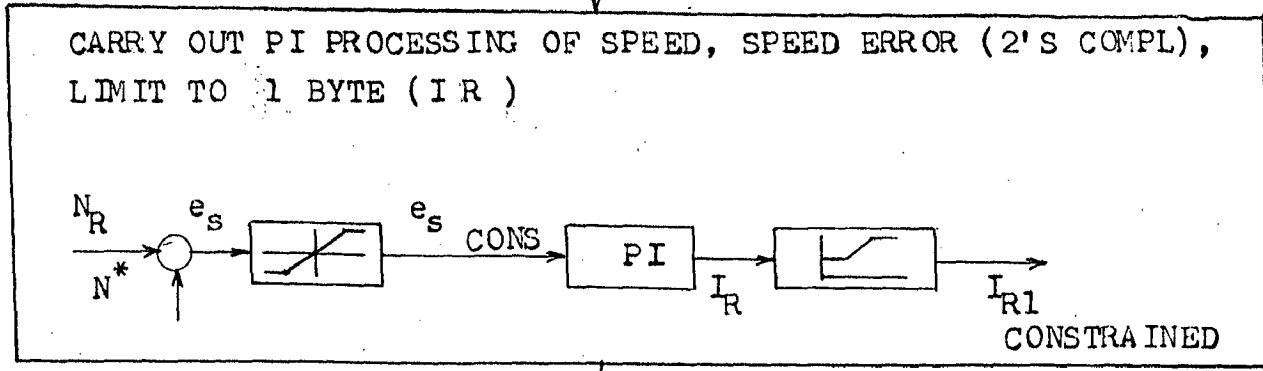
IS
SMT = 01
?

NO

YES
SPEED MEAS OVER

XXX

- CALCULATE ACTUAL SPEED (1 BIT = 1 RPM), STORE
- INITIALISE ACTUAL MEAS BY SMT = 00, FI = 00
- TM2 WITH 200 MSEC, UNMASK IR1, IR3, EI

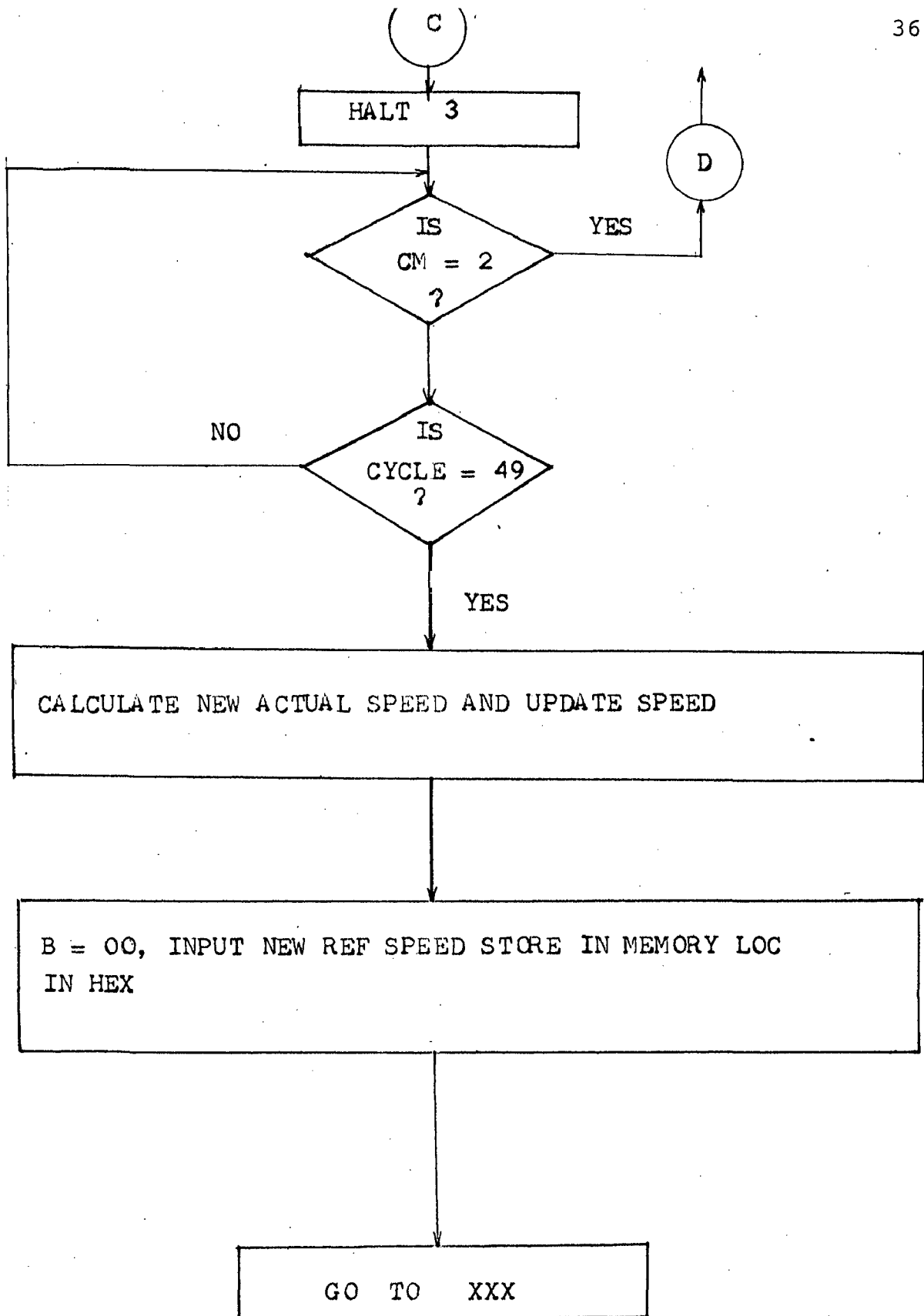


(D)

ENTER PI FOR CURRENT (10 mSEC SAMPLING)

- INDEX CM = 00
- MEAS CURRENT VIA ADC (Ia)
- CURRENT ERROR CALCULATION
- PI PROC OF CURRENT
- CONSTRAIN T_{ON} AND CALCULATE T_{OFF}

(C)



FLOW CHART FOR MAIN PROGRAM

b) Firing of Thyristors by RST 6.5 ISS:

The microprocessor controlled firing scheme is as shown in Fig. 4.3. Bits PB_0 and PB_1 of Port B of 8255 are used to trigger monoshots 74121 which are configured in positive edge triggered mode. The pulse width at the output of these monoshots is designed to be 300 μ sec to ensure proper firing of the Thyristors.

$$\text{i.e. } 0.7 RC = 300 \times 10^{-6}$$

choosing $C = 0.01 \mu\text{f}$, $R = 42.8\text{K}$ (33K is used)

These pulses are AND ed with high frequency output of a 555 Timer using triple input AND gate 7411 and are amplified using a pulse amplifier. The pulses at the output of pulse transformer secondary are given to the Gates of the thyristors. RST 6.5 Interrupt is used to generate the firing pulses for both Main and Auxiliary thyristors at required instants and is explained as below. The T_{ON} and T_{OFF} values (in Hex) are calculated for a particular reference speed as explained before. The main thyristor is fired by making PB_0 HIGH and the TML is loaded with a count equal to T_{ON} and its Gate is enabled. The timer starts down counting and RST 6.5 interrupt which is connected to OUT of TML is generated on terminal count. In RST 6.5 interrupt the Auxiliary Thyristor is fired by making PB_1 HIGH and it loads the TML with count T_{OFF} enabling its Gate. Thus the above procedure is repeated again when RST 6.5 interrupt

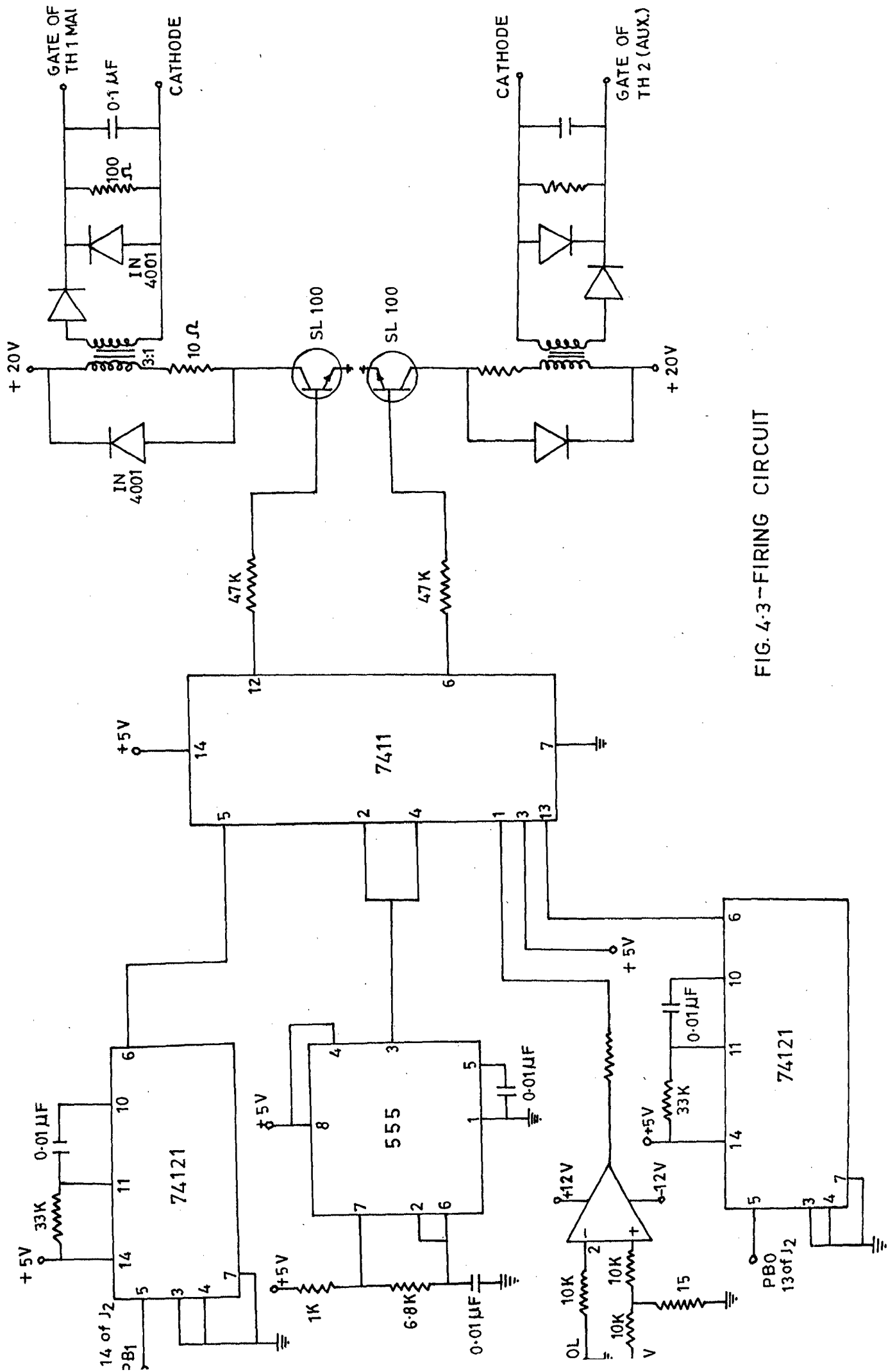


FIG. 4-3-FIRING CIRCUIT

is generated after a period T_{OFF} is reached.

RST 6.5 I.S.S.

Name of

Subroutine : RST 6.5 ISS

Inputs : Interrupt generated when TMI OUT becomes HIGH on terminal count.

Outputs : Loads TMI either with T_{ON} or T_{OFF} for next interrupt.

CALLS : None.

Description : This routine fires main thyristor, makes firing index $I=01$, loads TMI with T_{ON} or fires auxiliary thyristor makes $I=00$, loads TMI with T_{OFF} .

Note : It uses values T_{ON} , Index I, T_{OFF} , cycle from the memory.

The relevant flow chart is given in the next page.

c) Digital Measurement of speed using IR1 and IR3 ISS:

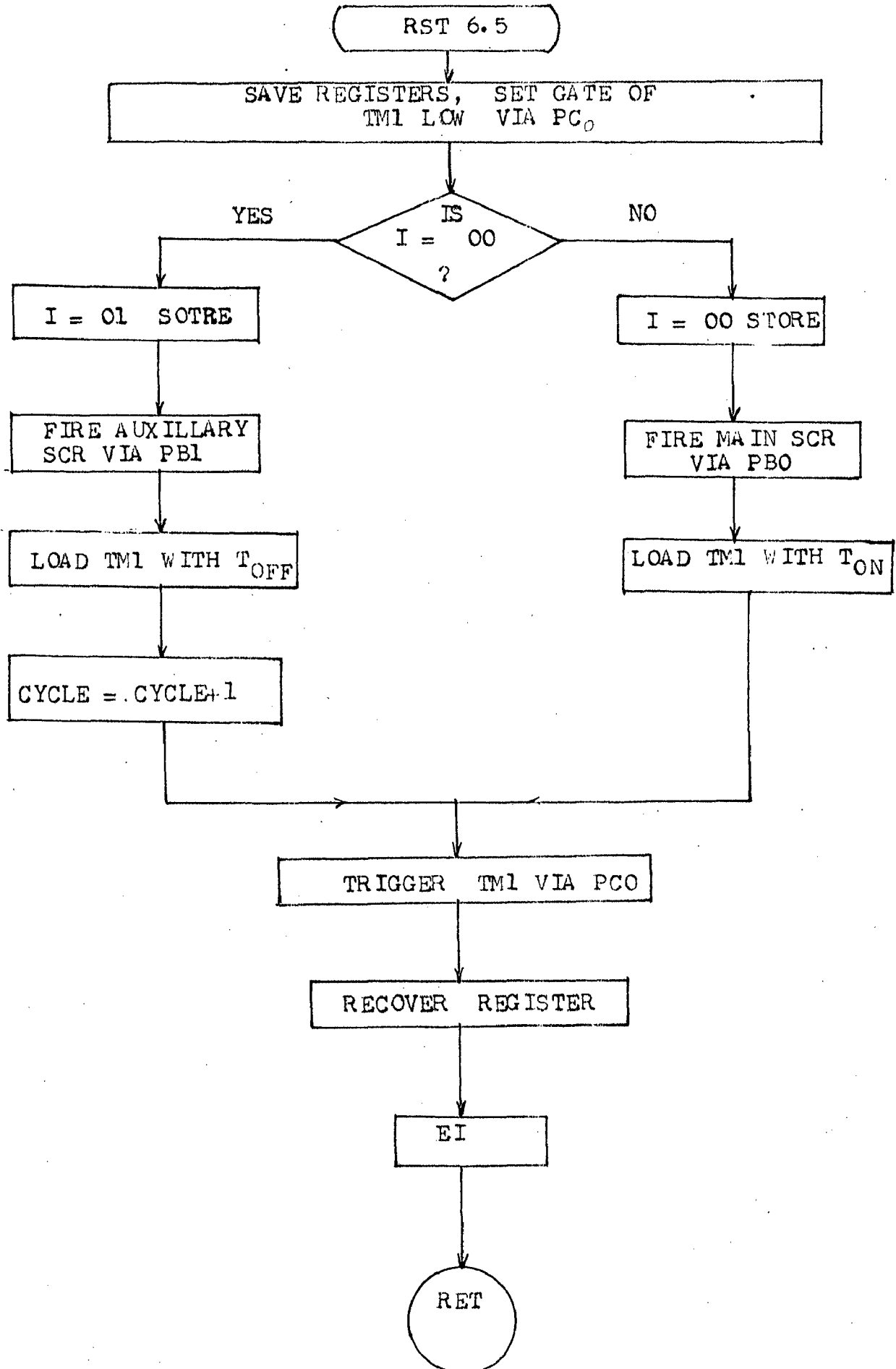
The interfacing circuitary for the digital measurement of speed is shown in Fig. 4.2. The optical shaft encoder used has 60 holes (H) on its periphery. If the actual speed of the machine is N RPM,

$$\text{Number of revolutions/sec } (n_s) = N/60$$

$$\text{Number of pulses generated/sec} = N/60 \times H$$

$$= N/60 \times 60 = N$$

RST 6.5 ISS



FLOW CHART FOR RST 6.5 ISS

Hence if we sample the speed encoder pulses for a period of 1 sec, the number of pulses counted (COUNT) would directly give the speed in RPM. As the sampling is actually done for 200 msec, the actual speed of the machine is equal to $COUNT * 5 \text{ rpm}$ (The relation between the actual speed and the speed as measured by up is given in Appendix B.

The counting of the speeder pulses is for 200 msec. It is done with the execution of IR1 and IR3 ISS, generated by the IR1 and IR3 interrupts of the PIC, and is explained as below.

IR1 ISS is executed every time the speeder pulse is generated during the sampling period. When IR1 ISS is executed for the first time upon the generation of the first speeder interrupt (FI), the timer TM2 is loaded with a 200 msec count and its gate is enabled. During the subsequent execution of IR1 ISS, the COUNT is incremented by one. In the mean time, TM2 starts down counting and its OUT connected to IR3 goes HIGH upon zero count. Occurrence of the IR3 interrupt heralds the completion of 200 msec time and IR3 ISS further disables all the speeder pulses interrupts.

IR1 ISS for measurement of speeder pulses

Name of SR	:	IR1 ISS
Input	:	Interrupt recognised upon the generation of each speeder pulse.
Output	:	The speeder pulses COUNT in HL rp.

CALLS : None

Destroys : None

Description : Other interrupts are automatically disabled during this ISS. It loads the TM1 with 200 msec constant during the first execution and makes index FI=01. During subsequent execution for a max. period of 200 msec, COUNT is incremented and restored back in HL rp.

IR3 ISS

Name of SR : IR3 ISS

Input : Interrupt generated when the OUT of TM2 loaded with a 200 msec constant, goes HIGH.

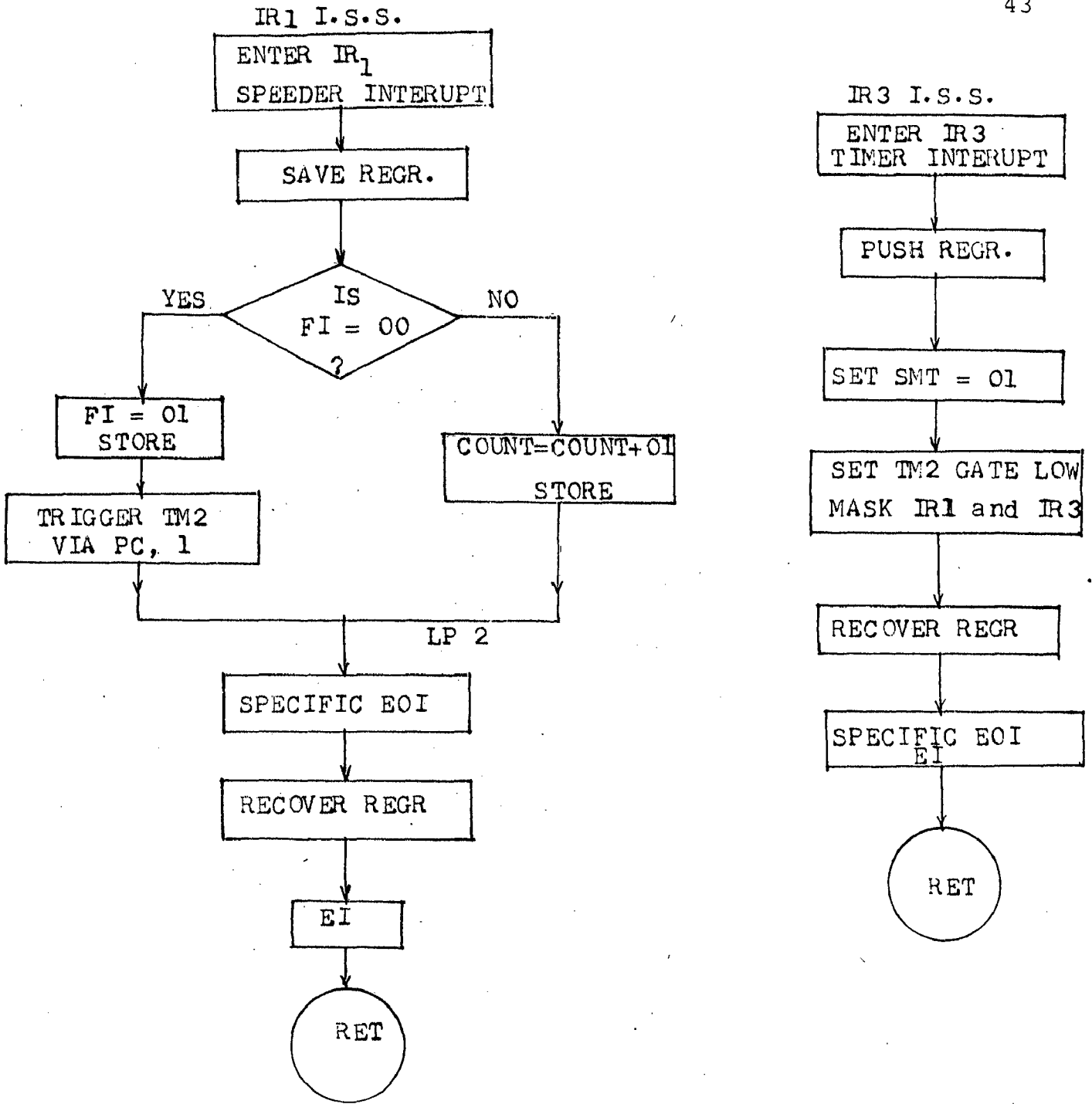
Output : Makes speed measurement time index SMT=01 (i.e. speed measurement is over)

CALLS : None

Destroys : None

Description : This interrupt coming after 200 msec of speed measurement initialisation indicates completion of speed measurement, and sets the gate of TM2 low via PC₁ and masks all IR's of PIC, thus disabling any further speeder interrupt.

The flow charts for IR1 and IR3 SR's are given in the next page.



FLOW CHART FOR IR1 AND IR3 ISS

d) Digital Measurement of current

The actual armature current is sampled i.e. tapped across a low resistor in series with the armature circuit. As this current is pulsating, it is passed through a filter and amplified to a suitable voltage level so that maximum armature current of 8A corresponds to an analog signal of 5V. This analog signal is converted to its equivalent digital value using ADC 0809 as shown in Fig. 4.2.

The current is sampled once in 10 msec by the μ p program in the closed loop. Firstly, a pulse is given at the start of conversion pin (SOC) of ADC via PC2. The end of conversion EOC is tested by μ p via EOC pin. Once EOC is high, the digital information is input from the ADC via the input port A bits ($PA_7 - PA_0$) and stored in a particular memory location for further processing.

ADC S.R. for measurement of current

Name of S.R.	:	ADC S.R.
Inputs	:	None
Outputs	:	None
CALLS	:	None
Destroys	:	None
Description	:	Inputs the digital equivalent of armature current through ADC and stores in appropriate location for further Processing.

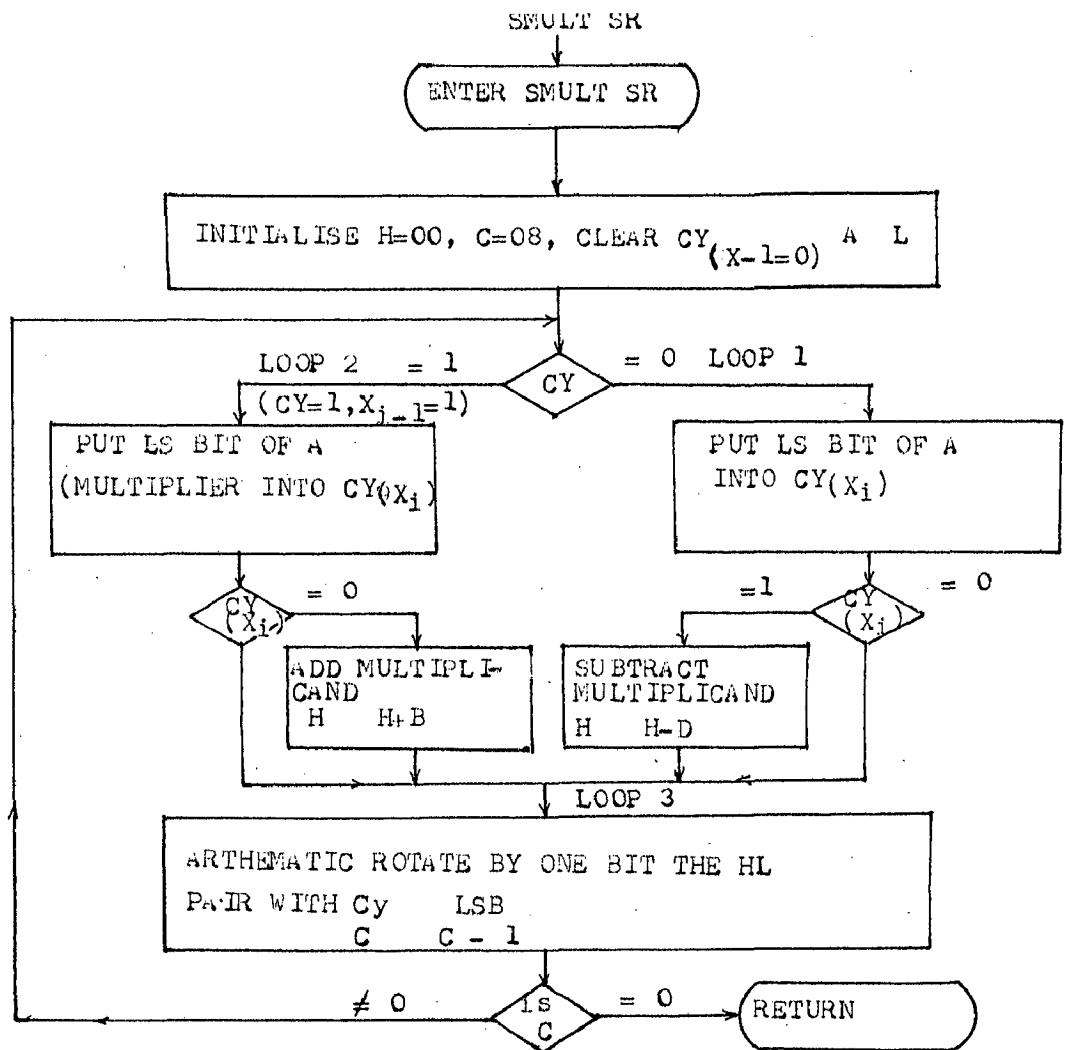
Note : Other interrupts like RST 6.5 and RST 7.5 are already enabled during the execution of this SR.

(The relation between the actual current and the current as measured by up is given in Appendix B).

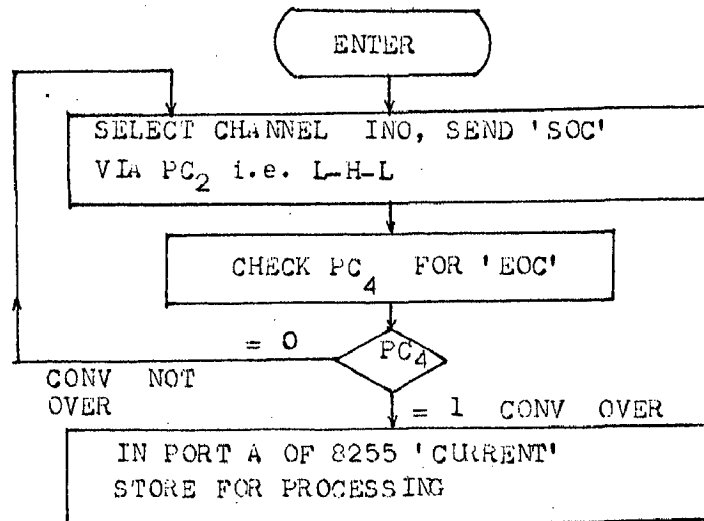
The relevant flow chart is given in the next page.

e) Subroutines for the multiplication and division of Two's Compliment numbers [32]:

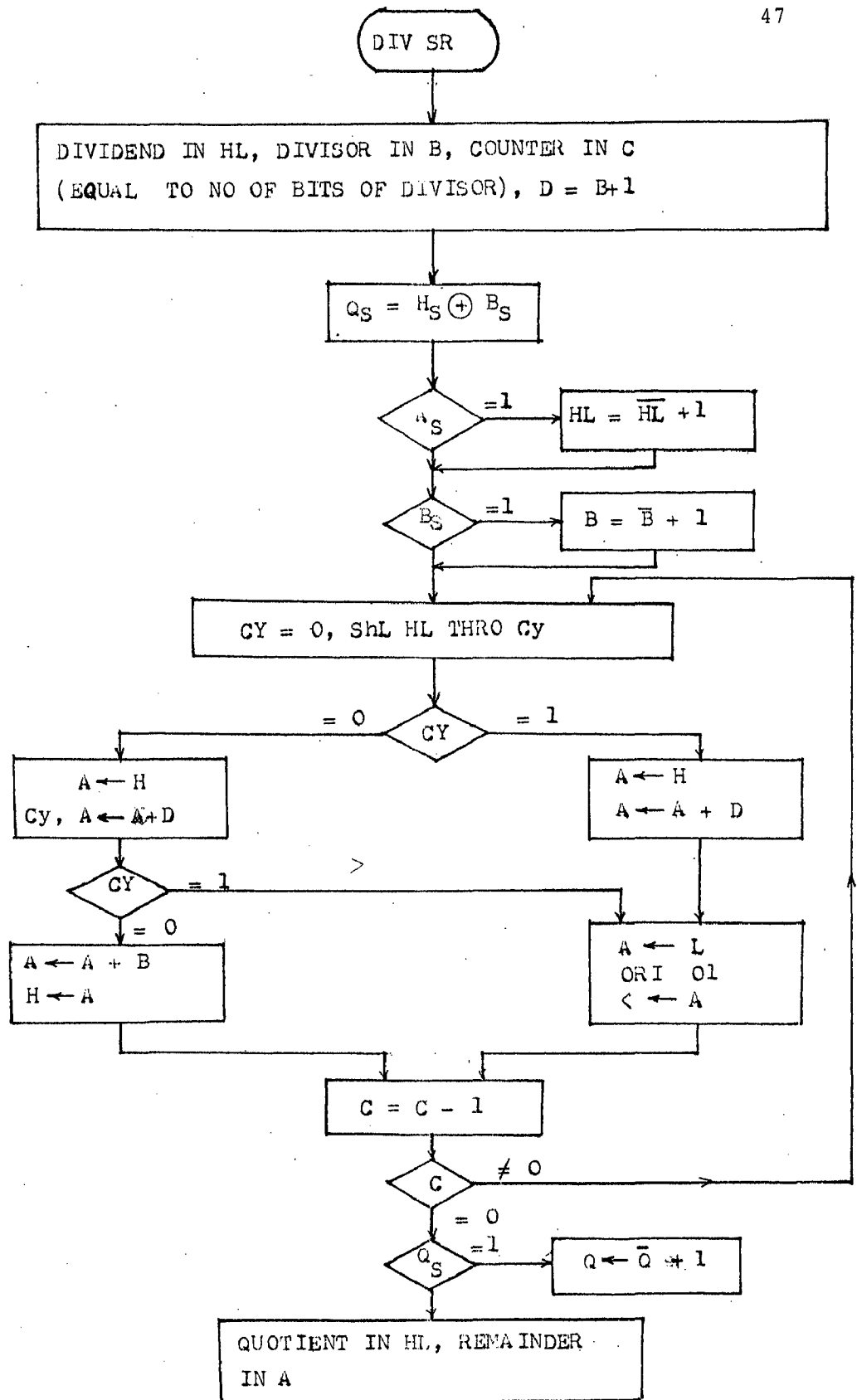
Name of S.R.	: SMULT
Inputs	: multiplier in B reg and multiplicand in L reg
Outputs	: product in HL rp
CALLS	: None
Destroys	: A and C registers
Description	: This S.R. multiplies two Two's compliment numbers and the product of multiplication is returned to the calling program in HL rp using Booth's algorithm
Name of S.R.	: DIV
Inputs	: Dividend in HL rp and divisor in B reg
Outputs	: quotient in HL rp
CALLS	: None
Destroys	: A,C,D,E
Description	: This SR divides a Two's compliment number in HL rp by another two's compliment number in B reg; the quotient also a Two's compliment number is returned to calling program in HL rp using Booth's algorithm



FLOW CHART FOR SMULT SR



FLOW CHART FOR 'ADC' SR



FLOW CHART FOR 'DIV' SR

4.4 Conclusion

This chapter deals with the complete μp implementation of the closed loop scheme. The block diagram of the closed loop scheme, the system hardware and most of the flow charts for the system software are given. How the different interrupts of the μp are used for the measurement of speed, the firing of the thyristors and the measurement of current are explained in detail.

CHAPTER - 5

Mathematical Modelling and Computer Simulation of the drive system

5.1 Introduction

After the microprocessor based drive system is designed and fabricated, it is the desire of the designer to achieve superior performance such as minimum overshoot, fast response in the transient state and zero error in the steady state condition. In order to achieve this, the drive system has to be suitably designed. As the different components of the drive system [32] such as, power converter, controller (and its type), and the plant are already fixed, the gains and time constants of the controller are the only feasible parameters that could be varied, and hence suitably designed.

To achieve the above said task, the first step is the preparation of the mathematical model of the system, from its differential equations and solve them in the time domain to predict the variation of different quantities. In case of higher order systems (as it is in our case), such a method would be difficult to achieve. Hence digital simulation, wherein a system of differential equations are solved step by step is sometimes used and seems to be a convenient mathematical tool for transient and steady state studies. Thus we have simulated our system on DEC 2050 main-frame computer, to design the controller values and the procedure is explained in this chapter.

5.2 Transfer function of various elements [34]

5.2.1 D.C. Motor

The differential equation of armature circuit of a separately excited dc motor, with constant field excitation is as follows,

$$e_a = e_b + R_a i_a + L_a \frac{d i_a}{dt}$$

where Back emf $e_b = K_b \omega_m$ volts with,

$$K_b = K_f I_f \text{ a constant,}$$

$$I_f = \text{constant field current} \quad (5.1)$$

The torque balance differential equation is

$$J \frac{d\omega_m}{dt} = T - T_L \quad (5.2)$$

where the Load Torque $T_L = B \omega_m$ Nw-mt and,

the Electromagnetic Torque $T = K_b i_a$ Nw-mt

The coulomb and static frictions are neglected for getting a linear model. The viscous friction is included in the load torque T_L . In the experimental set up, the dc motor is loaded by means of a dc generator supplying power to a resistive load. Neglecting the electrical time constant of the armature circuit of the dc generator, it can be shown that the load torque on the dc motor is proportional to speed. The viscous friction only increases this proportionality constant and was found out experimentally.

Taking Laplace transforms of equations 5.1 & 5.2

$$E_a(s) = E_b(s) + R_a I_a(s) + L_a \cdot s I_a(s)$$

$$E_b(s) = K_b \omega_m(s)$$

$$sJ\omega_m(s) = T(s) - T_L(s)$$

$$T_L(s) = B\omega_m(s)$$

$$T(s) = K_b I_a(s) \text{ and hence}$$

$$(sJ + B) \omega_m(s) = T(s) = K_b I_a(s) \quad (5.3)$$

The block diagram of the dc motor using the above equation can be drawn as shown in Fig. 5.1. From the block diagram the transfer function can be derived as follows

$$\begin{aligned} \frac{\omega_m(s)}{E_a(s)} &= \frac{G(s)}{1 + G(s) H(s)} \\ &= \frac{\frac{K_b}{(sL_a + R_a)(sJ+B)}}{1 + \frac{K_b^2}{(sL_a + R_a)(sJ+B)}} \\ &= \frac{1/K_b}{1 + \frac{JR_a}{K_b^2} \left(1 + s\frac{L_a}{R_a}\right) \left(s + \frac{B}{J}\right)} \end{aligned}$$

defining $\tau_a = \frac{L_a}{R_a}$ = electrical time constant of the motor armature circuit

and $\tau_m = \frac{JR_a}{K_b^2}$ = mechanical time constant.

the transfer function becomes

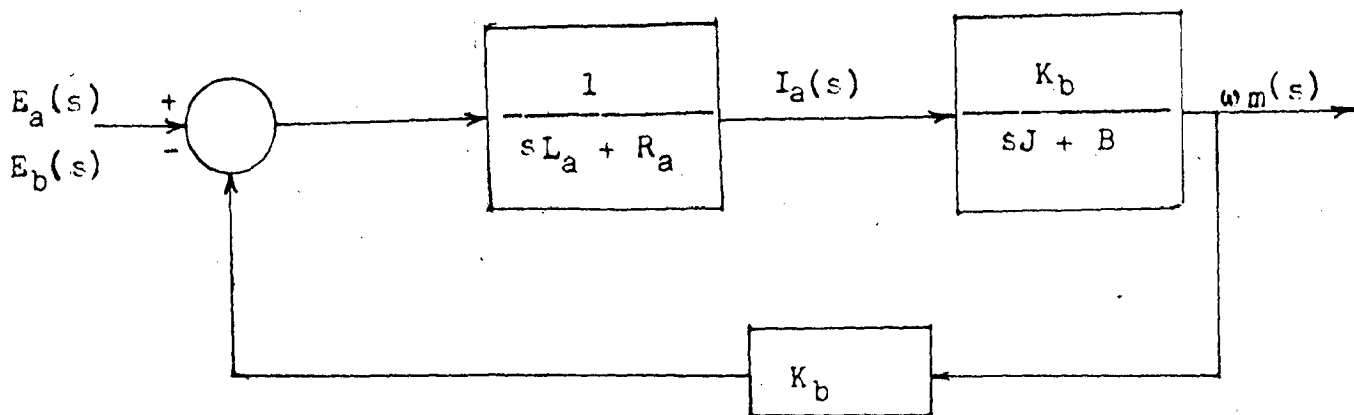


FIG. 5.1 BLOCK DIAGRAM OF D.C. MOTOR

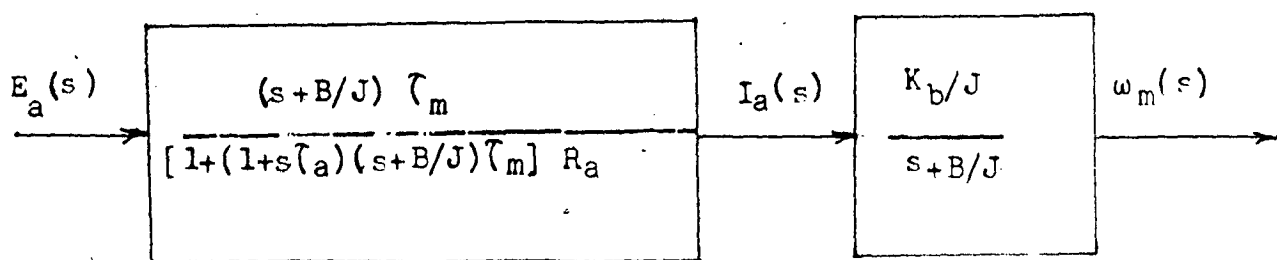


FIG. 5.2 REDUCED BLOCK DIAGRAM OF D.C. MOTOR

$$\frac{\omega_m(s)}{E_a(s)} = \frac{1/K_b}{1 + \tau_m(1 + s\tau_a)(s + B/J)} \quad (5.4)$$

$$\text{Also } \frac{\omega_m(s)}{I_a(s)} = \frac{K_b}{sJ + B} = \frac{K_b/J}{(s + B/J)}$$

$$\begin{aligned} \frac{I_a(s)}{E_a(s)} &= \frac{I_a(s)}{\omega_m(s)} * \frac{\omega_m(s)}{E_a(s)} \\ &= \frac{(s + B/J)}{K_b/J} * \frac{1/K_b}{1 + (1 + s\tau_a)(s + B/J)\tau_m} \\ &= \frac{(s + B/J)\tau_m}{[1 + (1 + s\tau_a)(s + B/J)\tau_m]R_a} \quad (5.5) \end{aligned}$$

The block diagram redrawn using 5.4 and 5.5 is as shown in Fig. 5.2.

5.2.2 Chopper

The input and the output voltage relationship of a chopper can be assumed to be linear and is as follows

$$V_{out} = V_{in} \frac{T_{ON}}{T_{ON} + T_{OFF}}$$

where $V_{in} = V_s$ the supply voltage,

$V_{out} = E_a$ the armature input voltage,

$T_{ON} + T_{OFF} = T_{CH}$ the time period of chopper a constant for PWM operation of chopper and

T_{ON} = the on time of chopper & is proportional to control V_{Cl}

Hence $E_a \propto V_{Cl}$ or

$$E_a = K V_{Cl}$$

where K is the transfer function of chopper

The numerical value of K is taken as 1 for the analytical study. Although, there is a delay (maximum of, $T_{ON\ MAX}$) in the propagation of information V_{C1} to be reflected on E_a , it is neglected for all practical purposes.

Thus the thyristor power converter consisting of chopper and firing circuit is approximated as a linear continuous element although it is a nonlinear sampled data element in reality.

5.2.3 Current Controller

A PI controller has been chosen for current control and its transfer function can be written as

$$\frac{V_{C1}(s)}{e_{C1}(s)} = \frac{K_1(1 + T_{C1}s)}{T_{C1}s} \quad (5.7)$$

5.2.4 Speed Controller

A PI controller has been chosen for speed control also, and its transfer function is

$$\frac{V_{C2}(s)}{e_{C2}(s)} = \frac{K_2(1 + T_{C2}s)}{T_{C2}s} \quad (5.8)$$

5.2.5 Current Transducer

As was already explained in section 4.3 the transfer function of the current transducer can be written with a dead time lag as

$$\frac{I^*(s)}{I_a(s)} = R e^{-sT_1}$$

where I^* = feed back signal for actual armature current I_a

R = equivalent resistance of sampler, filter and
is equal to 0.5412 ohms.

T_1 = sampling time for current and is equal to 0.01 secs.

5.2.6 Speed Transducer

It is already explained in section 4.3.b that the speed feed back should be in rpm for the speed processing. Hence the speed transducer with a dead time lag has the transfer function

$$\frac{N^*(s)}{\omega_m(s)} = H_W e^{-sT_2} \quad (5.9)$$

where N^* = speed of the machine in rpm as fed back

ω_m = actual speed of the machine in rads/sec

H_W = $60/2\pi$ conversion factor

T_2 = sampling time of speed and is equal to 0.245 secs.

5.3 System State Model

The system model is shown in detail in Fig. 5.3. The state variables are defined as follows;

$$x_1 = V'_{C1}$$

$$x_2 = V'_{C2}$$

$$x_3 = I_a$$

$$x_4 = \omega_m$$

from the block diagram (Fig. 5.3)

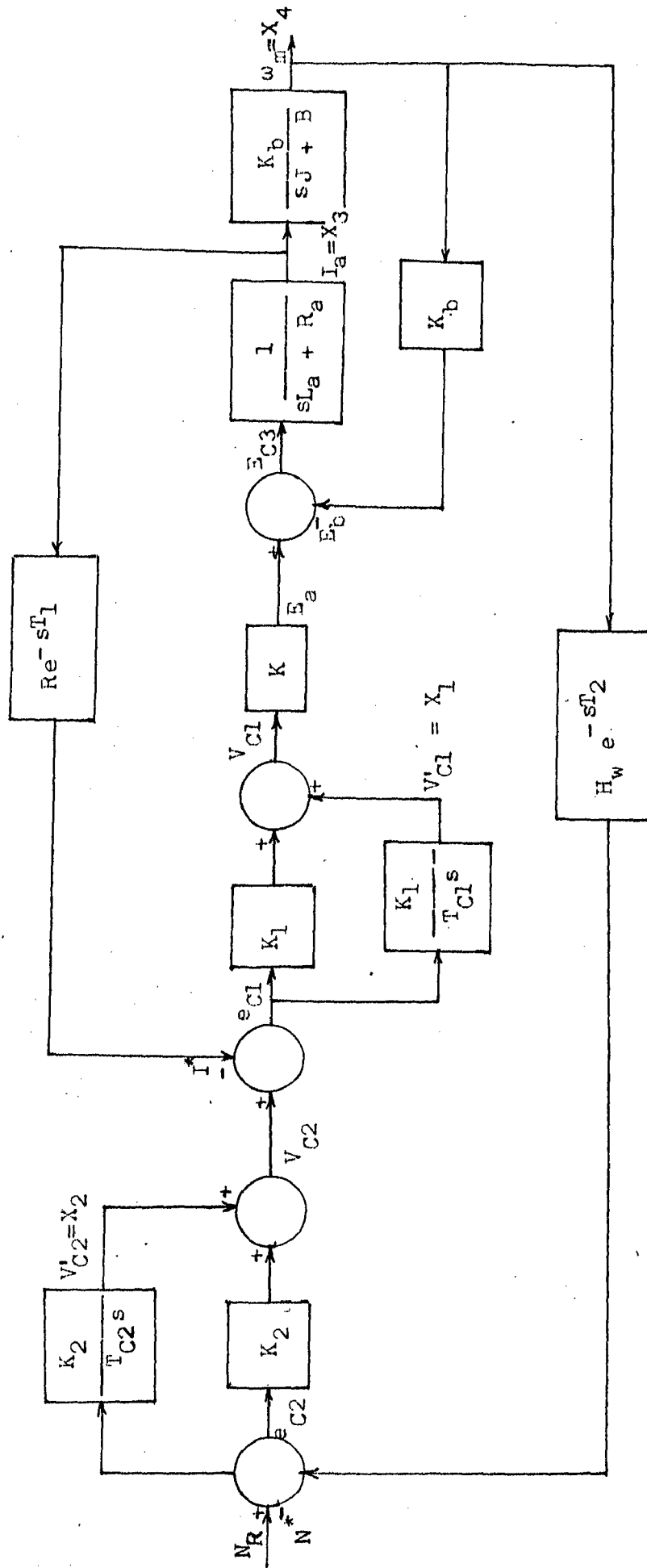


FIG. 5.3 SYSTEM BLOCK DIAGRAM WITH ALL STATE VARIABLES

$$e_{C2} = N_R - N^* \text{ where } N^* = H_W e^{-sT_2} X_4$$

$$X_2 = \frac{K_2}{T_{C2}s} * e_{C2}$$

$$\text{or } sX_2 = \frac{K_2}{T_{C2}} * e_{C2}$$

Taking inverse Laplace transform

$$\frac{dX_2}{dt} = \frac{K_2}{T_{C2}} * e_{C2} \quad (5.10)$$

$$V_{C2} = X_2 + e_{C2} K_2, \text{ also } V_{C2} = I_R$$

$$e_{C1} = I_R - I^* \text{ where } I^* = R e^{-sT_1} X_3$$

$$X_1 = \frac{K_1}{T_{C1}s} * e_{C1}$$

$$\text{or } sX_1 = \frac{K_1}{T_{C1}} * e_{C1}$$

Taking inverse Laplace transform

$$\frac{dX_1}{dt} = \frac{K_1}{T_{C1}} * e_{C1} \quad (5.11)$$

$$V_{C1} = X_1 + e_{C1} K_1$$

$$E_a = K * V_{C1}$$

$$e_{C3} = E_a - E_b \text{ where } E_b = K_b \omega_m$$

$$X_3 = e_{C3} / (sL_a + R_a)$$

$$\text{or } sX_3 = (e_{C3} - X_3 R_a) / L_a$$

Taking inverse Laplace transform

$$\frac{dX_3}{dt} = (e_{C3} - X_3 R_a) / L_a \quad (5.12)$$

$$X_4 = X_3 K_b / (sJ + B)$$

$$\text{or } sX_4 = (X_3 K_b - X_4 B) / J$$

Taking inverse Laplace transform

$$\frac{dx_4}{dt} = (X_3 K_b - X_4 B) / J \quad (5.13)$$

5.4 Design of Controllers

5.4.1 Current Controller

A PI Controller is used for the current controller and its transfer function is given as $K_1(1 + T_{Cl}s)/T_{Cl}s$. Before the two parameters, gain K_1 and time constant T_{Cl} could be designed, they have to be first coordinated in parameter plane so that stability of the system is assured. The method of stability used is as described in appendix A. Now considering only current loop, its characteristic equation is given below. The current loop can be delinked from the speed loop due to the fastness of the current loop in comparison to machine speed variation. The block diagram given in figures 5.2 and 5.3 are used here.

$$1 + G(s) H(s) = 0$$

$$1 + K_1 \left(1 + \frac{1}{T_{Cl}s}\right) \frac{K(s+B/J)\tau_m/R_a}{[1+(1+s\tau_a)(s+B/J)\tau_m]} * R e^{-sT_1} = 0$$

$$1/K_1 + \left(1 + \frac{1}{T_{Cl}s}\right) \frac{K(s+B/J)\tau_m/R_a}{[1+(1+s\tau_a)(s+B/J)\tau_m]} * R e^{-sT_1} = 0$$

Defining $\alpha_1 = 1/K_1$ and $\beta_1 = 1/T_{Cl}$ the equation becomes

$$\alpha_1 + \left(1 + \frac{\beta_1}{s}\right) \frac{K(s+B/J)\tau_m/R_a}{[1+(1+s\tau_a)(s+B/J)\tau_m]} * R e^{-sT_1} = 0$$

Let $F_1(s) = K R \tau_m e^{-sT} (s+B/J)/R_a$

and $F_2(s) = [1+(1+s\tau_a) (s+B/J)\tau_m]$

then, $\alpha_1 + (1 + \beta_1/s) \frac{F_1(s)}{F_2(s)} = 0$

or $\alpha_1 s F_2(s) + \beta_1 F_1(s) + s F_1(s) = 0$

Separating the real and imaginary parts of the above equation, for a complex value of the Laplacian operators

$$\alpha_1 \operatorname{Re}[s F_2(s)] + \beta_1 \operatorname{Re}[F_1(s)] + \operatorname{Re}[s F_1(s)] = 0 \quad (5.14)$$

$$\text{and } \alpha_1 \operatorname{Im}[s F_2(s)] + \beta_1 \operatorname{Im}[F_1(s)] + \operatorname{Im}[s F_1(s)] = 0 \quad (5.15)$$

Solving the equations 5.14 and 5.15 for α_1 and β_1 ,

$$\alpha_1 = \frac{\operatorname{Re}[F_1(s)] \operatorname{Im}[s F_2(s)] - \operatorname{Re}[s F_1(s)] \cdot \operatorname{Im}[F_1(s)]}{\Delta}$$

$$\text{and } \beta_1 = \frac{\operatorname{Re}[s F_1(s)] \cdot \operatorname{Im}[s F_2(s)] - \operatorname{Re}[s F_2(s)] \cdot \operatorname{Im}[s F_1(s)]}{\Delta}$$

where $\Delta = \operatorname{Re}[s F_2(s)] \cdot \operatorname{Im}[F_1(s)] - \operatorname{Re}[F_1(s)] \cdot \operatorname{Im}[s F_2(s)]$

Putting $s = -\sigma + j\omega d$ and $s = -\xi\omega_n + j\omega_n\sqrt{1-\xi^2}$, two different sets of D partition boundaries* are obtained as shown in Figs. 5.4, 5.5, 5.6. To ensure maximum relative stability, σ and ξ are increased from minimum values of zero. It is found that the region with higher degree of relative stability goes on decreasing as σ and ξ are increased. Thus the regions with highest possible σ and ξ are obtained. Frequency scanning method is used to check the stability of a particular region with the relevant values of σ , α_1 , β_1 (or ξ , α_1 , β_1) and is shown in figs. 5.7, 5.8.

*Refer Appendix A.

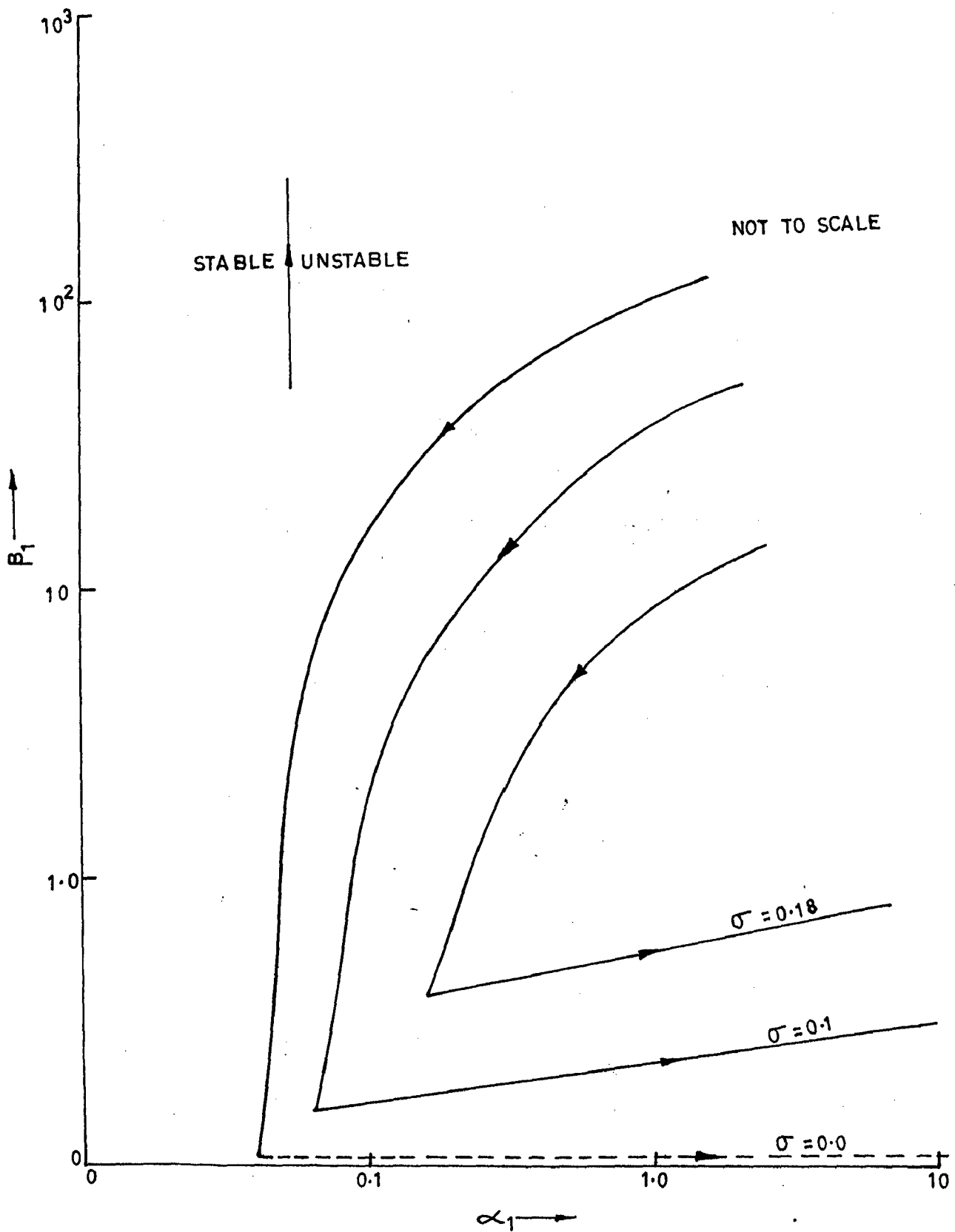


FIG.5.4 — D-PARTITION CURVE FOR CURRENT CONTROLLER WITH VARIATION IN σ

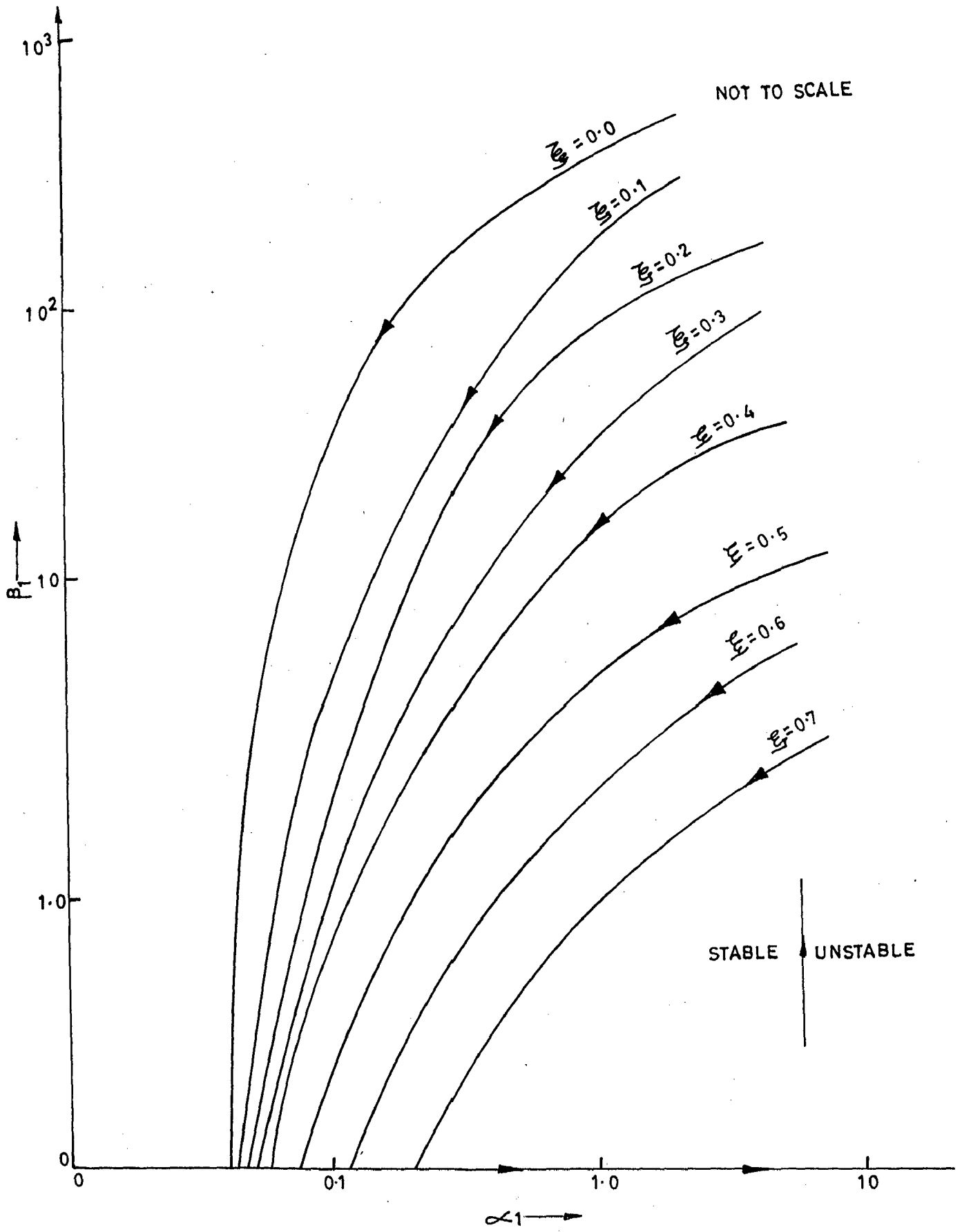


FIG. 5.5 - D-PARTITION CURVE FOR CURRENT CONTROLLER WITH VARIATION IN ζ

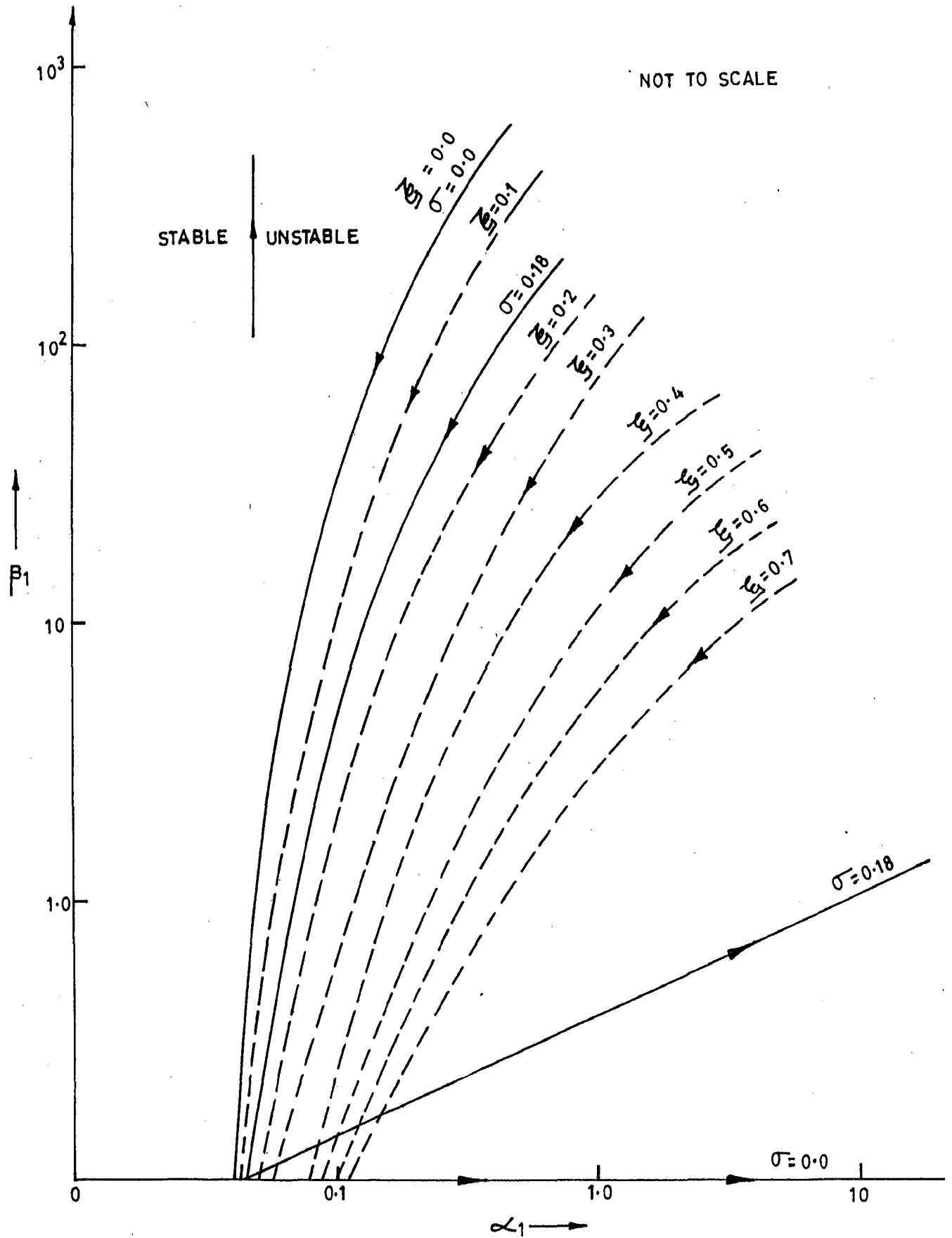


FIG. 5.6—COMBINATION OF FIGS. 5.4, & 5.5

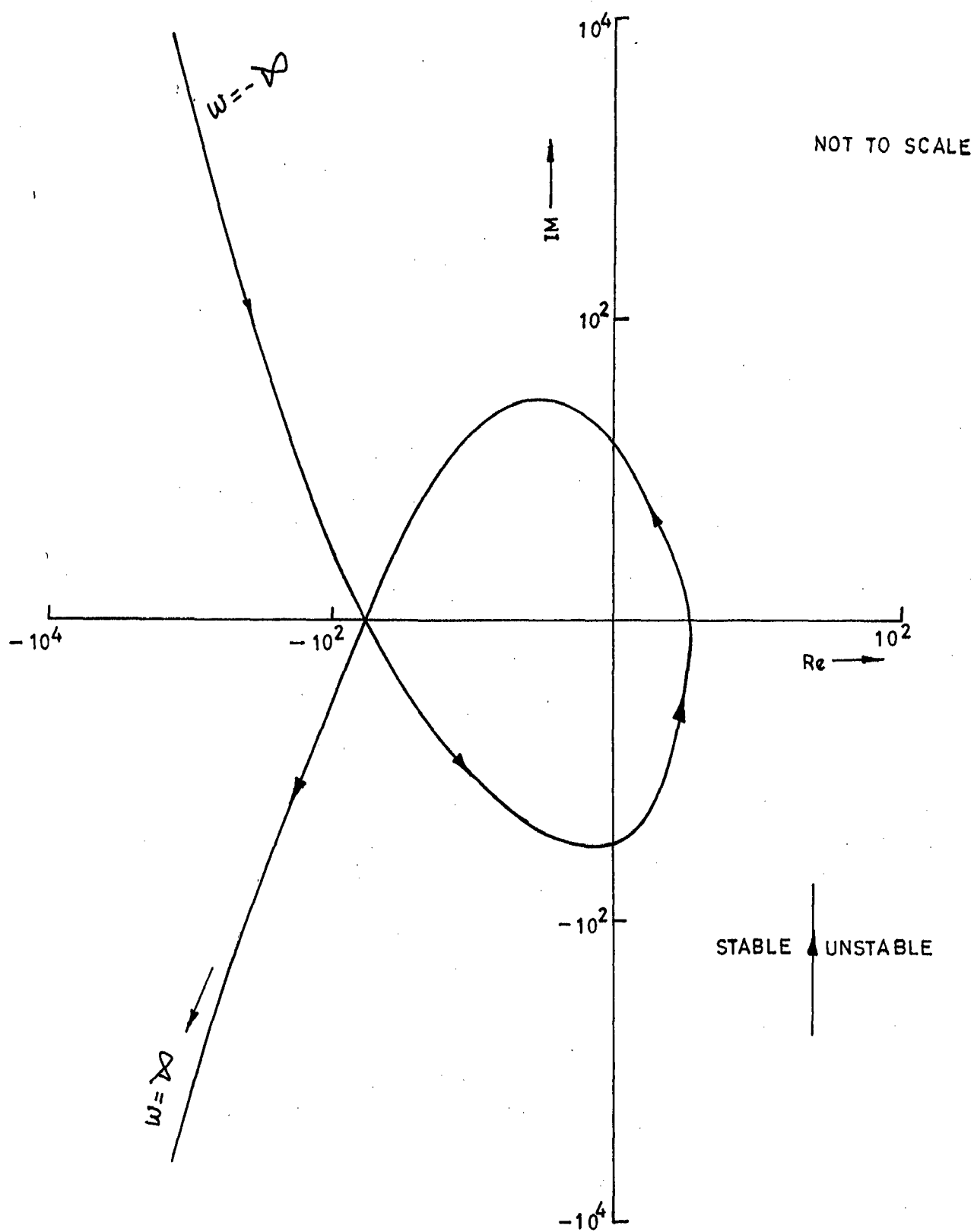


FIG.5.7-STABILITY CHECK FOR CURRENT CONTROLLER
 ($\sigma = 0.18$ $\alpha_f = 1.0$ $\beta_f = 10$)

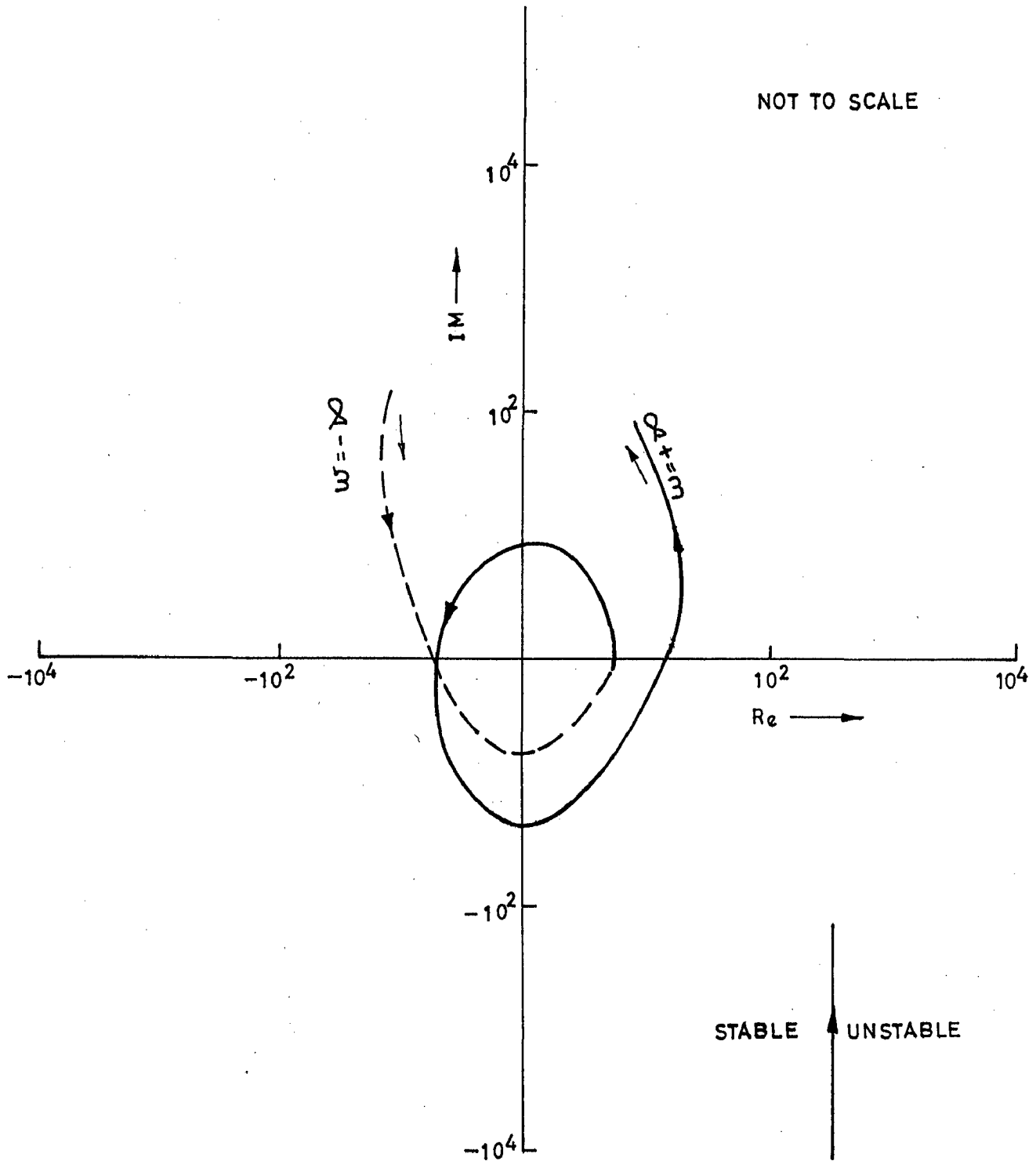


FIG. 5.8 - STABILITY CHECK FOR CURRENT CONTROLLER
 ($\xi = 0.9$, $\alpha_1 = 1.0$, $\beta_1 = 30.0$)

After ensuring the stability of the most probable stable region, the final selection of the two parameters (gain and time constant) are made comparing the time response of the current loop for a standard test signal (step) for different values of gains and time constants. The relevant computer programs for obtaining the D-partition boundary curves, frequency scanning check and the time response are given in Appendix D.

The state model of the current loop is now determined. The modified current loop is as shown in Fig. 5.9 wherefrom the state variables are selected as (Fig. 5.9),

$$V'_{Cl} = X_1$$

$$I_a = X_2$$

The reference current input (step), $I_R = 1.0$. From the block diagram of Fig. 5.9,

$$e_{Cl} = I_R - I^*$$

$$X_1 = \frac{K_1}{T_{Cl}s} * e_{Cl}$$

$$sX_1 = \frac{K_1}{T_{Cl}} * e_{Cl}$$

Taking the inverse Laplace transform

$$\frac{dx_1}{dt} = \frac{K_1}{T_{Cl}} * e_{Cl} \quad (5.16)$$

also
$$V_{Cl} = X_1 + e_{Cl}K_1$$

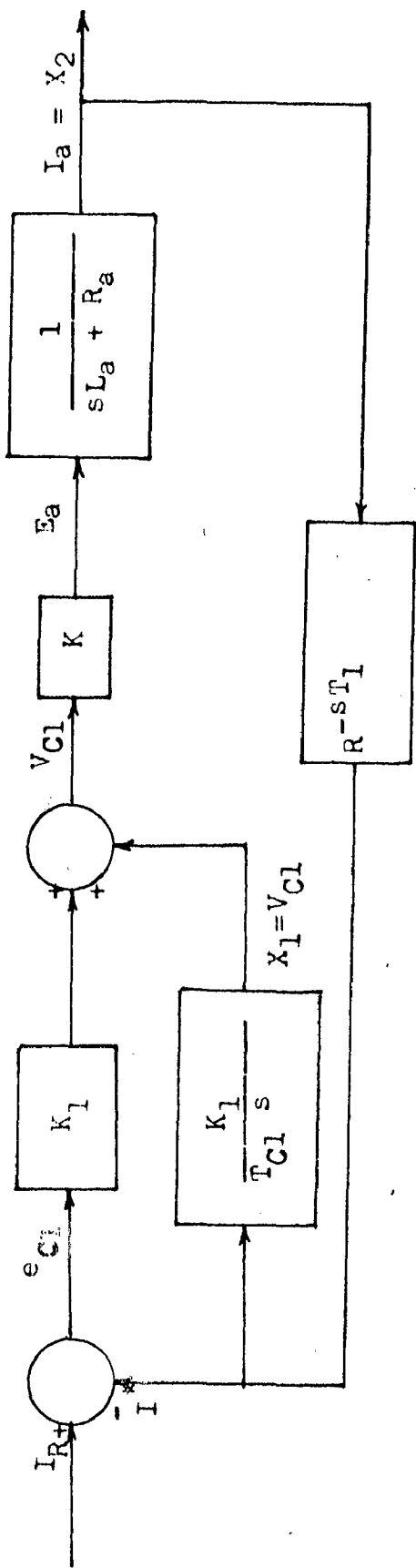


FIG. 5.9 BLOCK DIAGRAM OF CURRENT LOOP WITH ALL STATE VARIABLES

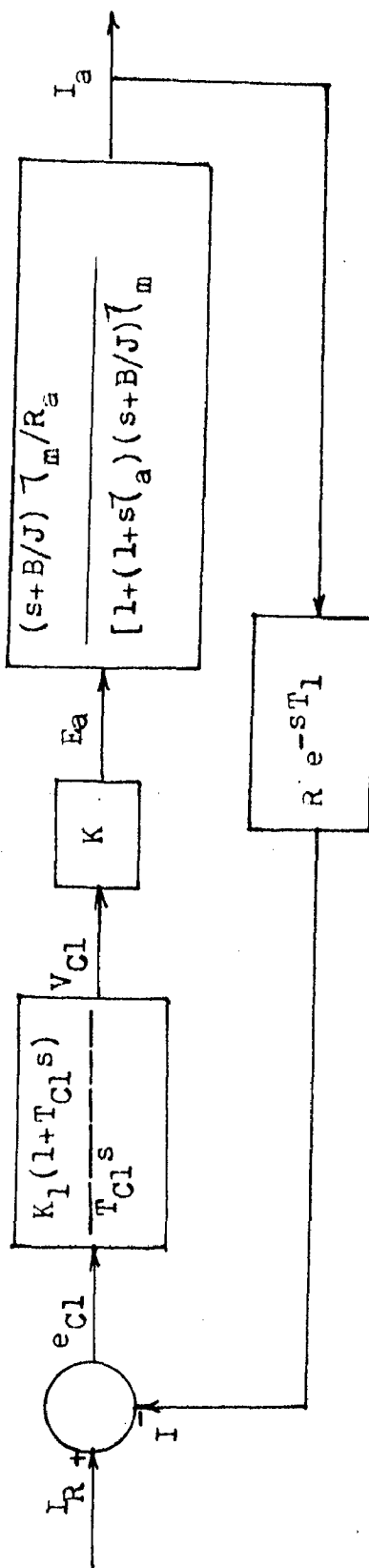


FIG. 5.14 BLOCK DIAGRAM OF CURRENT CONTROL LOOP

$$E_a = K * V_{C1}$$

$$X_2 = \frac{K}{(sL_a + R_a)} * V_{C1}$$

$$\text{or } sX_2 = (KV_{C1} - R_a X_2)/L_a$$

Taking the inverse Laplace transform

$$\frac{dX_2}{dt} = (K V_{C1} - R_a X_2)/L_a \quad (5.17)$$

Using the equations 5.16 and 5.17 the time response was computed and plotted for different values of K_1 and T_{C1} as shown in Fig. 5.10, 5.11, 5.12, 5.13.

Values $K_1 = 10$ and $T_{C1} = 0.025$ are chosen as with these values, the time response is close to the desired one.

5.4.2 Speed Controller

The transfer function of PI controller used for speed control is $K_2(1+T_{C2}s)/T_{C2}s$. The parameters K_2 and T_{C2} are to be designed using the same procedure that is used for the current loop. The inner current loop is reduced to a single block Fig. 5.14.

$$\text{T.F. of current loop} = G_1(s)/[1+G_1(s)H_1(s)]$$

$$\begin{aligned} \text{where } G_1(s) &= \frac{K_1(1 + \frac{1}{T_{C1}}s) \cdot K (s+B/J)\tau_m/R_a}{[1+(1+s\tau_a)(s+B/J)\tau_m]} \\ &= \frac{K_1(1+sT_{C1}) K (s+B/J)\tau_m/R_a}{sT_{C1} [1+(1+s\tau_a)(s+B/J)\tau_m]} = \frac{F_1(S)}{F_2(S)} \end{aligned}$$

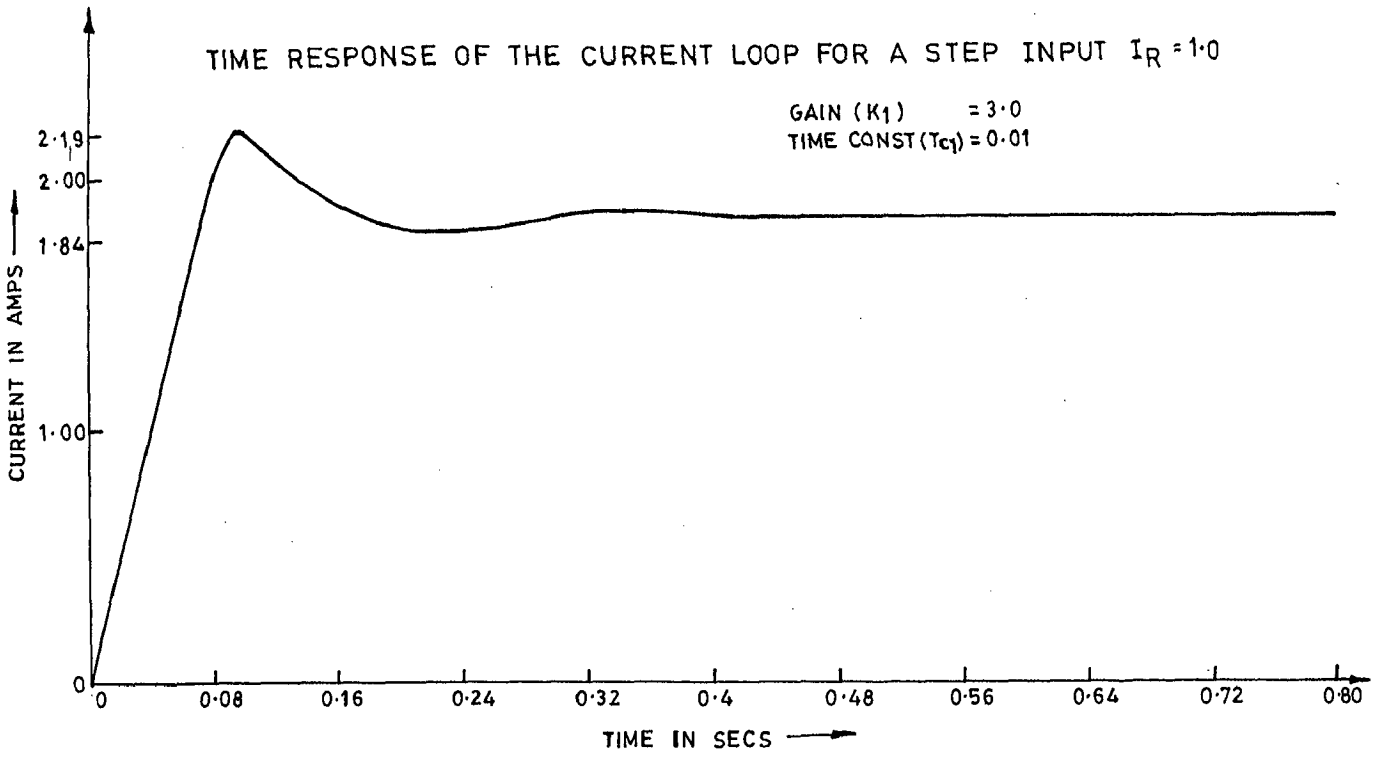


FIG. 5.10

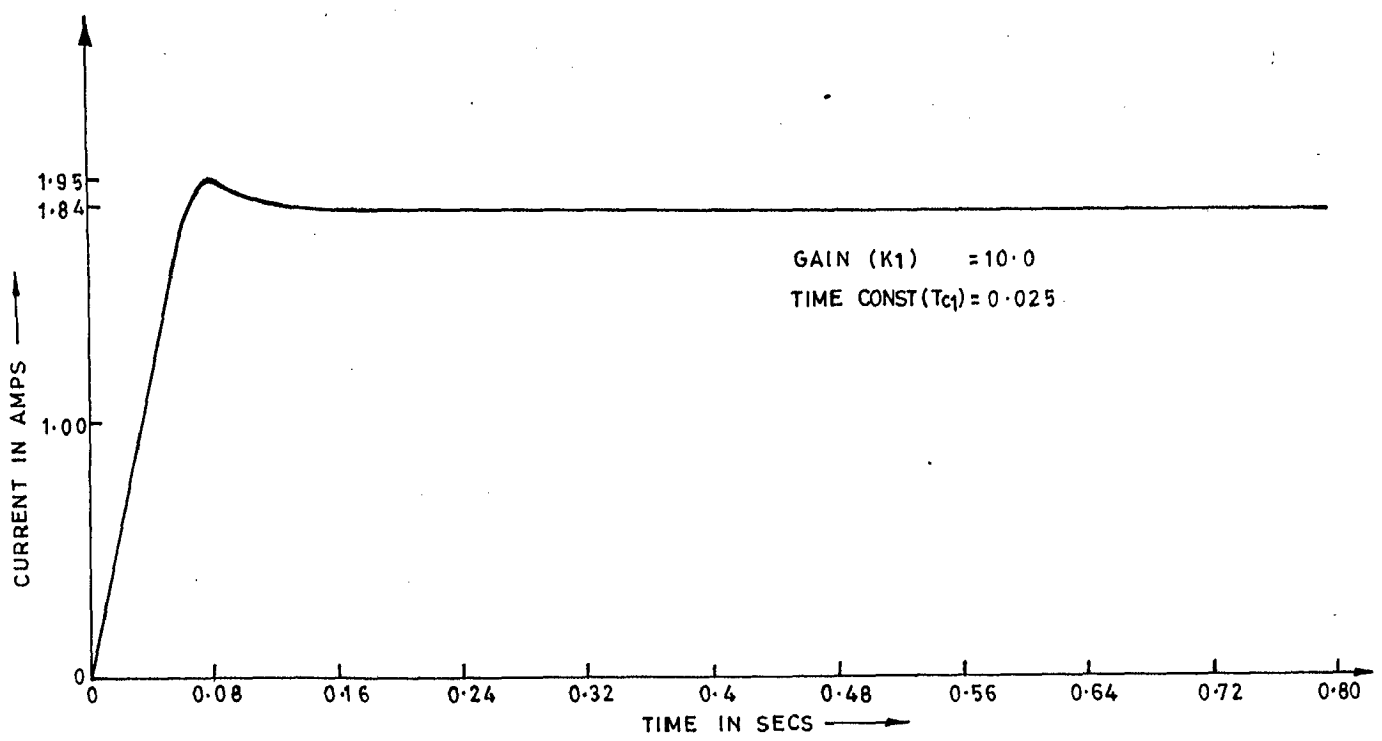


FIG. 5.11

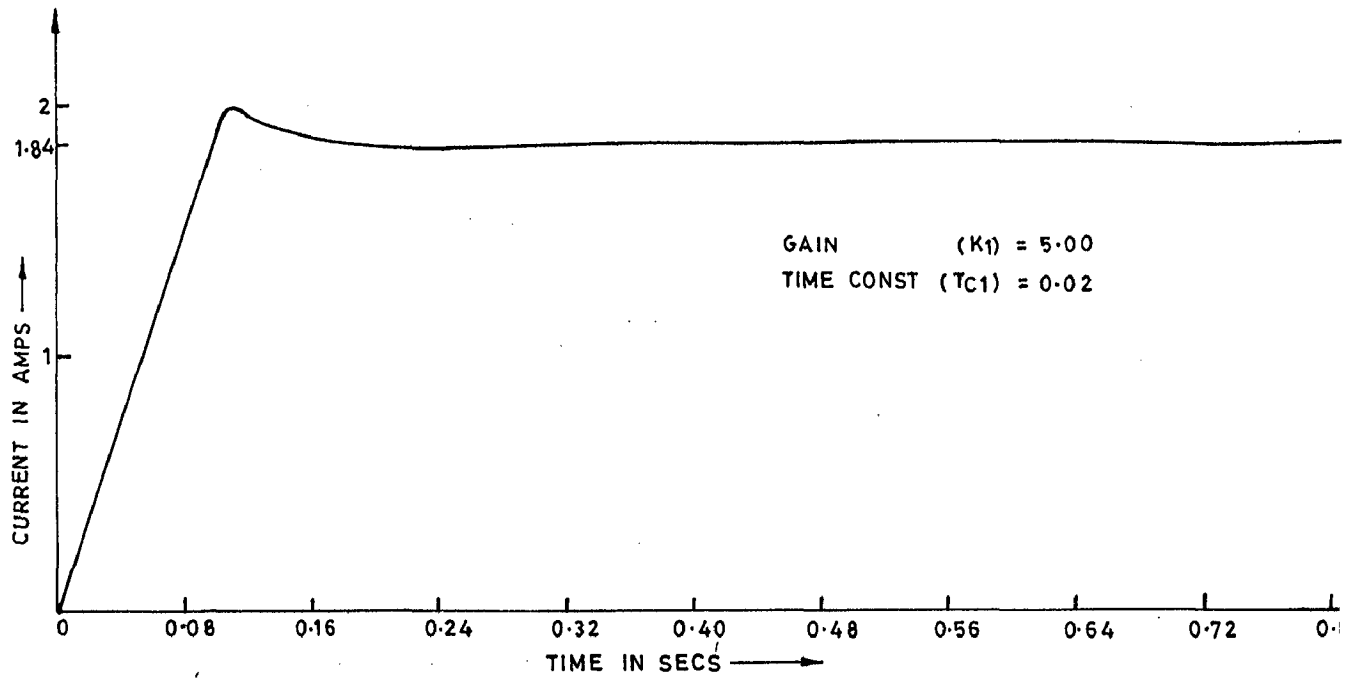


FIG. 5.12

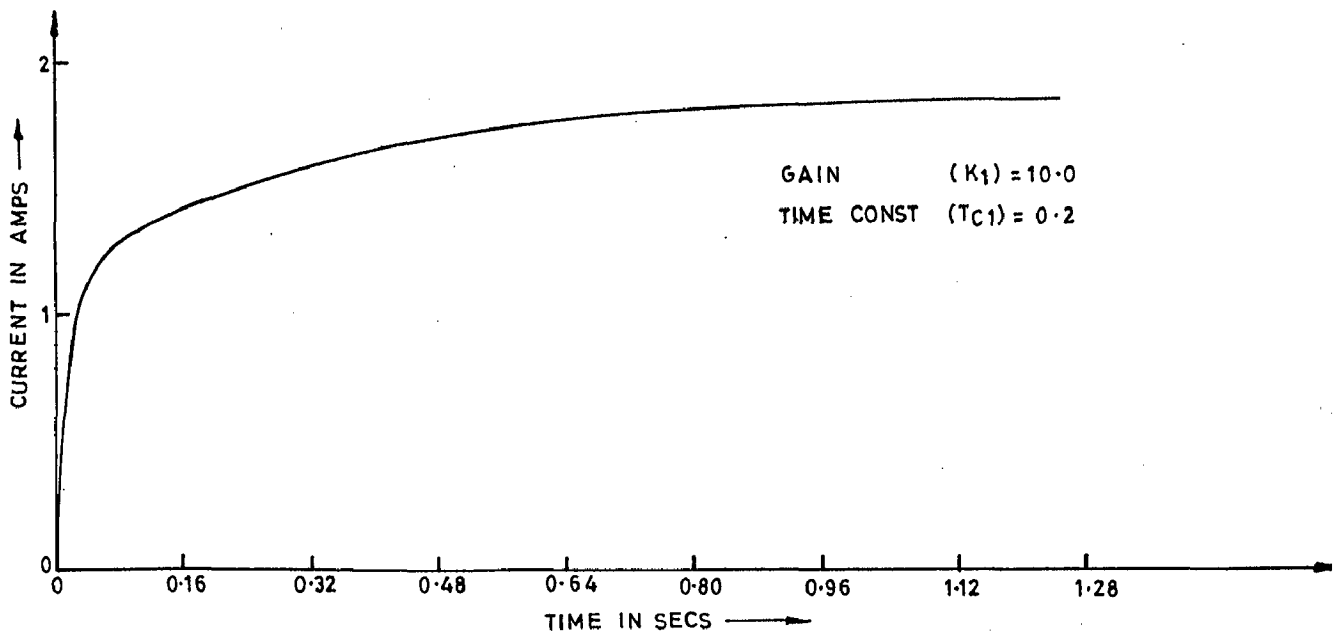


FIG. 5.13

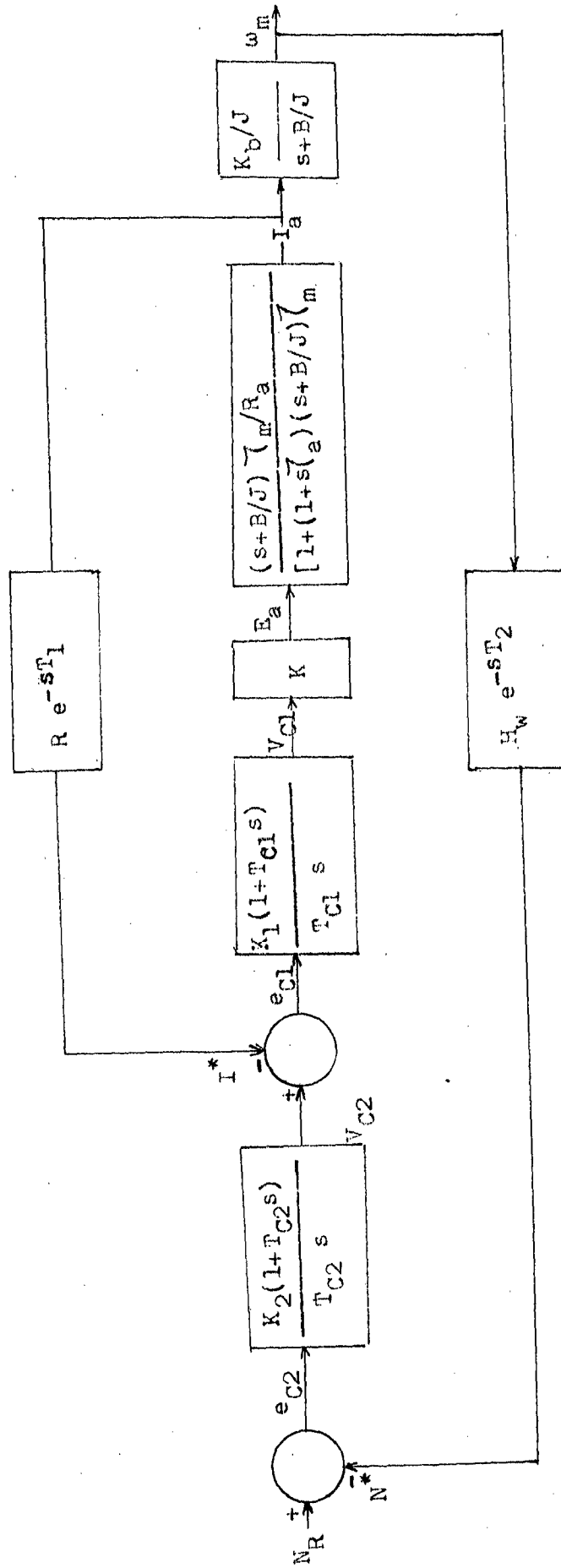


FIG. 5.14 SCHEMATIC BLOCK DIAGRAM

$$\text{and } H_1(s) = Re^{-sT_1}$$

$$\begin{aligned} \text{T.F. of current loop} &= \frac{F_1(s)/F_2(s)}{1 + \frac{1}{F_2(s)} Re^{-sT_1}} \\ &= \frac{F_1(s)}{F_2(s) + F_1(s) Re^{-sT_1}} \end{aligned}$$

Now the characteristic equation of the complete system is

$$1 + G'(s) H'(s) = 0$$

$$\text{where } G'(s) = K_2 \left(1 + \frac{1}{T_{C2}s}\right) \frac{F_1(s)}{[F_2(s) + F_1(s) Re^{-sT_1}]} \frac{K_b/J}{(s+B/J)}$$

$$\text{and } H'(s) = H_W e^{-sT_2}$$

$$\text{i.e. } 1 + K_2 \left(1 + \frac{1}{T_{C2}s}\right) \frac{F_1(s)}{[F_2(s) + F_1(s) Re^{-sT_1}]} \frac{K_b/J}{(s+B/J)} H_W e^{-sT_2} = 0 \quad (5.18)$$

$$\text{Let } F_3(s) = F_1(s) (K_b/J) H_W e^{-sT_2}$$

$$F_4(s) = (F_2(s) + F_1(s) Re^{-sT_1}) (s+B/J)$$

$$\alpha_2 = 1/K_2 \quad \text{and}$$

$$\beta_2 = 1/T_{C2}$$

Eq. 5.18 can be written as

$$1/K_2 + \left(1 + \frac{1}{T_{C2}s}\right) \frac{F_3(s)}{F_4(s)} = 0$$

$$\text{i.e. } \alpha_2' s F_4(s) + \beta_2' F_3(s) + s F_3(s) = 0$$

As before, with this basic equation, the two sets of D-partition boundaries are drawn and the most probable

stable region is determined (Figs. 5.15, 5.16, 5.17). By frequency scanning method the stability is checked (Fig.5.18)

and the time response for a step input is plotted for different values of gains and time constants (Figs. 5.19, 5.20, 5.21, 5.22). Values $K_{C2} = 0.021$ and $T_{C2} = 0.1$ are chosen as with these values, the time response obtained closely meets the desired time specifications.

5.5 up Translation of the Controller Parameters

5.5.1 Speed Controller

As already given (Fig. 5.3), the speed controller is represented as $[K_2 e_n + \frac{K_2}{T_{C2}s} e_n]$. This is realised in the actual set up by using up as $K_{PS} \Delta e_n + K_{IS} e_{n-1}$. Hence, the Proportional Constant $K_{PS} = K_2$ and the Integral Constant $K_{IS} = \frac{K_2}{T_{C2}} \cdot T_2$, where $T_2 = 0.245$ with the values chosen (previous section), $K_{PS} = 0.021$ and $K_{IS} = 0.05$.

5.5.2 Current Controller

As already given (Fig. 5.3),* the current controller is represented as $[K_1 e_I + \frac{K_1}{T_{C1}} e_I]$. Again, this is realised in the actual set up by means of up as, $K_{PI} \Delta e_n + K_{II} e_{n-1}$, where all the quantities are in HEX numbers. As the actual current (Analog signal) fed back to the up is in HEX (via ADC), suitable conversion is necessary to convert A_{K1} and T_{C1} to get K_{PI} and K_{II} and is given as follows

$$E_{a_n} = K_1 \left[1 + \frac{1}{T_{C1}s} \right] [R I_R - R I_a e^{-sT_1}]$$

$$= R \cdot K_1 \left[(e_n) - \frac{K_1}{T_{C1}} \int_{-\infty}^n e_n dt \right] \text{ and}$$

*Refer Section 4.2 also.

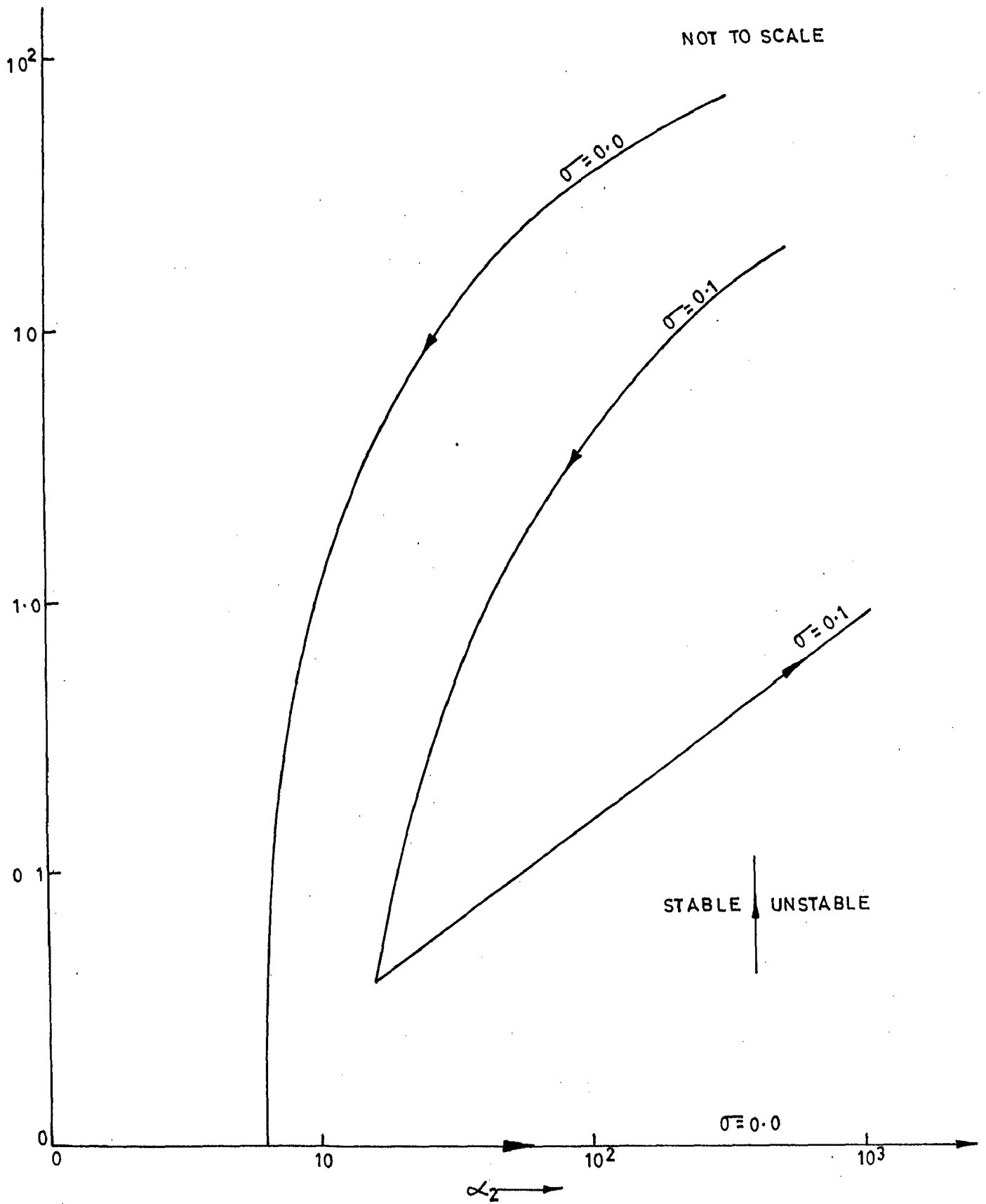


FIG. 5.15—D-PARTITION CURVE FOR SPEED CONTROLLER WITH VARIATION IN σ

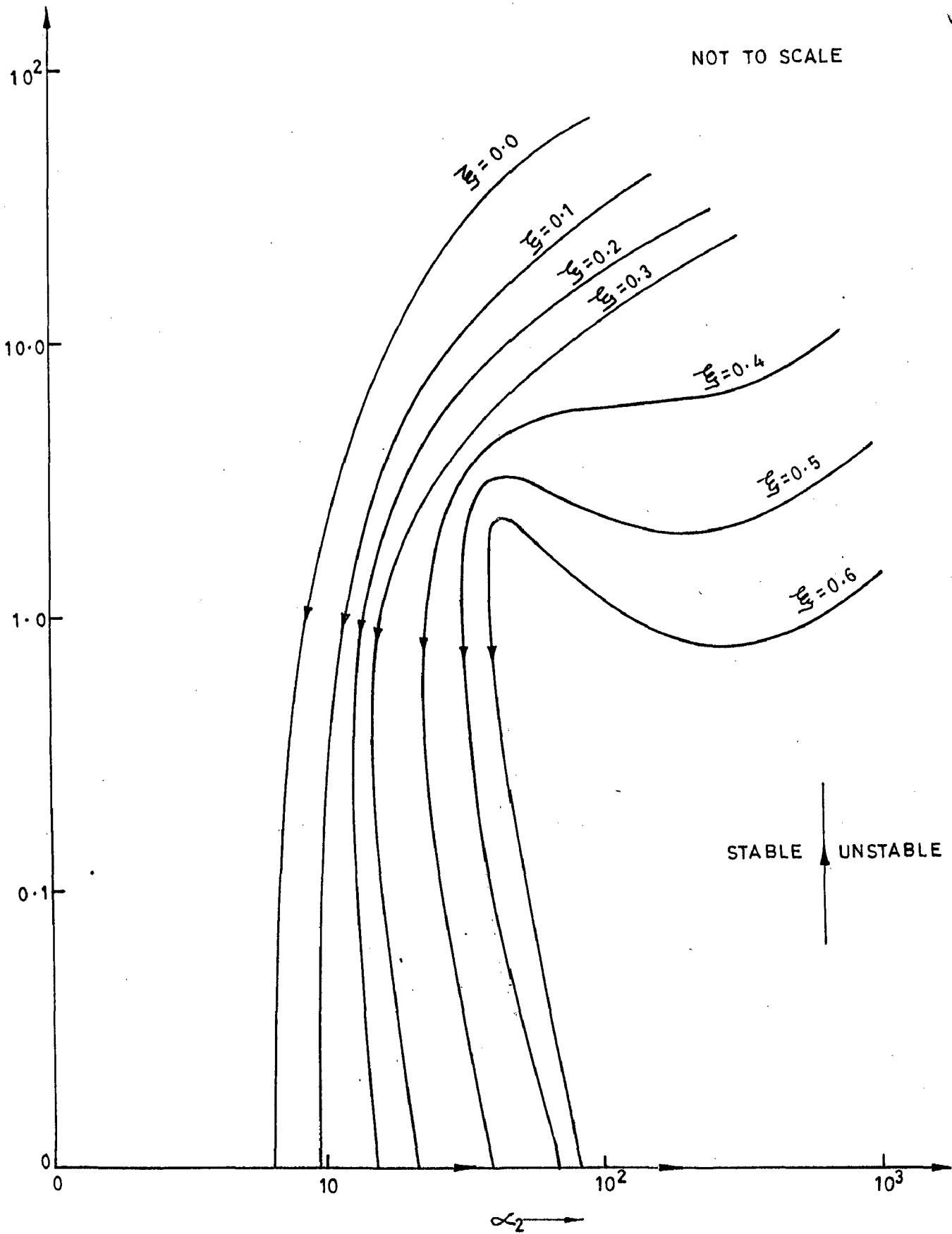


FIG.5-16 - D-PARTITION CURVE FOR SPEED CONTROLLER WITH THE VARIATION IN ξ

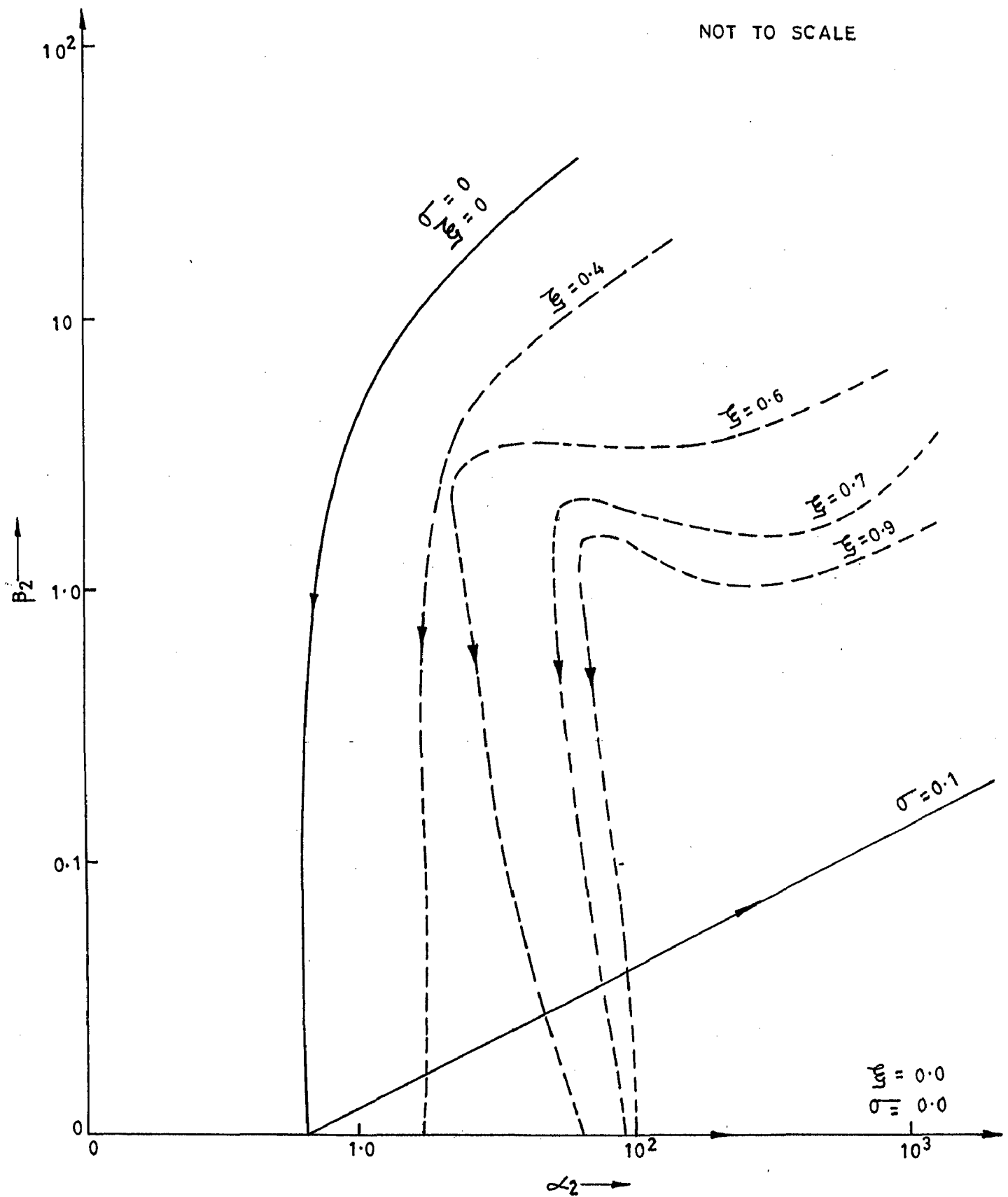


FIG. 5.17—COMBINATION OF FIGURES 5.15 & 5.16

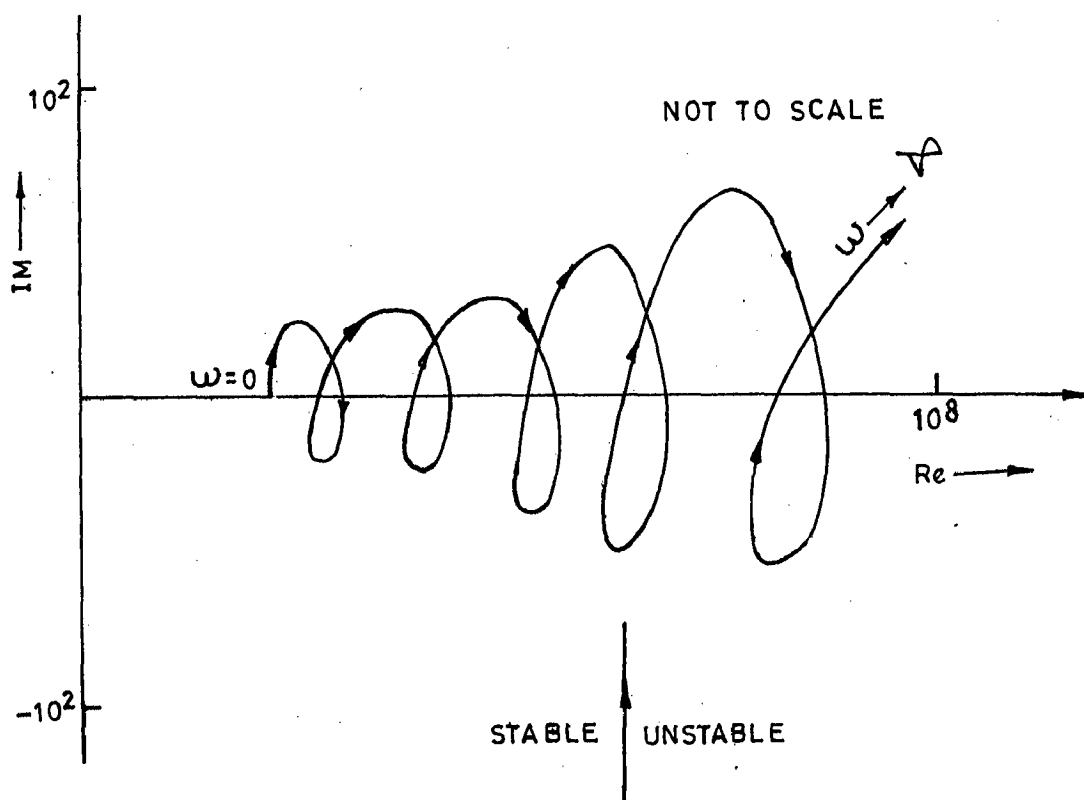


FIG. 5.18—STABILITY CHECK FOR SPEED CONTROLLER

$$\sigma = 0.1 \quad \alpha_2 = 10 \quad \beta_2 = 20$$

$$\xi = 0.1 \quad \alpha_2 = 10 \quad \beta_2 = 20$$

TIME RESPONSE OF SPEED LOOP FOR A STEP INPUT OF
SPEED $N_R = 200 \text{ RPM}$
 $= (20.91 \text{ RADS/SEC})$

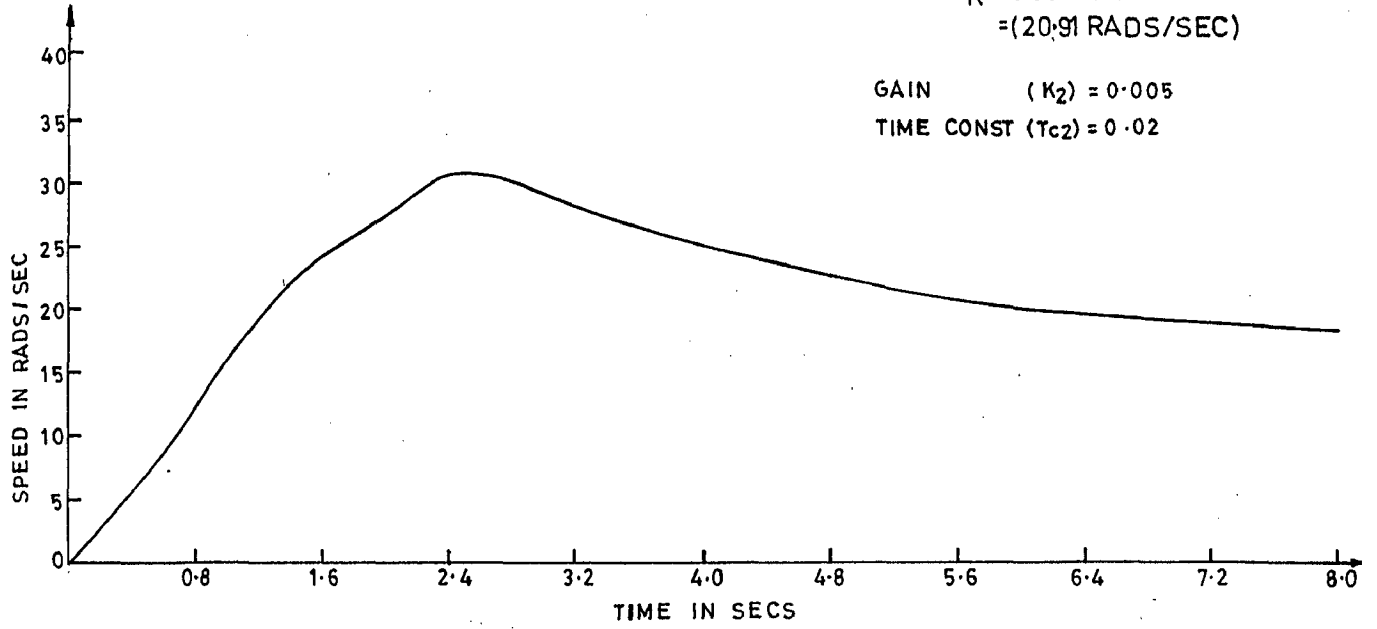


FIG. 5-19

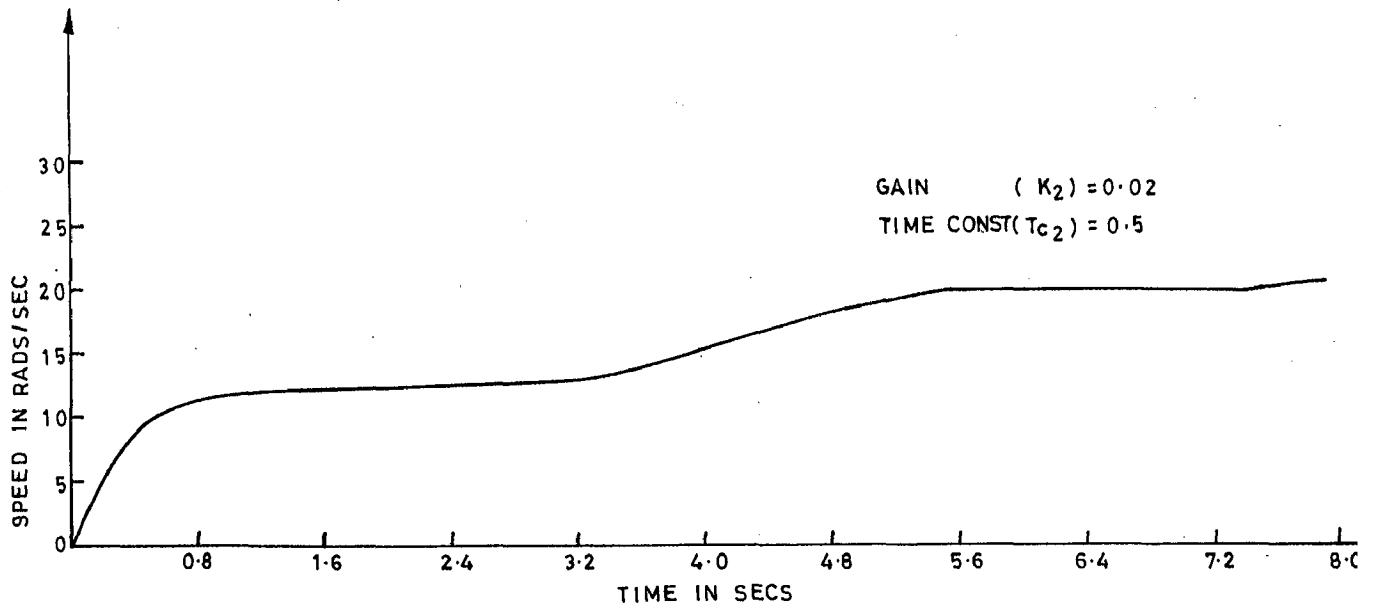


FIG. 5-20

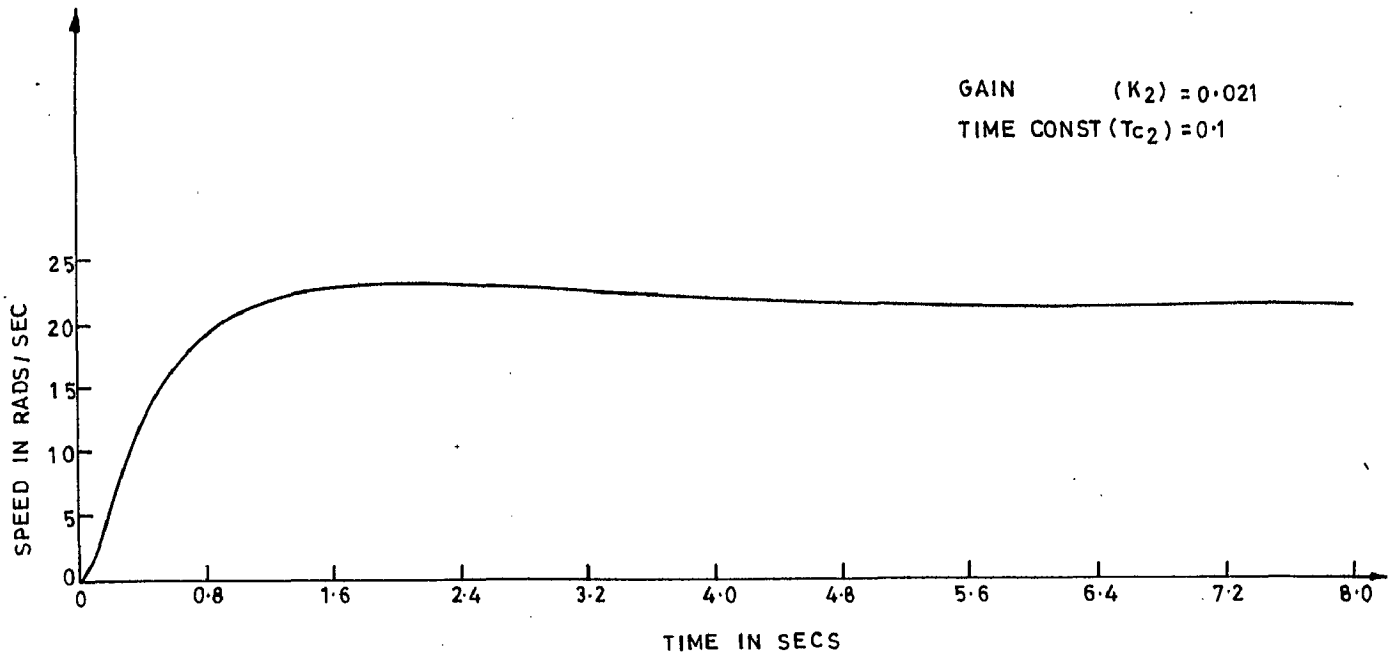


FIG. 5.21

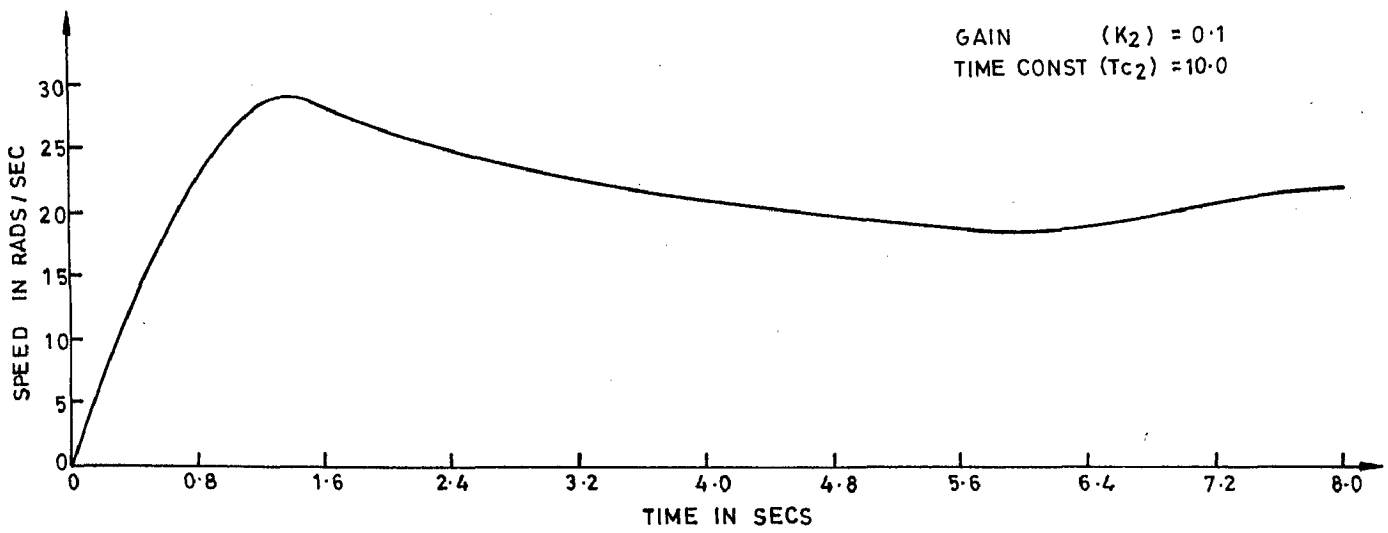


FIG. 5.22

$$E_{a_{n-1}} = K_1 [(e_{n-1}) - \frac{K_1}{T_{Cl}} \int_{-\infty}^{t_{n-1}} e_{n-1} dt]$$

$$\dots E_{a_n} - E_{a_{n-1}} = K_1 \Delta e_n + \frac{K_1}{T_{Cl}} e_n \cdot T_1$$

Where E_{a_n} = Current error at the n^{th} sampling instant in volts

$E_{a_{n-1}}$ = Current error at the $(n-1)^{\text{th}}$ sampling instant in volts

$$e_n = [RI_R - RI_a e^{-sT_1}] = R[I_R - I^*] \text{ in volts and}$$

$$\Delta e_n = [e_n - e_{n-1}]$$

$$T_1 = \text{sampling time of current loop} = 0.01 \text{ secs}$$

Converting all these values into numbers (in terms of COUNT),

$$\text{We have, } E = \frac{T_{ON}}{T_{ON} + T_{OFF}} V_{dc}$$

$$\Delta E = \frac{\Delta T_{ON}}{T_{CH}} V_{dc} = 220 \times \frac{\Delta T_{ON} \text{ sec}}{T_{CH} \text{ sec}}$$

$$\dots 220 \frac{\Delta T_{ON}}{T_{CH}} = R \cdot \frac{5}{256} [K_1 \Delta e_n + K_1 \left(\frac{T}{T_{Cl}}\right) e_n]$$

where, ΔT_{ON} , T_{CH} , Δe_n are all in COUNT and T , T_{Cl} are in secs.
as 5V represents 256 H in COUNT

$$\begin{aligned} \dots \Delta T_{ON} &= R \cdot \frac{T_{CH}}{220} \times \frac{5}{256} [K_1 \Delta e_n + \frac{K_1}{T_{Cl}} 0.01 e_n] \\ &= 0.5412 \times \frac{7675}{220} \times \frac{5}{256} [K_1 \Delta e_n + \frac{K_1}{T_{Cl}} (0.01) e_n] \\ &= 0.368 [K_1 \Delta e_n + \frac{K_1}{T_{Cl}} (0.01) e_n] \end{aligned}$$

With the designed values of $K_1 = 10.0$ and $T_{Cl} = 0.025$

the values $K_{PI} = 3.68$ and $K_{II} = 1.47$.

5.6 Conclusions

In this chapter, the transfer function of various elements are given. The theoretical studies are carried out with these transfer functions to design the values of the parameters of the controllers. The theoretically designed values are converted suitably into μp language.

CHAPTER 6

PERFORMANCE OF THE DRIVE SYSTEM

6.1 Introduction

This chapter deals with the experimental performance evaluation of the drive system. The performance of the drive system is determined based upon the performance characteristics, namely, (i) speed, (ii) current and (iii) % efficiency Vs output power of motor at different speed settings. The performance characteristics are plotted based on the results of the load test. The performance characteristics of the natural system (natural characteristics), μ p controlled open loop system and the μ p controlled closed loop system are plotted in order to draw a comparison between them. Theoretical determination of the parameters of the controllers are already described in chapter 5. However, during experimentation, these parameters were varied over a range and those parameters which gave best performance under the transient and steady state conditions were chosen for the load test of the μ p controlled system. The Table 6.1 shows the effect of the variation of the controller parameters upon the performance of the drive system.

6.2

Load test on the μ p controlled drive system

With the gain factors of the drive, as per theoretically determined values, the μ p controlled closed-loop drive

TABLE 6.1

N_{RPM}	K_{PS}	K_{IS}	K_{PI}	K_{II}	N_{RPM}^*		N_{av}^* RPM
					LOWER	UPPER	
500	0.1	0.1	06	05	450	550	500
	0.2	0.1	08	05	475	525	500
	0.5	0.1	10	05	475	500	488
500	0.2	0.2	04	02	450	550	500
	0.2	0.5	04	02	450	550	500
	0.2	0.5	04	04	475	525	500
	0.2	0.5	04	06	475	550	513
500	0.2	0.5	06	02	475	500	488
	0.2	0.5	06	04	455	520	488
	0.2	0.5	06	06	475	525	500

resulted in speed oscillations. Hence the gain values were experimentally adjusted about the theoretical value. At certain optimal setting, the speed oscillations were minimum with average speed close to the reference speed. For load test on closed-loop system such a set of gains was selected.

For conducting the load test, the values of the parameters of the controllers chosen are $K_{P_S} = 0.2$, $K_{I_S} = 0.5$, $K_{P_I} = 0.6$ and $K_{I_I} = 0.2$ as with these values, the oscillations in speed were minimum (Table 6.1). The load test was carried for different values of the reference speed settings, i.e. 100% (1000 rpm), 75% (750 rpm) and 50% (500 rpm) of the rated speed. Figs. 6.1, 6.2 and 6.3 show the speed Vs output power of the motor. From Fig. 6.1 it is seen that for the natural system, the speed drops from 1000 rpm to 930. For load variation from no load to 0.75 of the rated power output (for a 2 HP m/c, the rated output is $2 \times 735.5 = 1470$ watts).

For open loop μp controlled system, the speed drops from 1000 rpm to 675 rpm for the same load variation. For the μp controlled closed loop system, the speed was constant at 975 rpm irrespective of the variation in the load, exhibiting a steady state error of about 25 rpm. During this test, the total excitation was constant (fed from the rectifier output at $V_{dc} = 220V$) at $I_f = 0.8A$.

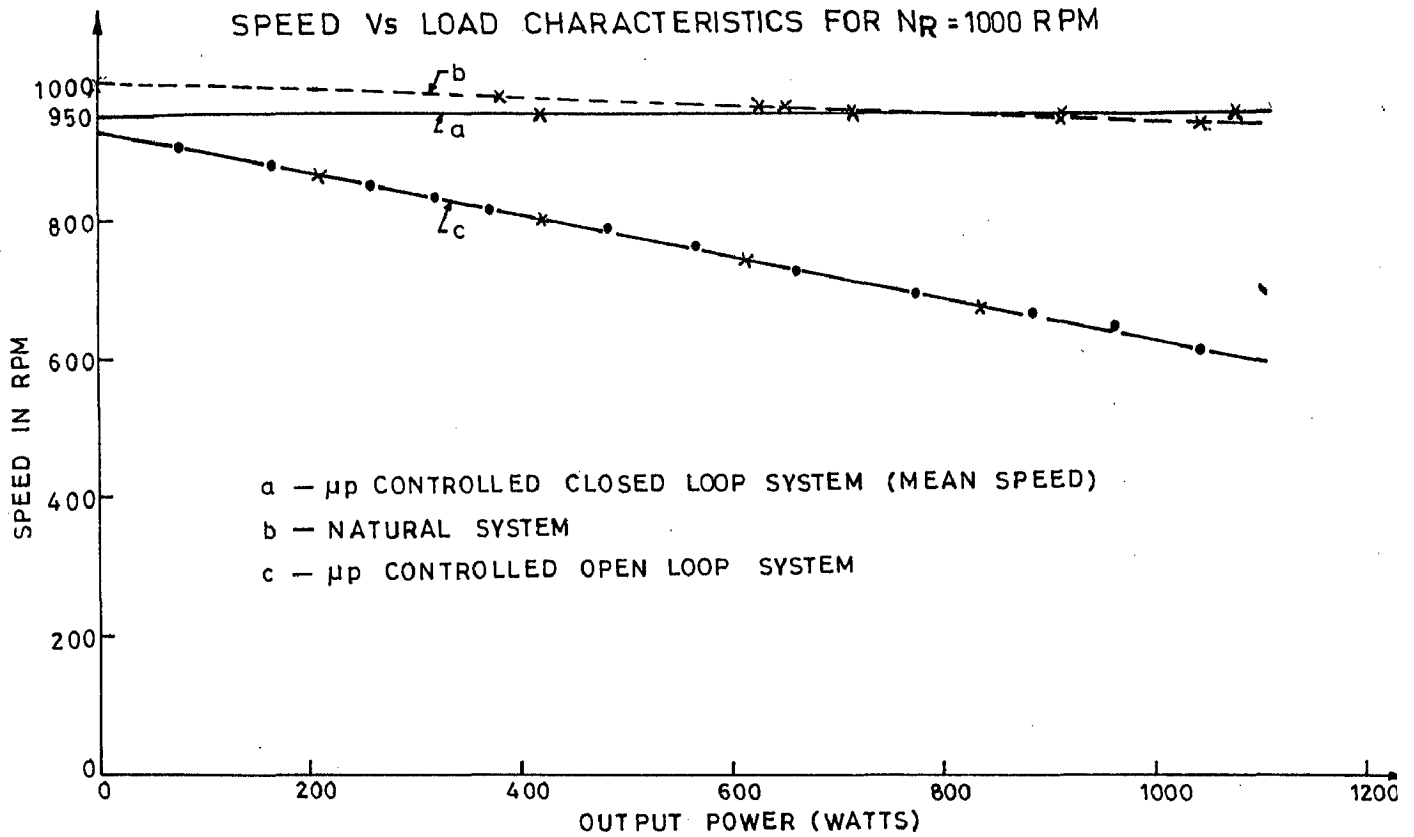


FIG. 6.1

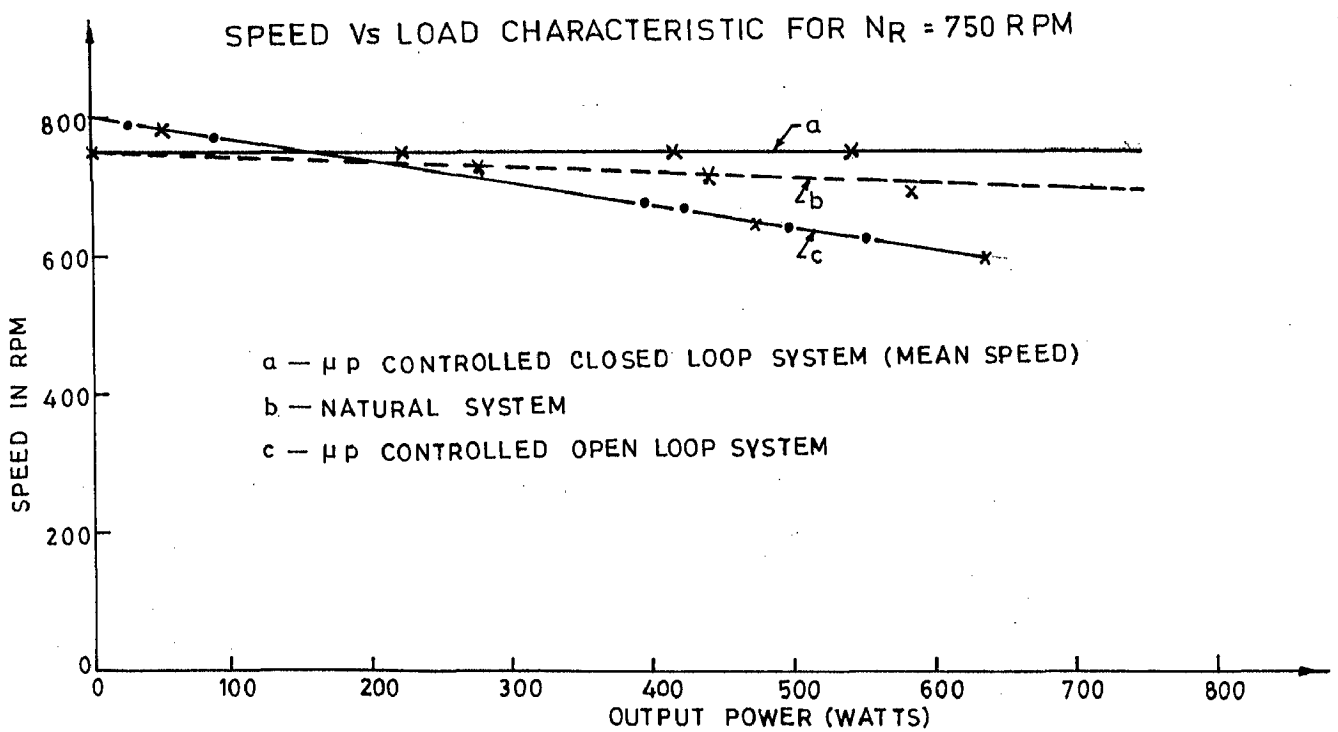


FIG. 6.2

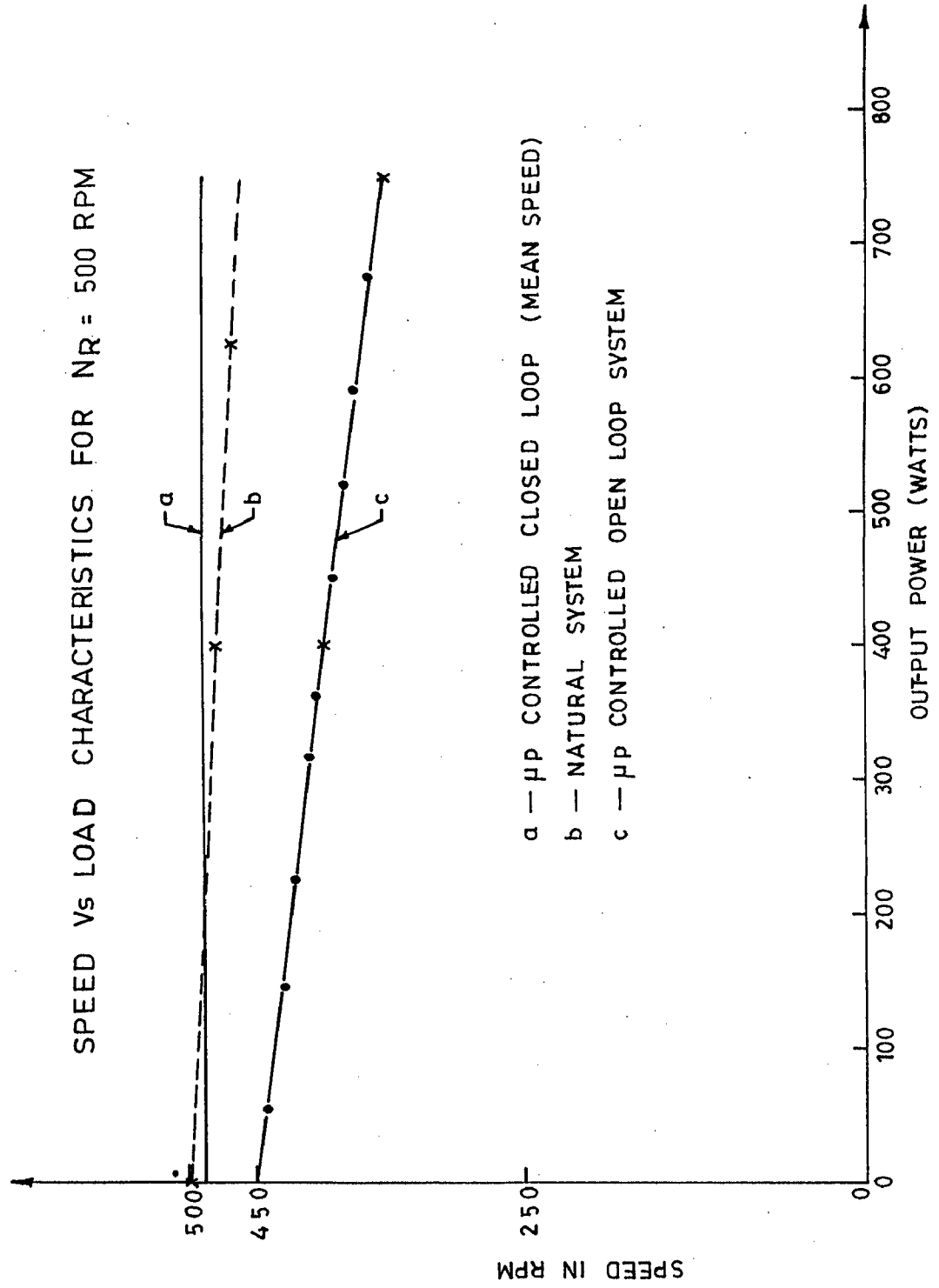
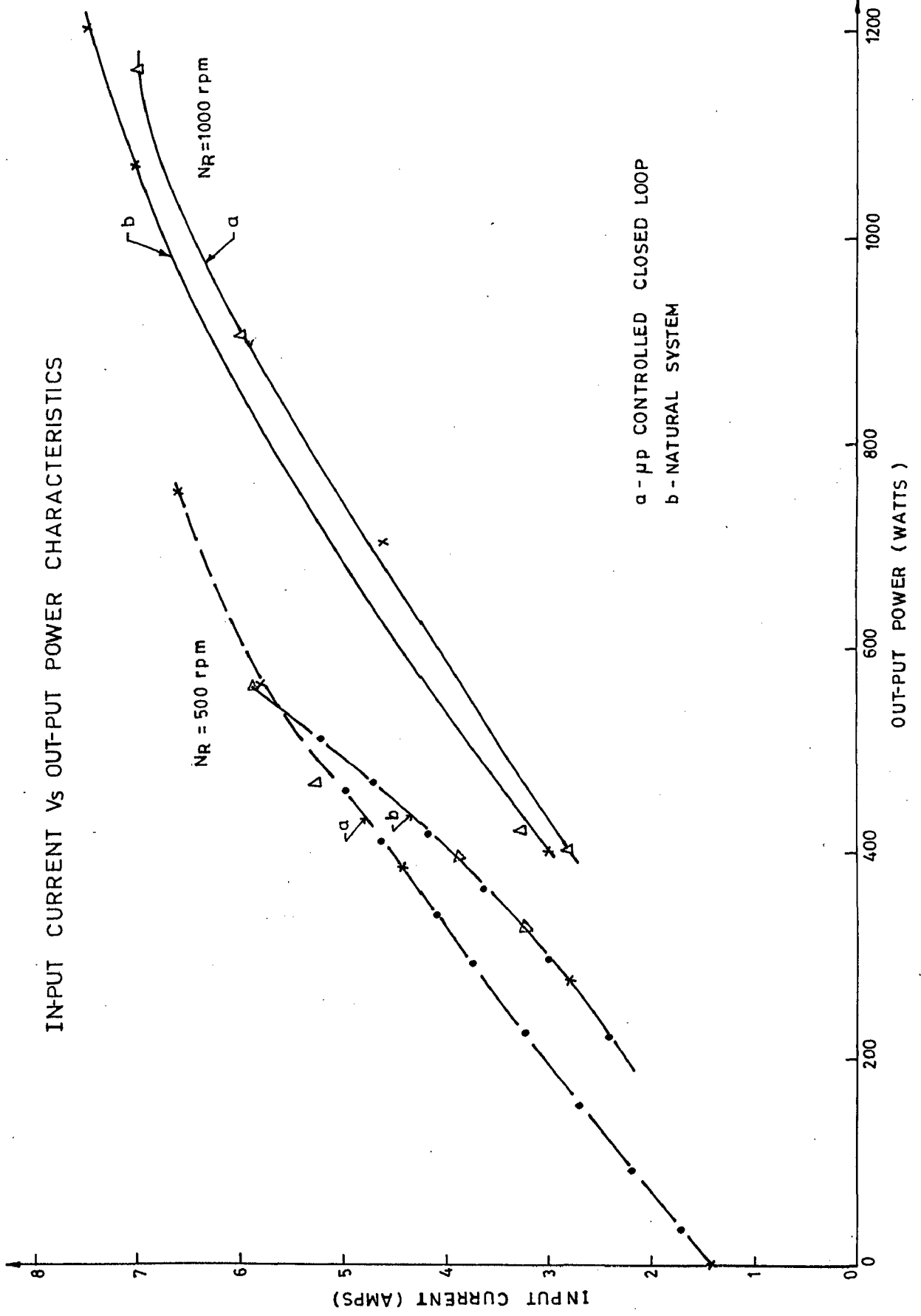


FIG. 6.3

Almost similar results were obtained for other speed settings also for natural system and the μ p controlled open loop system. However, for the μ p controlled closed loop system, there were oscillations in the speed of about 25 rpm (at lower speed settings) and 50 rpm (at higher speed settings). The above figures show the average value of the speed for this case.

With regard to the Input current Vs output power behaviour at any initial speed setting, the characteristics obtained (Fig. 6.4) for all the three systems were nearly the same, But in the μ p controlled closed loop system, the input current drawn from the supply was oscillating about a mean value. This was true for all the different speed settings. Also that, the input current was slightly less for the μ p controlled closed loop system for certain load condition. This is because the μ p controlled closed loop system maintained near constant machine speed with gradual increase in armature voltage to compensate for armature drop. Hence for same power output, the input current can be less. This behaviour is noted at high reference speed settings.

As far as the % efficiency ($\% \eta$) Vs output power relationship is concerned, the % efficiency was higher at higher speed settings and lower at lower speed settings as is expected of any drive system. This was true for



a - μp CONTROLLED CLOSED LOOP
 b - NATURAL SYSTEM

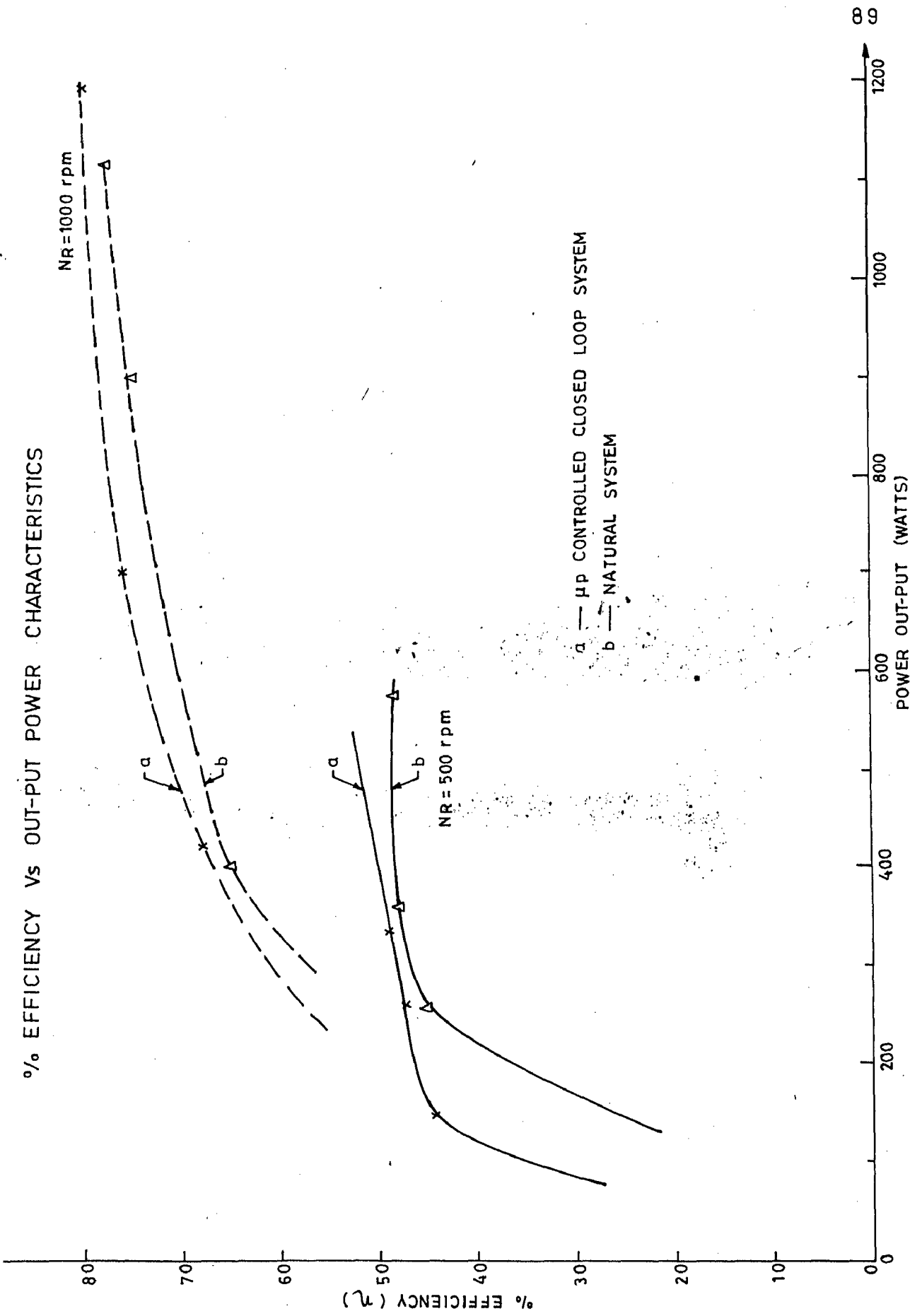
FIG. 6-4

all the three systems. However, for the μp controlled closed loops system, $\% \eta$ was higher compared to the other two systems (Fig. 6.5). The load test at different speed settings was carried out by having a resistance in series with the armature circuit and adjusting it at every load to feed a constant dc voltage across the armature, for the natural system. However, for η calculation losses in this series resistance are not included. The field in each case was excited by a constant voltage ($I_f=0.8A$).

6.3 Performance oscillograms

Photographs of various waveforms are shown in Fig. 6.6. (a-k). Figs. 6.6 (a-d) show the load voltage waveforms (upper) and load current (lower) at different instants, when the drive is first started by means of smooth start SR. We can see, that T_{on} is slowly increased from $T_{ON MIN}$ to $T_{ON DES}$ to bring the drive upto the reference speed which was 600 rpm in this case. Photograph 6.6 (e-f) show the same waveforms, when the drive is running in closed loop for $N_R=600$ rpm. The speed oscillations are due to the variation in T_{ON} which is easily seen in the photograph. Fig. 6.6g shows how the speeder pulses are properly wave shaped. Fig. 6.6h shows the filtering of the armature current before being given to the ADC. Fig. 6.6i shows the voltage across capacitor and TH1. Fig. 6.6j shows the firing pulses used to trigger

% EFFICIENCY VS OUT-PUT POWER CHARACTERISTICS



a — 1/2 HP CONTROLLED CLOSED LOOP SYSTEM
 b — NATURAL SYSTEM

FIG. 6.5

80
1200
1000
800
600
400
200
0

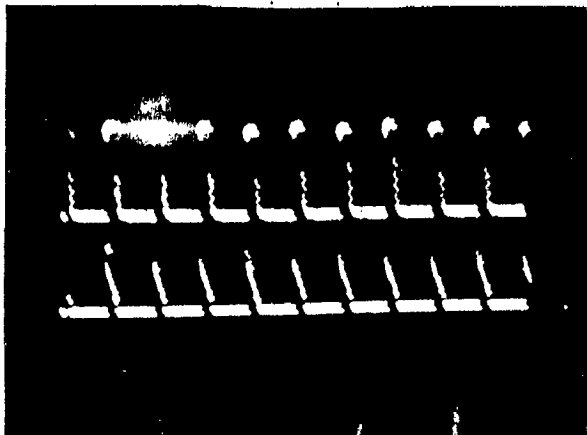
% EFFICIENCY (η)

POWER OUT-PUT (WATTS)

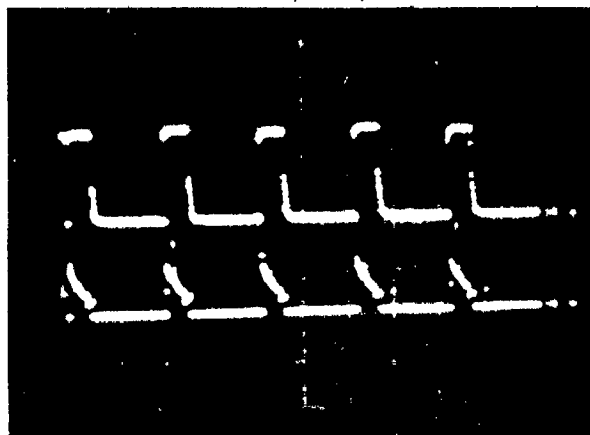
Photographs of the various waveforms

Scale upper channel 100 V/cm, lower channel 100 mv/cm

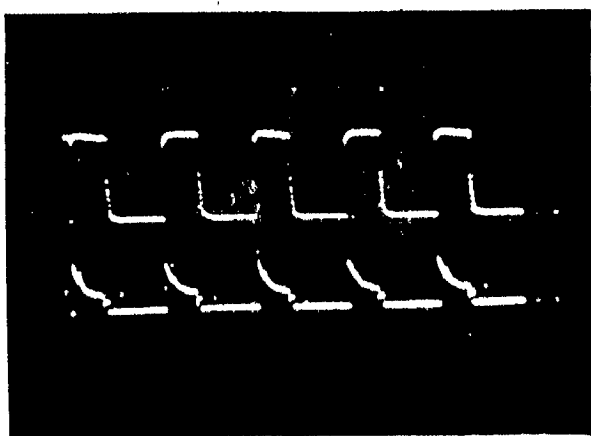
Time scale 0.1 sec/cm



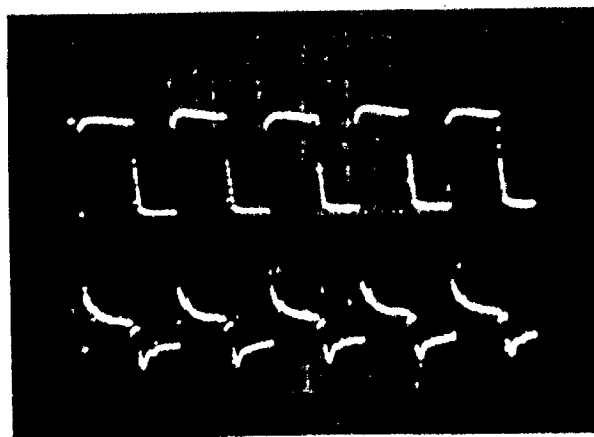
a) at the beginning of
smooth start
 $T_{ON} = T_{ON MIN}$



b) at an intermediate
instant

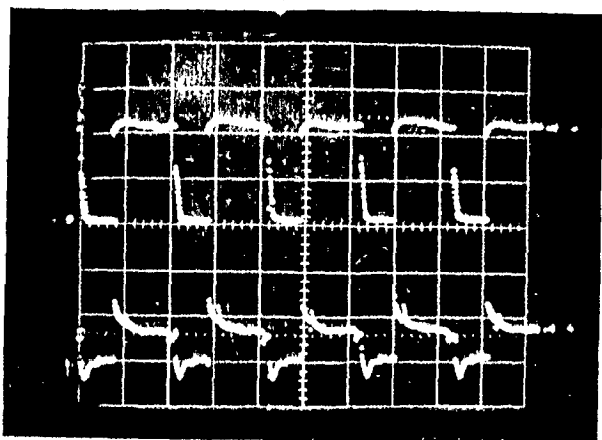


c) at an intermediate instant

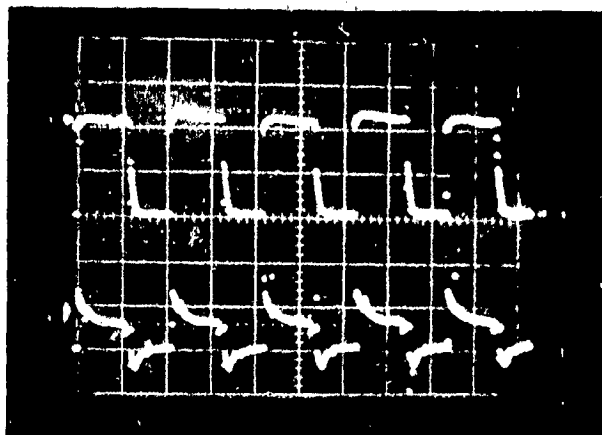


d) towards the end
 $T_{ON} = T_{ON DES}$ 60% duty cycle

Fig. 6.6 Load voltage (upper channel) and load current (lower channel) waveforms at different instants of smooth start for $N_R = 600$ rpm

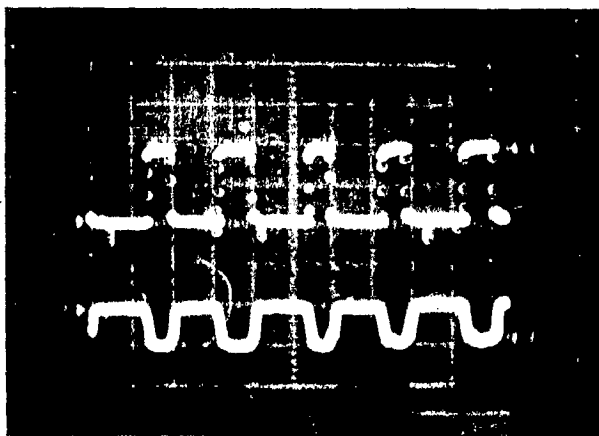


e) Instant at which speed oscillation is maximum

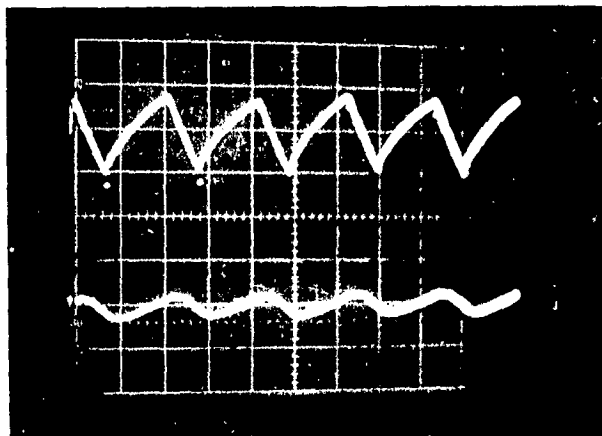


f) Instant at which speed oscillation is minimum

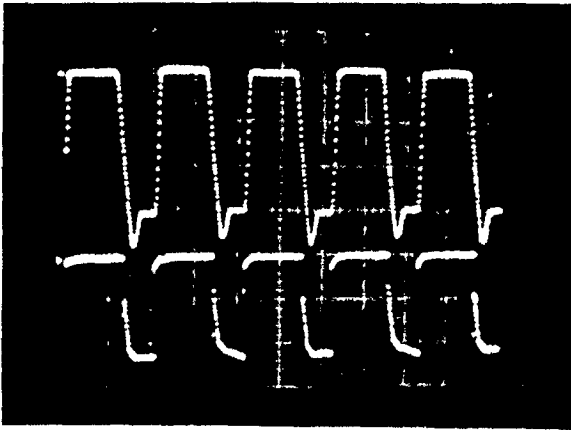
During the closed loop operation for $N_R=600$ rpm, $I_M=5A$



g) speeder pulses
 upper-after wave shaping
 scale 2V/cm
 lower-before wave shaping
 scale-5V/cm
 Time scale - 0.2 msec/cm

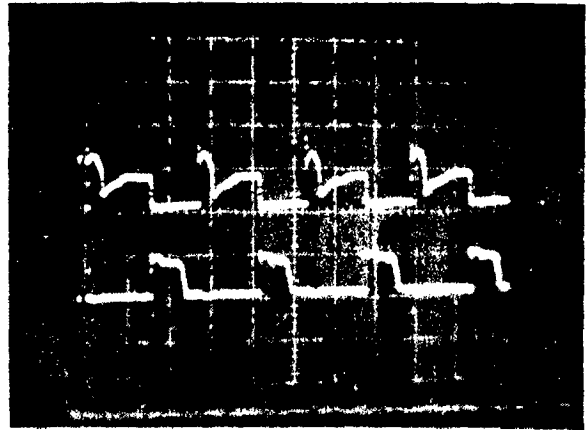


h) Motor armature current
 upper-before filtering
 scale-2V/cm
 lower-after filtering
 scale-2V/cm
 Time scale - 0.2 msec/cm



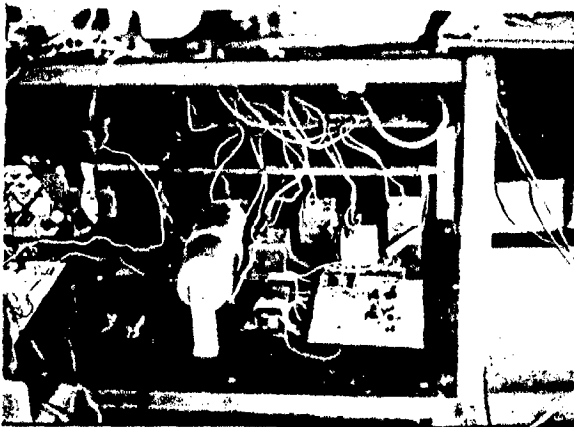
i) upper-voltage across C
lower-voltage across TH1
with the anode of TH1 as
common point

Scale - 100 V/cm
0.1 msec/cm

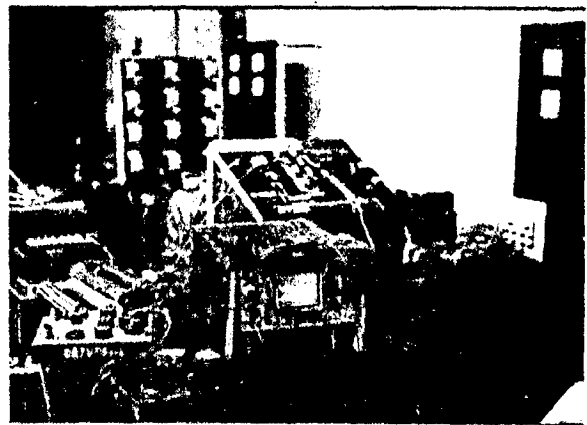


j) upper-firing pulse for TH1
lower-firing pulse for TH2
during CL operation for
 $N_B = 600$

Scale 1V/cm
0.2 msec/cm



j) Rear view of the set up



k) front view of the set up

the main and the auxiliary thyristors. The firing pulse for TH1 has this specific waveform, as, after firing of the TH1, the Gate to cathode junction behaves as a diode, having a certain voltage drop across it.

6.4 Conclusions

The performance of the μ p based drive system has been investigated experimentally and compared with that obtained under natural and μ p controlled open loop operating conditions. The μ p based closed loop system shows better performance over the other systems. However, this drive showed sustained speed oscillations. This calls for more rigorous analytical studies of the closed loop drive. The speed and current measurement loops need improvements so as to process the errors in shorter times.

CHAPTER 7

CONCLUSIONS

The design, fabrication and performance evaluation of a microprocessor based closed loop chopper fed separately excited DC drive has been discussed in this dissertation.

The power circuit used is a single quadrant, current commutated chopper with two thyristors and three power diodes. The commutating components L and C were designed and the operation principle of the power circuit was explained with waveforms. The closed loop control scheme incorporating speed and current loops was implemented entirely by the μ p software. The flow chart for most of the software was given. The drive system was simulated on a computer to theoretically design the controller parameters. Finally, the performance evaluation of the μ p based drive was done with the experimental results obtained.

It was found that the practical values used of the controller parameters were slightly different from those of the theoretical ones. The deviation was small for current controller parameters and large for that of the speed controller. This is obvious from the fact that, inherently, the current controller of the inner current loop imparts a restriction, on the speed controller of the outer speed loop. The other reasons may be

- 1) inaccuracies in the measurement of the motor parameters

which are used for the simulation studies,

- 2) inaccuracies in the preparation of the mathematical model i.e. certain time delays of the system are neglected. The drive must really be simulated as a discrete time system.
- 3) The inaccuracies in the computation methods (Runge-Kutta method for the numerical solution of the differential equation).

But, as already mentioned in Section 6.3, the different values of the parameters of the controller, closely conform with the region of stability determined analytically. The practical limitations of the actual set up also contribute for not achieving the desired performance of non oscillatory system (both in speed and current). They are

- 1) Inaccuracy in measurement of speed.

Taking 1 bit = 1 rpm, a maximum of ± 5 rpm error (since actual speed = COUNT * 5) can exist in the measurement of speed by the μ p.

- 2) Inaccuracy in current measurement.

The filtering of current used for feed back purpose is not perfect. This can cause oscillations in the drive variables.

- 3) The machine being a low inertia one, responded to the actual variation in T_{ON} and T_{OFF} in closed loop

and this discrepancy would not have been there, if the machine were to have high inertia.

But nevertheless, the microprocessor based system gives better performance than the conventional one as is obvious from our results.

Scope for Future Work

The author would like to suggest the following for the improvement of the system.

- 1) improvement in the optical shaft encoder so that, the speed sampling could be done at a fast rate.
- 2) using faster speed measurement algorithms.
- 3) using a faster processor such as INTEL 8086 to reduce the execution time.
- 4) the simulation of the drive as a discrete time system with a view to coordinate its parameters for satisfactory performance and investigate its transient performance.
- 5) at least 2 quadrant dc chopper to further improve the performance.
- 6) using modern adaptive control methods such as variable structure (vss) control method as against conventional one used.

REFERENCES

- [1] Sen, P.C., "Thyristor D.C. Drives", A Wiley - Inter science Publications, John Wiley and Sons, New York, 1981.
- [2] Zwicky, R., 'Modern development in Electric drives', Brown Boweri Review, May/June 1967, pp. 212.
- [3] S.N. Singh and D.R. Kohli, "Analysis and performance of a chopper controlled separately excited D.C. Motor", IEEE Trans. on Industrial Electronics, Vol. II, No. 1, Feb. 1982.
- [4] K.B. Naik, 'Estimation of Critical Inductance for a D.C. separately excited motor fed by load dependent chopper', Electromechanics and power systems 1985 Vol. 10.
- [5] G.K. Dubey, S.R. Doradla, A. Joshi, R.M.K. Sinha, "Thyristorised Power Controllers", Wiley Eastern Limited, 1986.
- [6] Pradeep Kumar, Y., 'Design Fabrication and Performance evaluation of a Microprocessor - Controlled Thyristorised D.C. Drive system', Thesis, M.E., Electrical Engg. Deptt., UOR, Roorkee 1979.
- [7] Irie, H., Fujii, J. and Ishizula, T., 'Thyristor chopper for separately excited dc motor control', Elect. Engg. in Japan, Vol. 88, No. 4, pp 1-9, 1968.
- [8] E.A. Parrish, EUGENE S. McVEY, 'A Theoretical Model for Single Phase Silicon Controlled Rectifier systems', IEEE Trans. on Automatic Control', Vol. AC-12, No. 5, p-577, Oct. 1967.

- [9] Nitta, K., Okitsu, H., Suzuki, T. and Kinouchi, Y., 'A separately excited dc motor driven by discontinuous current', *Elect. Engg. in Japan* Vol. 89, No.11, pp 19-26, 1969.
- [10] N. Matsui and S. Miyairi, 'Transfer function estimation of dynamic behaviour of separately excited dc motor controlled by the thyristor chopper circuit', *Elect. Engg. in Japan*, Vol. 96, No.2, 1976.
- [11] Naik, K.B., V.K. Jain, G.K. Dubey, 'Dynamic model of a dc chopper fed separately excited motor', *Electric Machines and Electromechanics*, Vol. 7, No.6, NOV/DEC. 1982.
- [12] T. Jinzenji, T. Kanzaki, T. Koga, 'Characteristics of Two phase Double superimposed Auxiliary impulse commutated chopper', *IEEE Trans. on IA*, vol. IA-16, No. 1, JAN/FEB. 1980.
- [13] WILLIAM MC MURRAY, 'Thyristor Commutation in DC Choppers - A Comparative study', *IEEE Trans. on IA*, Vol. IA-14, No. 6, NOV/DEC. 1978.
- [14] Keiju Malsui and Noraiki Sato, 'A new high frequency thyristor chopper with improved commutating efficiency', *Electrical Engg. in Japan*, Vol. 97, No. 3, 1977, pp 103.
- [15] T. Krishnan and B. Ramaswami, 'A Fast Response DC Motor Speed Control System', *IEEE Trans. on IA*, Vol. IA-10, No.5, pp 643-651, Sept/Oct. 1974.

- [16] R.R. Sule, Balakrishna J. Vasanth, Thadiappan Krishnan, and Mudit Kumar, 'Microprocessor - Based Speed Control system for High-Accuracy Drives', IEEE Trans. on IE, Vol IE-32, No.3, AUG. 1985.
- [17] E.S.N. Prasad, Gopal, K. Dubey, And srinivasa S. Prabhu, 'High - performance DC Motor Drive with Phase - Locked Loop Regulation', IEEE Trans. on IA, Vol. IA-21, No.1, JAN/FEB. 1985.
- [18] W.G. Dunfor and S.B. Dewan, 'Design of a control circuit for a Two-Quadrant Chopper based on the Motorola 6800 Microprocessor', IEEE Trans. on IA, Vol. IA-16, No. 4, July/Aug. 1980.
- [19] Kenneth R. Zelenka and Thomas A. Barton, 'A fast acting current limit for a dc motor drive', IEEE Trans. on IA, Vol. IA-22, No.5, Sep/Oct. 1986.
- [20] A.K. Lin and W.W. Koepsel, 'A Microprocessor Speed Control System', IEEE Trans. on IECI, Vol IECI-24, No. 3, AUG.1977.
- [21] Pradeep K. Nandam, Paresh C. Sen, 'Analog and Digital Speed Control of DC Drives using Proportional - Integral and Integral - Proportional Control Techniques', IEEE Trans. on IE Vol IE-34, No.2, MAY 1987.
- [22] Tsutomu Ohmae, Toshihiko Matsuda, Toshitaka Suzuki, Noboru Azusawa, Kenzo Kamiyama, and Tsutomu Konishi, 'A Microprocessor Controlled fast response speed Regulator

with Dual Mode Current Loop for DCM Drives", IEEE Trans. on IA, vl. IA-16, No.3, pp 383-394, May/June 1980.

- [23] S.B. DEWAN and ALI MIRBOD, 'Microprocessor based optimum Control for Four Quadrant Chopper', IEEE Trans. on IA, Vol. IA-17, No.1, JAN/FEB. 1981.
- [24] P.C. Sen and S.R. Doradla, "Evaluation of Control schemes for Thyristor - Controlled DC Motors", IEEE Trans. on IECI, Vol IECI-25, No.3, pp 247=255, Aug. 1978.
- [25] C. Chellamuttu and V.V. Sastry, 'Simulation of Chopper Fed DC Motor Drive System - Problem Oriented Approach', Elect. Machines and Electromechanics, Vol. 6, No.5, Sep-Oct. 1981.
- [26] Pramod Agarwal and V.K. Verma, "parameter Plane Synthesis of A Dual Converter Fed Variable Speed D.C. Drive System', Electric Machines and Power Systems, 12:57-68, 1987.
- [27] B.M. Bird and K.G. King, "An Introduction to Power Electronics", John Wiley and Sons, 1983.
- [28] DAVID FINNY; Power Thyristor and its applications.
- [29] S.B. Dewan and Straughen, 'Power Semiconductor Circuits', John Wiley and Sons, New York, 1975.
- [30] Fitzgerald, A.E., Kingley C. and Kusko, A: 'Electric Machinery', (Mc Graw Hill, New York, 1971).
- [31] Hriao - Chuan Wang, "Sampling Period and Stability Analysis for the Microprocessor Based Motor Control systems", IEEE Trans. on IECI, Vol. IECI-28, No.2, pp-98-102, May 1981.

- [32] M. Morris Mano, "Computer system Architecture".
- [33] I.I. Nagarath Gopal and M. Gopal, "Control Systems Engineering", Wiley Eastern Limited, 1982.
- [34] Pramod Agarwal, 'Design, Fabrication and Performance Investigation of a Dual Converter Fed Variable Speed D.C. Drive system', M.E. Dissertation.
- [35] Paul W. Franklin, 'Theory of the D.C. Motor Controlled by Power Pulses', Part I, II, IEEE Trans. on PAS Vol.91, No. 1, pp.249-253, Jan/Feb 1972.
- [36] M.A. Aizerman, 'Theory of Automatic Control", Pergamon Press, 1963.
- [37] "INTEL Periferal Design Hand Book", Published by INTEL Corporation, Santa Clara, August, 1981.
- [38] VMC 85/9 User's Manual.

APPENDIX - A

PARAMETER PLANE SYNTHESIS METHOD

A process is said to be stable if for any small initial deviations, the equilibrium is restored to the control system as a result of the action of the controller, and the process is said to be unstable if the controller does not restore operating state which existed in the system before the appearance of these initial deviations. In the case of linear model, if it is stable for small disturbances then it is stable with respect to any other disturbance. The necessary and sufficient condition for the stability (i.e. in the case when the process is described by a set of linear differential equations) is that all the real roots of the characteristic equation be negative and all complex roots have a negative real part.

Usually the techniques employed for studying the stability have been the Routh - Hurwitz's criterion, Nyquist method and Root locus method. These methods have been successfully used to study the effect of only one parameter of the control system on the system performance. An improvement over the above methods is the D-partition method. This method was presented first by Neimark in 1948. This method can be used to study the effect of two parameters of the control system on stability and transient performance.

With regard to stability analysis, the method provides a possibility of defining the relative stability of control system as the numbers of roots of characteristic equation relative to a specified s-plane contour of a general shape. The plane with the two adjustable parameters as coordinate axes is termed as 'Parameter Plane'. The parameter plane method can also be extended in case of non-linear and sample data system.

Parameter Mapping

The idea of system design is to obtain a simple correlation between the system parameters and the characteristic roots so that the roots can be set at a desired location by adjusting the system parameters. This can be done by parameter plane synthesis method.

The parameter plane method is based on a mapping procedure that transform points from the complex $s(\sigma, \omega)$ plane on to the parameter $\alpha - \beta$ plane. In the general case, the mapping function is an n^{th} degree algebraic equation

$$F(s) = \sum_{k=0}^n a_k s^k = 0$$

where s is the complex variable defined by

$$s = -\sigma + j\omega_d,$$

and a_k are the coefficients that are functions of two real parameters α and β i.e.

$$a_k = a_k(\alpha, \beta), \quad k = 0, 1, 2, \dots, n$$

(for $\omega_d \neq 0$ or ∞) are simply oriented in accordance with the shading of complex boundaries. The shading of such a spatial line must be done twice on the same side as that on the complex root boundary at their point of intersection. The spatial lines at $\omega_d = 0$ and $\omega_d = \infty$ are also shaded with this rule but they are shaded only once. The root leaves the contour if it goes from a shaded region to the unshaded region and enters the contour if it goes from unshaded to shaded region. After the boundaries are appropriately shaded, the relative number of roots in each bounded region is easily determined. For doing this, firstly the region with maximum values of roots on the left side in the s-plane is established by inspection of the plot. For ascertaining stable region point in the region with maximum number of roots is selected and the stability of the system is checked by the Frequency Scanning Technique. If the system is stable at this point then this entire enclosed region is also a stable region.

Frequency Scanning Technique (The Mikhailov Criterion)

A system is said stable, provided its characteristic equation

$$F(s) = a_0 s^n + a_1 s^{n-1} + \dots + a_n = 0 \quad (\text{A.9})$$

where

$$s = j\omega$$

satisfies the following conditions:

- (i) $F(j\omega) \neq 0$ at $\omega = 0$ i.e. $a_n \neq 0$

Separating terms containing α and β results in following two equations:

$$u(\sigma, \omega_d, \alpha, \beta) = \alpha S_1(\sigma, \omega_d) + \beta Q_1(\sigma, \omega_d) + R_1(\sigma, \omega_d) = 0 \quad (\text{A.5})$$

$$v(\sigma, \omega_d, \alpha, \beta) = \alpha S_2(\sigma, \omega_d) + \beta Q_2(\sigma, \omega_d) + R_2(\sigma, \omega_d) = 0 \quad (\text{A.6})$$

Solving equations (A.5) and (A.6) with respect of α and β for each ω_d give

$$\alpha = \frac{\begin{vmatrix} -R_1 & Q_1 \\ -R_2 & Q_2 \end{vmatrix}}{\begin{vmatrix} S_1 & Q_1 \\ S_2 & Q_2 \end{vmatrix}} = \frac{Q_1 R_2 - Q_2 R_1}{S_1 Q_2 - S_2 Q_1} \quad (\text{A.7})$$

$$\beta = \frac{\begin{vmatrix} S_1 & -R_1 \\ S_2 & -R_2 \end{vmatrix}}{\begin{vmatrix} S_1 & Q_1 \\ S_2 & Q_2 \end{vmatrix}} = \frac{S_2 R_1 - S_1 R_2}{S_1 Q_2 - S_2 Q_1} \quad (\text{A.8})$$

The equations (A.5) and (A.6) determine one value of α and one value of β as given by equations (A.7) and (A.8) for each ω_d , only when these equations are simultaneous and independent.

If for some value of ω_d , say ω_c , the numerator and denominator becomes zero, then for this value of ω_d , the two equations (A.5) and (A.6) are linearly dependent to each other and a straight line is obtained instead of a point

in the $\alpha - \beta$ plane, known as spatial line. In this case, either of the equations (A.5) and (A.6) is the equation of the straight line when this value of ω_d is substituted. If the coefficient of the highest term of the characteristic equation depends on the parameter α and β , then by equating this coefficient to zero spatial line at $\omega_d = \infty$ is obtained. Similarly, a spatial line at $\omega = 0$ is obtained by equating the coefficient of the lowest (free) term of the characteristic equation to zero.

In order to find the number of roots in the various region obtained in the parameter plane by the plotted boundaries it is necessary to know whether a root is leaving or entering the s-plane contour as shown in Figs. (A.1), (A.2), (A.3) at the instant that point goes over a boundary in the parameter plane. In order to know whether the roots are leaving or entering the s-plane contour, the boundary curves should be appropriately shaded. The side of the boundary to be shaded is determined according to sign of the denominator

Δ where $\Delta = \begin{vmatrix} S_1 & Q_1 \\ S_2 & Q_2 \end{vmatrix}$. Facing the direction in which ω_d is

increasing the boundary curves in the $\alpha - \beta$ plane are shaded on the left side if $\Delta > 0$ and on the right side if $\Delta < 0$. Usually, the curve is traversed twice, once when ω_d goes from $-\infty$ to 0 and next when it changes from 0 to $+\infty$. It is shaded both the times on the same side, as the sign of Δ changes with change in sign of ω_d (Δ is an odd function of ω_d). After the complex root boundaries are shaded, the spatial lines

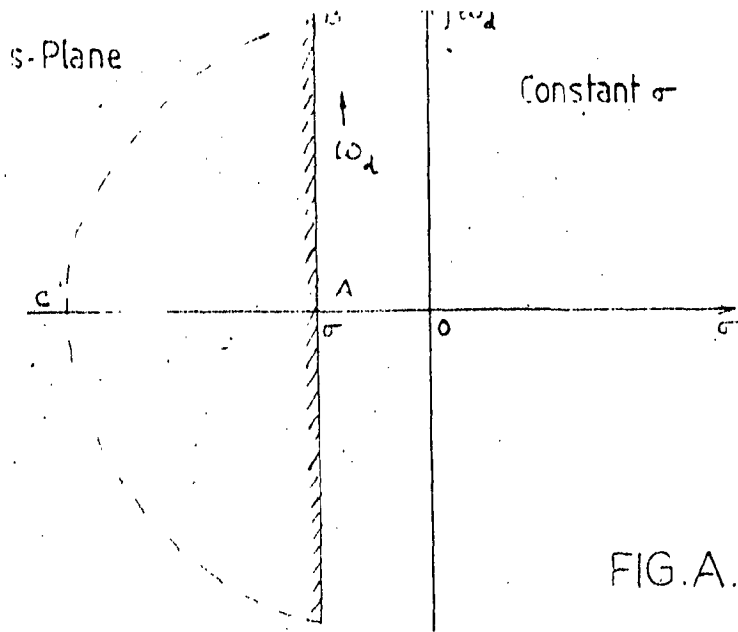


FIG. A.1

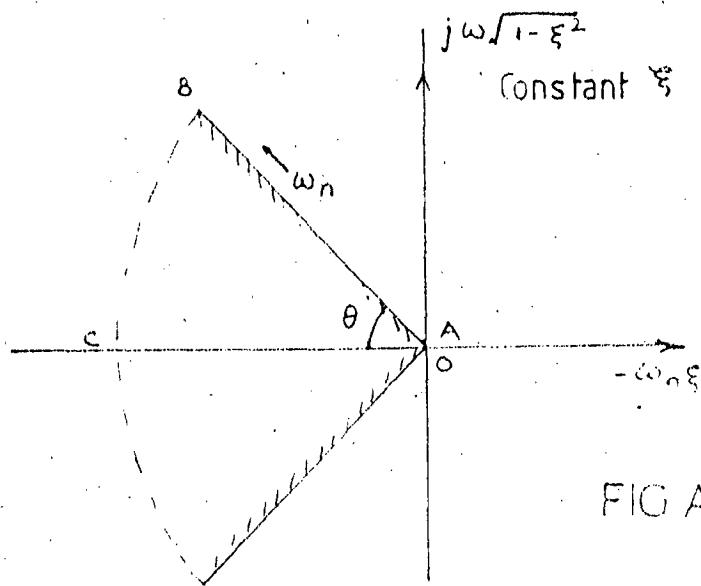


FIG. A.2

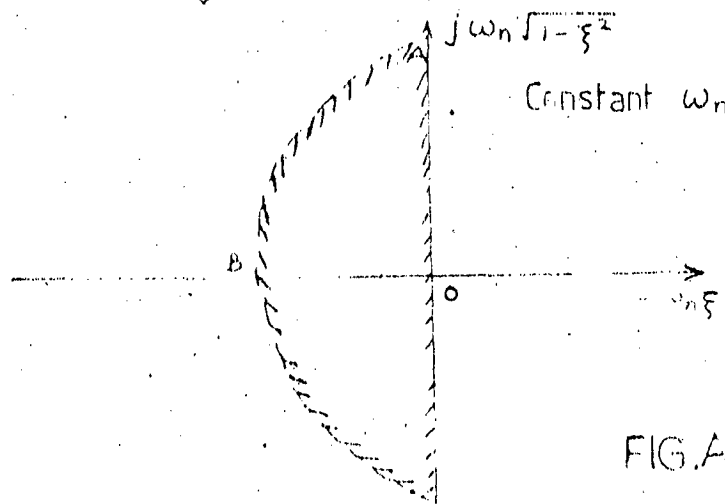


FIG. A.3

s-PLANE CONTOURS

If to a given pair of number (σ_1, ω_{d1}) there corresponds a pair of numbers (α_1, β_1) so that mapping equation $F(s) = 0$ is satisfied, then for α_1 and β_1 , the equation has a root pair $s_1 = -\sigma_1 \pm j\omega_{d1}$. Therefore, the defined mapping can be regarded as a transformation of the points (σ, ω_d) for the complex s -plane, which represents root values of the algebraic equation $F(s) = 0$, to certain points of parameter $\alpha - \beta$ plane. This is referred to as parameter mapping. The same theory is also applicable for $s = -\xi\omega_n \pm j\omega_n\sqrt{1-\xi^2}$ in (ξ, ω_n) plane.

Now, considering the case when two parameters α and β enter into the characteristic equation linearly so that the characteristic equation can be reduced to the form.

$$F(s) = \alpha S(s) + \beta Q(s) + R(s) = 0 \quad (\text{A.1})$$

Substituting $s = -\sigma + j\omega$ in equation (A.1) and separating real and imaginary parts, results in following equation.

$$\alpha S(-\sigma + j\omega_d) + \beta Q(-\sigma + j\omega_d) + R(-\sigma + j\omega_d) = 0$$

$$\text{or } u(\sigma, \omega_d, \alpha, \beta) + jv(\sigma, \omega_d, \alpha, \beta) = 0 \quad (\text{A.2})$$

In order to construct the boundary of the D-partition it is necessary to determine α and β for each ω_d by solving simultaneously the two equations:

$$u(\sigma, \omega_d, \alpha, \beta) = 0 \quad (\text{A.3})$$

$$v(\sigma, \omega_d, \alpha, \beta) = 0 \quad (\text{A.4})$$

(ii) The locus of the end points of the vector $F(j\omega)$, when ω varies from 0 to ∞ , traverses in succession by 'n' quadrants in anti-clock wise manner for an equation of n^{th} order.

Let the roots of the equation (A.9) be z_1, z_2, \dots, z_n . then provided $a_0 = 1$, equation (A.9) can be expressed in the form

$$F(s) = (s-z_1) (s-z_2) \dots (s-z_n)$$

Substituting $s = j\omega$

$$F(j\omega) = (j\omega-z_1) (j\omega-z_2) \dots (j\omega-z_n)$$

$F(j\omega)$ constitutes a vector whose modulus is equal to the product of the moduli of all the vectorial factors and whose argument is equal to the sum of the arguments of all the vectorial factors.

At $\omega = 0$, the vector $F(j\omega)$ has a pure real value, $F(0)$ with its arguments equal to zero. As ω is varied from 0 to ∞ , the angle of term associated with a real root changes by $\pi/2$, and for each pair of conjugate roots by π . Consequently for an n^{th} order equation, if all the roots lie on the left hand side of imaginary axis, the total angle by which $F(j\omega)$ changes is equal to $n(\pi/2)$.

APPENDIX - B

B.1 Measurement of DC Machine parameters

The armature resistance R_a of motor as measured by voltmeter - ammeter method is found to be 4.0 ohms. The impedance Z_a of the armature as measured at ac supply frequency of 50 Hz is found to be 46.27 ohms. Therefore, armature inductance is equal to 0.147 H. The back emf constant K_b of the motor is obtained by running the machine as a generator at constant field current and is found to be 1.86 volts/rad/sec.

The dc motor is loaded by means of a dc generator (with constant field excitation) supplying a fixed resistor. Therefore the load torque T_L is proportional to the speed ω_m and the proportionality constant B is defined by the equation

$$T_L = B \omega_m$$

The viscous friction only increases this proportionality constant. For the operating condition used, this proportionality constant (viscous friction constant included in load on the motor) is determined experimentally and is found to be 0.08 Nw-mt/rad/sec.

The moment of inertia of the motor together with load generator is determined by the retardation or Running down test method. In this method, the machine is run slightly above the rated speed and then supply is cut off from the

armature. Consequently the armature slows down and its kinetic energy is used to meet rotational losses i.e. friction, windage and iron loss.

$$\begin{aligned} \text{Loss due to rotation } p &= d/dt \text{ (K.E.)} \\ &= d/dt \left(\frac{1}{2} J \omega_m^2 \right) \\ &= J \omega_m \frac{d\omega_m}{dt} \end{aligned}$$

Since $\omega_m = 2\pi n/60$, n is motor speed in rev/min

$$\text{and } \frac{d\omega_m}{dt} = \frac{2\pi}{60} \frac{dn}{dt}$$

$$\dots p = \left(\frac{2\pi}{60} \right)^2 J n \frac{dn}{dt} = 0.0109 J n \frac{dn}{dt}$$

$$\begin{aligned} \text{Average load current during retardation test } I_a &= \frac{1.5 + 1.4}{2} \\ &= 1.45 \text{ A} \end{aligned}$$

The time is measured for approximately 10% drop in speed i.e. from 220 V to 200 V at fixed field excitation. The tests gave following readings:

- a) Without additional load $t = 0.65$ secs.
- b) With additional load $t' = 0.45$ secs.

$$\text{Rotational losses } p = p' \frac{t'}{t-t'}$$

where p' = losses due to additional load

$$\dots p = p' \frac{0.45}{0.65-0.45} = 2.25 p'$$

$$\begin{aligned} \text{Average voltage during retardation test} &= \frac{220 - 200}{2} \\ &= 210 \text{ V} \end{aligned}$$

also $p' = 1.45 \times 210 = 304.5$ Watts

.. $p = 2.25 \times 304.5 = 685.12$ Watts

For determination of $\frac{dn}{dt}$, a graph is plotted between armature voltage (proportional to speed) as a function of time as shown in Fig. B.1.

The speed of the motor $n = 1050$ rpm

Since 220 V corresponds to 1200 rpm, hence 1 V corresponds to 5.45 rpm.

From graph,

$$\frac{dn}{dt} = 5.45 \times \frac{5}{0.2} = 136 \text{ rpm/sec}$$

$$\begin{aligned} \therefore J &= \frac{p}{0.0109 n \left(\frac{dn}{dt}\right)} \\ &= \frac{685.12}{0.0109 \times 1050 \times 136} \\ &= 0.4389 \text{ kg.m}^2 \end{aligned}$$

$$\begin{aligned} \text{The mechanical time constant } \tau_m &= \frac{JR_a}{K_b^2} \\ &= \frac{0.4389 \times 4.0}{(1.86)^2} \\ &= 0.503 \text{ sec} \end{aligned}$$

The electrical time constant τ_a of the armature circuit is found to be 37 msec.

B.2 Speed Transducer

As already described, the speed transducer consists of an optical shaft encoder and the speed is measured by μp . If N^* is the speed fed back to the μp (in rpm) and ω_m is

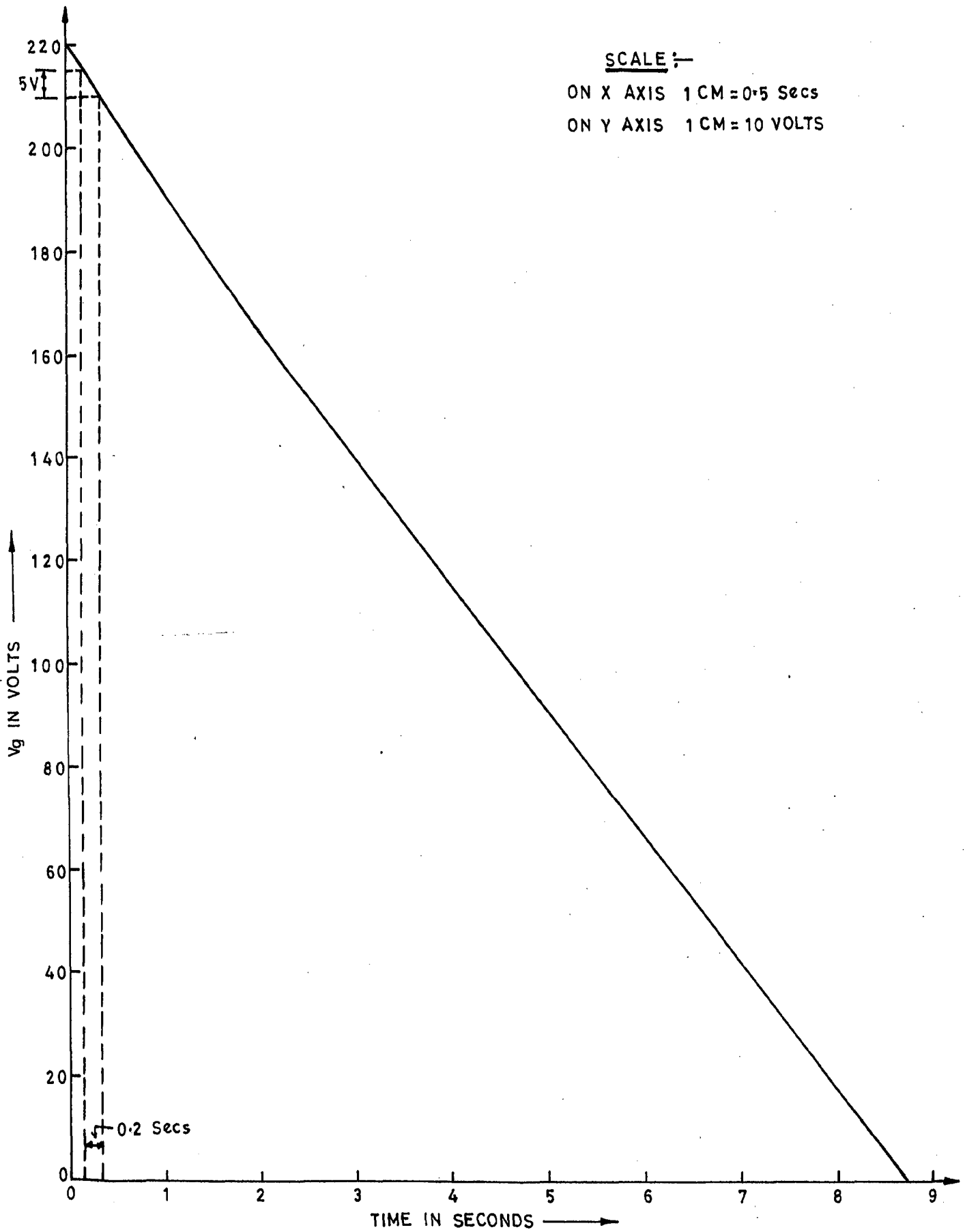


FIG. B-1—RETARDATION TEST

the actual speed in rad/sec, the gain of the speed transducer is given as

$$H_W = \frac{N^*}{\omega_m} = 9.54$$

The relation between the actual speed as measured by the tachometer and the microprocessor is shown by means of Fig. B.2.

B.3 Current Transducer

As already mentioned, the armature current is sampled, and is measured by μp through ADC. If I_a is the actual current and I^* is the current fed back to the μp then, the gain of the current transducer is given as

$$R = \frac{I^*}{I_a} = 0.5412 \text{ (Section 5.2.5)}$$

The relation between the actual current as measured by, the Armature and the microprocessor is shown by means of Fig. B.3.

Actual speed in RPM	Speed as Meas by μp (RPM)	Actual current in AMPS	Current as measured by μp AMPS
100	105	1	.89
200	205		
300	308	2	1.92
400	410		
500	510	3	2.98
600	610		
700	709	4	3.90
800	815		
900	915	5	4.80
1000	1017		

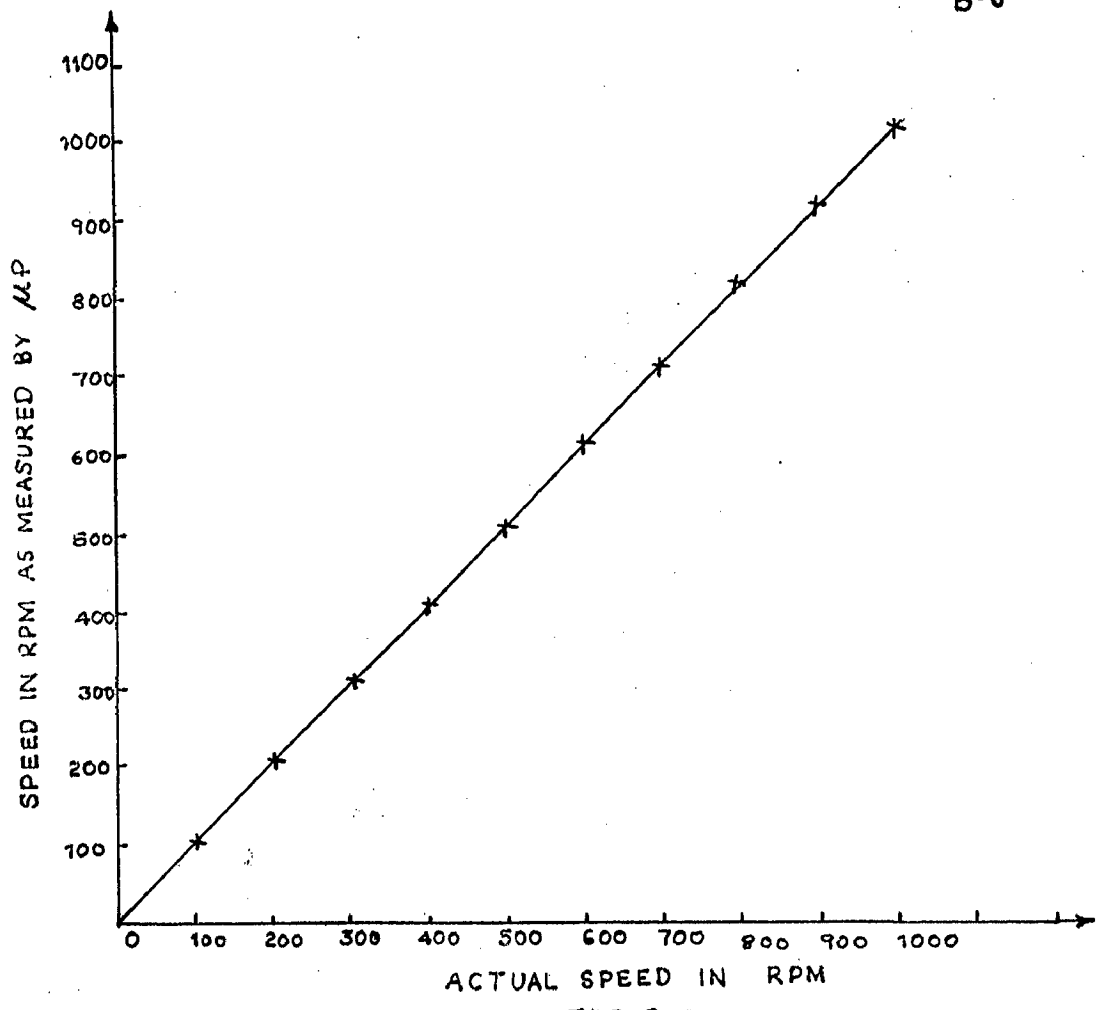


FIG. B-2

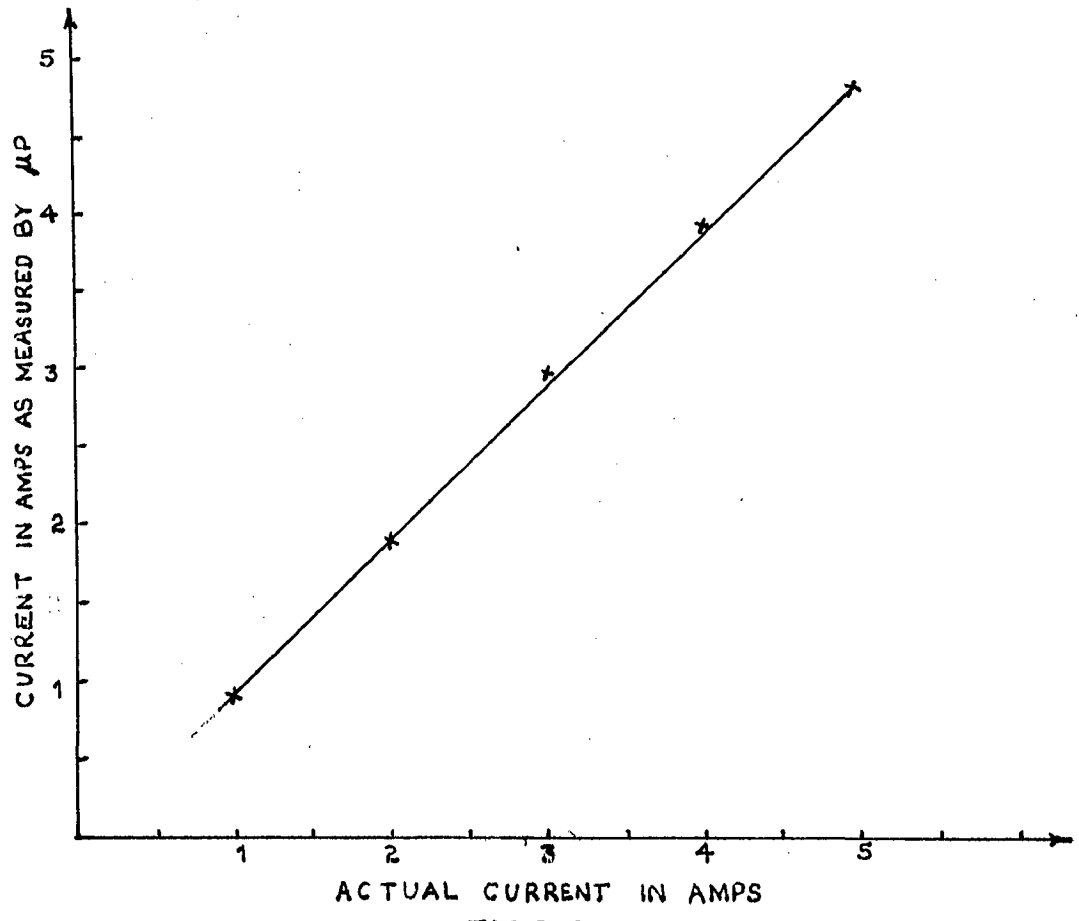


FIG. B-3

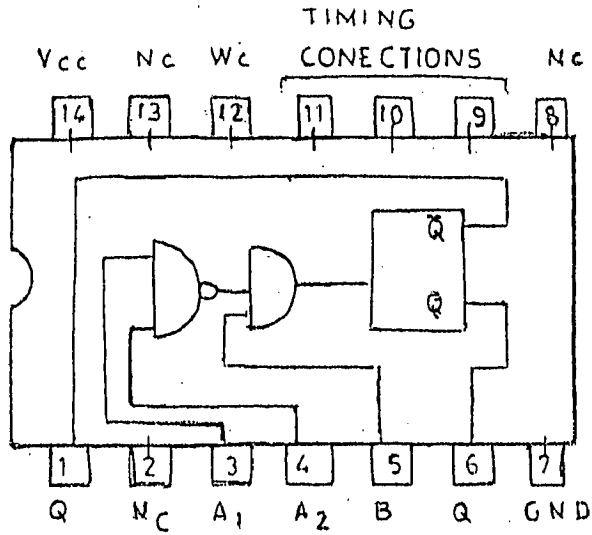


FIG. C-2 74121 MONOSTABLE MULTIVIBRATOR) PIN CONFIGURATION

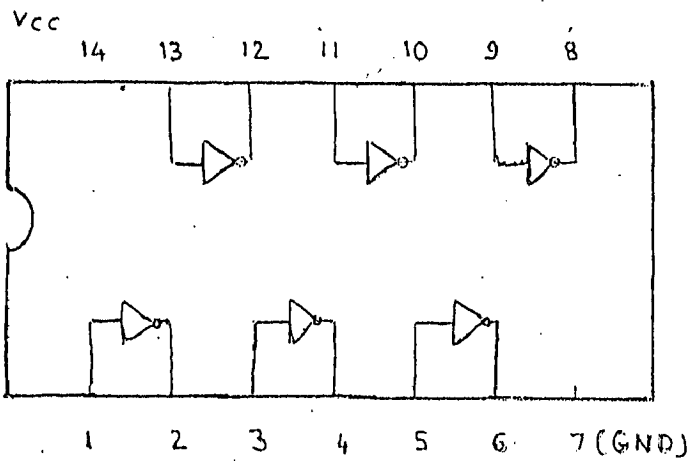


FIG. C-3 7404 (HEX INVERTER) PIN CONFIGURATION

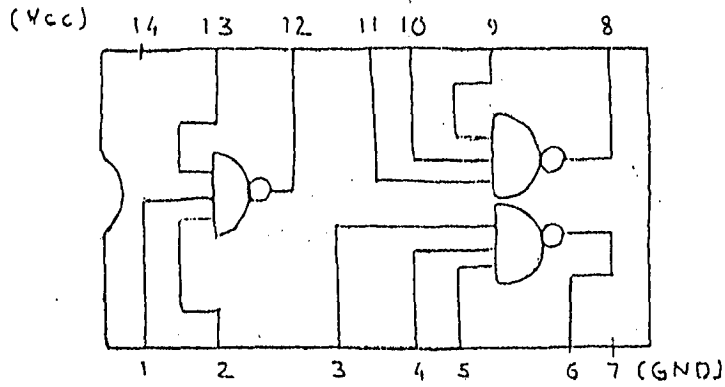


FIG. C. 4 7410 (TRIPLE-INPUT NAND GATE)
PIN CONFIGURATION

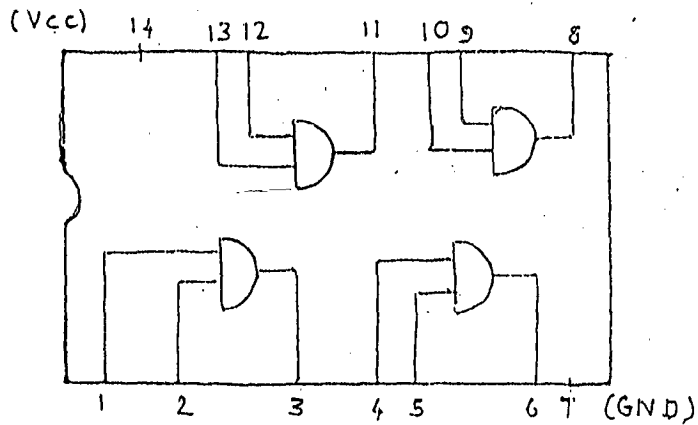
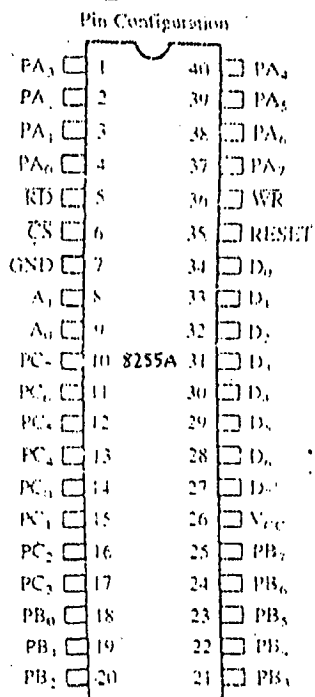


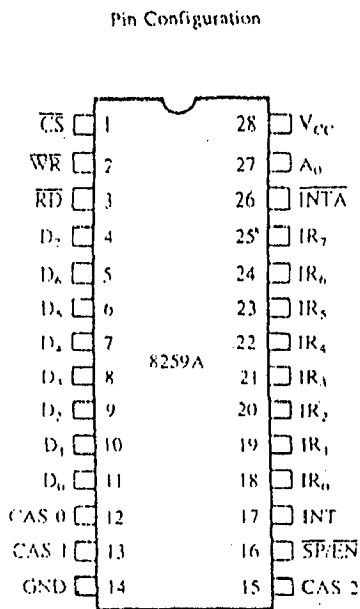
FIG. C. 5 7408 (QUAD 2-INPUT NAND GATE)
PIN CONFIGURATION



Pin Names

D ₀ -D ₇	Data Bus (Bidirectional)
RESET	Reset Input
CS	Chip Select
RD	Read Input
WR	Write Input
A ₀ , A ₁	Port Address
PA ₇ -PA ₀	Port A (Bit)
PB ₇ -PB ₀	Port B (Bit)
PC ₇ -PC ₀	Port C (Bit)
V _{CC}	+5 Volts
GND	0 Volts

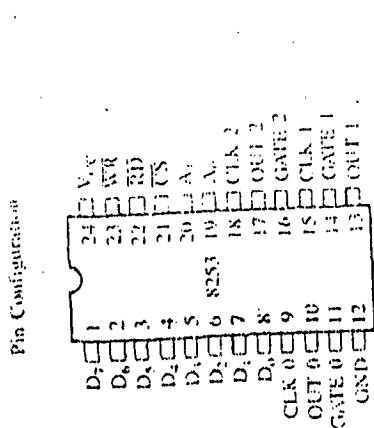
FIGURE C-8 8255A Block Diagram



Pin Names

D ₀ -D ₇	Data Bus (Bidirectional)
RD	Read Input
WR	Write Input
A ₀	Command Select Address
CS	Chip Select
CAS ₀ -CAS ₂	Cascade Lines
SP/EN	Slave Program-Enable Buffer
INT	Interrupt Output
INTA	Interrupt Acknowledge Input
IR ₀ -IR ₇	Interrupt Request Inputs

FIGURE C-10 The 8259A Block Diagram



Pin Names

D ₀ -D ₇	Data Bus (Bit)
CLK N	Counter Clock Inputs
GATE N	Counter Gate Inputs
OUT N	Counter Outputs
RD	Read Counter
WR	Write Command of Data
CS	Chip Select
A ₀ -A ₁	Counter Select
V _{CC}	+5 Volts
GND	Ground

FIGURE C-9 8253 Block Diagram

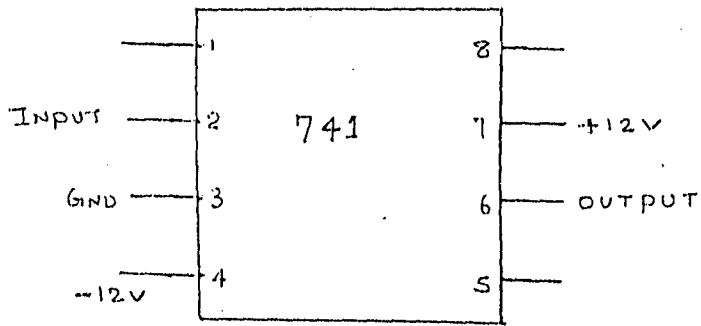


FIG. C.6. 741 I.C (AS COMPARATOR)

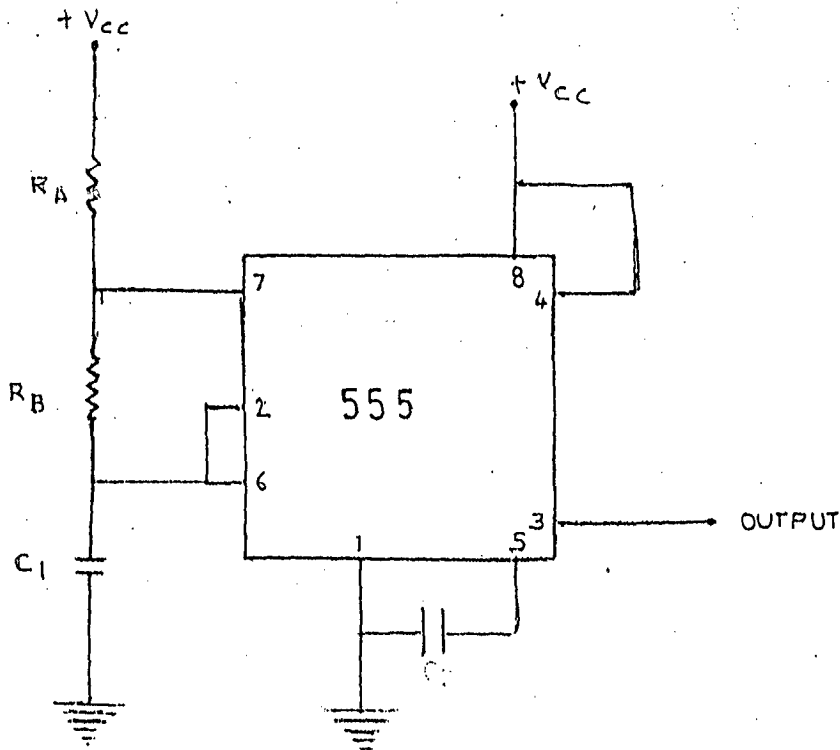
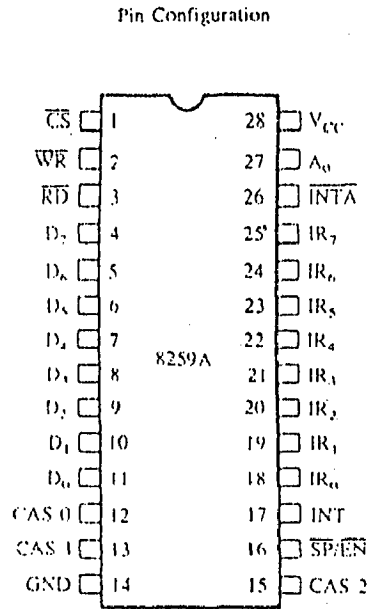
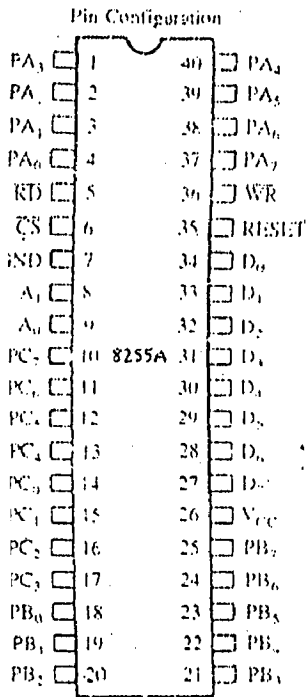


FIG. C.7. 555 TIMER (AS AN OSCILLATOR)
PIN CONNECTION DIAGRAM



Pin Names

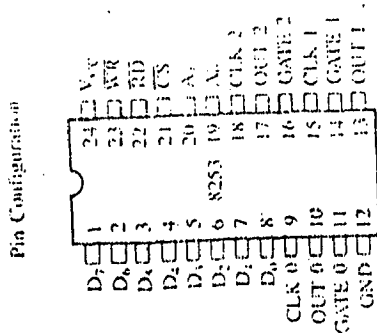
D ₇ -D ₀	Data Bus (Bidirectional)
RESET	Reset Input
CS	Chip Select
RD	Read Input
WR	Write Input
A ₀ , A ₁	Port Address
PA ₇ -PA ₀	Port A (Bit)
PB ₇ -PB ₀	Port B (Bit)
PC ₇ -PC ₀	Port C (Bit)
V _{CC}	+5 Volts
GND	0 Volts

Pin Names

D ₇ -D ₀	Data Bus (Bidirectional)
RD	Read Input
WR	Write Input
A ₀	Command Select Address
CS	Chip Select
CAS ₀ -CAS ₂	Cascade Lines
SP/EN	Slave Program-Enable Buffer
INT	Interrupt Output
INTA	Interrupt Acknowledge Input
IR ₇ -IR ₀	Interrupt Request Inputs

FIGURE C-8 8255A Block Diagram

FIGURE C-10 The 8259A Block Diagram



Pin Names

D ₇ -D ₀	Data Bus (Bidirectional)
CLK 0	Counter Clock Inputs
GATE 0	Counter Gate Inputs
OUT 0	Counter Outputs
RD	Read Counter
WR	Write Command to Data
CS	Chip Select
A ₀ -A ₁	Counter Select
V _{CC}	+5 Volts
GND	Ground

FIGURE C-9 8253 Block Diagram

```

00100 C      PROGRAM NO 1
00200 C      *****
00300 C      DETERMINATION OF THE REGION OF RELATIVE STABILITY
00400 C      OF CURRENT LOOP IN THE PLANE OF TWO PARAMETERS
00500 C      ALPHA AND BETA WITH THE VARIATION IN SIGMA
00600 C      USING D-DECOMPOSITION METHOD
00700 C      *****
00800 C      VARIABLES USED
00900 C      *****
01000 C      ALPHA=INVERSE OF GAIN K1
01100 C      BETA=INVERSE OF THE TIME CONSTANT TC1
01200 C      S=COMPLEX FREQUENCY
01300 C      ALR=COEFF.OF ALPHA OF REAL EQUATION
01400 C      ALI=COEFF. OF ALPHA OF IMAGINARY EQUATION
01500 C      BTR=COEFF. OF BETA OF REAL EQUATION
01600 C      BTI=COEFF. OF BETA OF IMAGINARY EQUATION
01700 C      COEFR=CONSTANT TERM IN REAL EQUATION
01800 C      COEFI=CONSTANT TERM IN IMAGINARY EQUATION
01900 C      *****
02000      COMPLEX S,F1,F2,SF1,SF2
02100      F1(S)=CH*R*TM*CEXP(-S*T)*(S+B/AJ)/RA
02200      F2(S)=(1.+(1.+S*TA)*(S+B/AJ)*TM)
02300      OPEN(UNIT=1,FILE='ST1.DAT')
02400      READ(1,*)CH,R,TM,B,AJ,RA,TA,T
02500      PRINT 5, CH,R,TM,B,AJ,RA,TA,T
02600 5      FORMAT(5X,'CH=',F7.5,'R=',F7.5,'TM=',F7.5,'B=',
02700      1F7.5,'AJ=',F7.5,'RA=',F7.5,'TA=',F7.5,'T=',F7.5)
02800      OMEGA=0.0
02900      SIGMA=0.15
03000 20     S=CMPLX(-SIGMA,OMEGA)
03100      SF2=S*F2(S)
03200      SF1=S*F1(S)
03300      ALR=REAL(SF2)
03400      ALI=AIMAG(SF2)
03500      BTR=REAL(F1(S))
03600      BTI=AIMAG(F1(S))
03700      COEFR=REAL(SF1)

```


SIMULATION PROGRAMS

```

03800      COEFI=AIMAG(SF1)
03900      DEN=BTI*ALR-BTR*ALI
04000      ANUM=BTR*COEFI-BTI*COEFR
04100      BNUM=ALI*COEFR-ALR*COEFI
04200      IF (DEN.NE.0.) GO TO 10
04300      IF (ANUM.NE.0.) GO TO 200
04400 C      *****
04500 C      CALCULATION OF SPATIAL LINE COORDINATES
04520      PRINT 60,SIGMA ,OMEGA ,ALR,BTR, COEFR,COEFI,ALI,BTI
04540 60     FORMAT(5X,'SIGMA=',F7.3,'OMEGA=',F7.3,'ALR='
04560      1,F7.3,'BTR=',E12.5,'COEFR=',E12.5,'COEFI=',E12.5,'
04580      2,ALI=',E12.5,'BTI=',E12.5)
04600 C      *****
05000      AL=0.
05100      DO 25 K=1,60
05200      BT=- (AL*ALR+COEFR)/BTR
05300      PRINT 26,AL,BT
05400 26     FORMAT(5X,'AL=',E12.5,5X,'BT=',E12.5)
05500      AL=AL+10.
05600 25     CONTINUE
05610      PRINT 27
05620 27     FORMAT(/5X,'S=', 28X,' ALPHA=',13X,'BETA=',9X,'ANUM
05640      1=',9X,'BNUM=',9X,'DEN=',9X,'OMEGA='//)
05700 C      *****
05800      GO TO 200
05900 10     ALPHA=ANUM/DEN
06000      BETA=BNUM/DEN
06100      PRINT 30, S,ALPHA,BETA,ANUM,BNUM,DEN,OMEGA
06200      IF (OMEGA.GE.200) GO TO 800
06300 200    OMEGA=OMEGA+2
06400      GO TO 20
06500 30     FORMAT(5X,8(E12.4,3X))
06600 800    STOP
06700      END
00100 C      PROGRAM NO 2
00200 C      *****
00300 C      DETERMINATION OF THE REGION OF RELATIVE STABILITY

```

SIMULATION PROGRAMS

```

00400 C      OF CURRENT LOOP IN THE PLANE OF TWO PARAMETERS
00500 C      ALPHA AND BETA WITH THE VARIATION IN DAMPING RATIO
00600 C      USING D-DECOMPOSITION MMETHOD
00700 C      *****
00800 C      VARIABLES USED
00900 C      *****
01000 C      ALPHA=INVERSE OF GAIN K1
01100 C      BETA=INVERSE OF THE TIME CONSTANT TC1
01200 C      S=COMPLEX FREQUENCY
01300 C      ALR=COEFF.OF ALPHA OF REAL EQUATION
01400 C      ALI=COEFF. OF ALPHA OF IMAGINARY EQUATION
01500 C      BTR=COEFF. OF BETA OF REAL EQUATION
01600 C      BTI=COEFF. OF BETA OF IMAGINARY EQUATION
01700 C      COEFR=CONSTANT TERM IN REAL EQUATION
01800 C      COEFI=CONSTANT TERM IN IMAGINARY EQUATION
01900 C      *****
02000      COMPLEX S,F1,F2,SF1,SF2
02100      F1(S)=CH*R*TM*CEXP(-S*T)*(S+B/AJ)/RA
02200      F2(S)=(1.+(1.+S*TA)*(S+B/AJ)*TM)
02300      OPEN(UNIT=1,FILE='ST1.DAT')
02400      READ (1,*) CH,R,TM,B,AJ,RA,TA,T
02500      PRINT 5, CH,R,TM,B,AJ,RA,TA,T
02600 5      FORMAT(5X,'CH=',F7.5,'R=',F7.5,'TM=',F7.5,'B=',
02700      1F7.5,'AJ=',F7.5,'RA=',F7.5,'TA=',F7.5,'T=',F7.5)
02800      OMEGA=0.0
02900      ZHI=0.0
02950      RR=-OMEGA*ZHI
02975      AA=OMEGA*SQRT(1.-ZHI**2)
03000 20      S=CHPLX(RR,AA)
03100      SF2=S*F2(S)
03200      SF1=S*F1(S)
03300      ALR=REAL(SF2)
03400      ALI=AIMAG(SF2)
03500      BTR=REAL(F1(S))
03600      BTI=AIMAG(F1(S))
03700      COEFR=REAL(SF1)
03800      COEFI=AIMAG(SF1)

```

SIMULATION PROGRAMS

```

00500 C      *****
00600      COMPLEX S, F1,F2,SF2,SF1,D
00700      F1(S)=CH*R*TM*CEXP(-S*T)*(S+B/AJ)/RA
00800      F2(S)=(1.+(1.+S*TA)*(S+B/AJ)*TM)
00900      OPEN (UNIT=1,FILE='ST1.DAT')
01000      READ (1,*) CH,R,TM,B,AJ,RA,TA,T
01100      PRINT 5, CH,R,TM,B,AJ,RA,TA,T
01200 5      FORMAT(5X,'CH=',F7.5,'R=',F7.5,'TM=',F7.5,'B=',
01300      1F7.5,'AJ=',F7.5,'RA=',F7.5,'TA=',F7.5,'T=',F7.5)
01400      SIGMA=-0.15
01500      ALPHA=40
01600      BETA=100
01700      PRINT *, ALPHA,BETA,SIGMA
01800      OMEGA=0.0
01900      PRINT 140
02000 140   FORMAT(//,16X,'OMEGA=',19X,'D',//)
02100      DO 150 I=1,200
02200      S=CMPLX(SIGMA,OMEGA)
02300      D=ALPHA*S*F2(S)+BETA*F1(S)+S*F1(S)
02400      PRINT 160 ,OMEGA,D
02500      TYPE 160, OMEGA,D
02600 160   FORMAT(5X,E21.5,15X,2E13.5)
02700 150   OMEGA=OMEGA+2.0
02800      STOP
02900      END
00100 C      PROGRAM NO 4
00200 C      *****
00300 C      FREQUENCY SCANNING TECHNIQUE FOR CURRENT LOOP WHIT
00400 C      THE VARIATION IN DAMPING RATIO
00500 C      *****
00600      COMPLEX S, F1,F2,SF2,SF1,D
00700      F1(S)=CH*R*TM*CEXP(-S*T)*(S+B/AJ)/RA
00800      F2(S)=(1.+(1.+S*TA)*(S+B/AJ)*TM)
00900      OPEN (UNIT=1,FILE='ST1.DAT')
01000      READ (1,*) CH,R,TM,B,AJ,RA,TA,T
01100      PRINT 5, CH,R,TM,B,AJ,RA,TA,T
01200 5      FORMAT(5X,'CH=',F7.5,'R=',F7.5,'TM=',F7.5,'B=',

```

SIMULATION PROGRAMS

```

01300      1F7.5, 'AJ=',F7.5,'RA=',F7.5,'TA=',F7.5,'T=',F7.5)
01400      ZHI=0.7
01500      ALPHA=10
01600      BETA=10
01700      PRINT *, ALPHA,BETA,ZHI
01800      OMEGA=0.0
01900      PRINT 140
02000 140   FORMAT(//,16X,'OMEGA=',19X,'D',//)
02100      DO 150 I=1,600,10
02200      RR=-OMEGA*ZHI
02300      AA=OMEGA*SQRT(1.-ZHI*ZHI)
02400      S=CMPLX(RR,AA)
02500      D=ALPHA*S*F2(S)+BETA*F1(S)+S*F1(S)
02600      PRINT 160 ,OMEGA,D
02700 160   FORMAT(5X,E21.5,15X,2E13.5)
02800 150   OMEGA=OMEGA+2
02900      STOP
03000      END
00100 C     PROGRAM NO 5
00200 C     *****
00300 C     TRANSIENT RESPONSE OF SPEED LOOP WITH A STEP REFERENE
00400 C     INPUT FOR DIFFERENT VALUES OF SPEED CONTROLLER GAIN AND
00500 C     TIME CONSTANT
00600 C     *****
00700 C     VARIABLES USED
00800 C     T = INDEPENDENT VARIABLE (TIME)
00900 C     DT = DESIRED TIME STEP FOR NUMERICAL INTEGRATION
01000 C     NEQ= NUMBER OF FIRST ORDER DIFFERENTIAL EQUATIONS
01100      DIMENSION TIME(1000),X(1000,2),XX(2),F(2),YI(2),YJ(2),
01200      1YK(2),YL(2),UU(2)
01300      COMMON T1,CF
01400      OPEN (UNIT=1,FILE='PA3.DAT')
01500      XX(1)=0.0,XX(2)=0.0,XX(3)=0.0,XX(4)=0.0
01600      CF = R*XX(2)
01700      T1=0.0,NEQ=2,DT=0.04,T=0.0
01800      NSTEP=1000
01900      DO 40 I=1,NSTEP

```

SIMULATION PROGRAMS

```

02000          CALL RUNGE(T,DT,NEQ,XX,F,YI,YJ,YK,YL,UU)
02100          TIME(I)=T
02200          DO 20 J=1,NEQ
02300 20        X(I,J)=XX(J)
02400          WRITE (1,111) (TIME(I),X(I,2))
02500 111      FORMAT(5X,2(F12.5,3X))
02600 40      CONTINUE
02700          END
02800 C        *****
02900          SUBROUTINE RUNGE(T,DT,NEQ,XX,F,YI,YJ,YK,YL,UU)
03000 C        *****
03100          DIMENSION YI(NEQ),YJ(NEQ),YK(NEQ),YL(NEQ),XX(NEQ),F(NEQ),UU(NEQ)
03200          COMMON T1,CF
03300          DO10 I=1,NEQ
03400 10        UU(I)=XX(I)
03500          CALL FTN(XX,F,NEQ,T)
03600          DO 50I=1,NEQ
03700          YI(I)=F(I)*DT
03800 50        XX(I)=UU(I)+YI(I)/2.0
03900          T=T+DT/2.0
04000          CALL FTN(XX,F,NEQ,T)
04100          DO 30I=1,NEQ
04200          YJ(I)=F(I)*DT
04300 30        XX(I)=UU(I)+YJ(I)/2.0
04400          CALL FTN(XX,F,NEQ,T)
04500          DO 80I=1,NEQ
04600          YK(I)=F(I)*DT
04700 80        XX(I)=UU(I)+YK(I)
04800          T=T+DT/2.0
04900          CALL FTN(XX,F,NEQ,T)
05000          DO90I=1,NEQ
05100          YL(I)=F(I)*DT
05200 90        XX(I)=UU(I)+(YI(I)+2.0*YJ(I)+2.0*YK(I)+YL(I))/6.0
05300          RETURN
05400          END
05500 C        *****
05600          SUBROUTINE FTN(XX,F,NEQ,T)

```

SIMULATION PROGRAMS

```

05700 C *****
05800 DIMENSION XX(NEQ),F(NEQ)
05900 COMMON T1,CF
06000 OPEN(UNIT=2,DEVICE='DSK',FILE='PX9.DAT')
06100 READ(2,*)CH,R,AL,AK1,TC1,B,AJ,RA,TA,TA,TM
06200 VC2=1.0
06300 IF ((T-T1).GE.0.01) GO TO 10
06400 GO TO 20
06500 10 CF=R*XX(2)
06600 T1=T
06700 20 EC1=VC2-CF
06800 VC1=XX(1)+AK1*(EC1)
06900 F(1)=AK1/TC1*(EC1)
07000 EA=VC1*CH
07100 IF(EA.GE.200) EA=200
07200 IF (EA.LE.33) EA=33
07300 F(2)=(EA-XX(2)*RA)/AL
07400 RETURN
07500 END

00100 C PROGRAM NO 6
00200 C *****
00300 C DETERMINATION OF THE REGION OF RELATIVE STABILITY
00400 C OF SPEED LOOP IN THE PLANE OF TWO PARAMETERS
00500 C ALPHA AND BETA WITH THE VARIATION IN SIGMA
00600 C USING D-DECOMPOSITION METHOD
00700 C *****
00800 C VARIABLES USED
00900 C *****
01000 C ALPHA=INVERSE OF GAIN K1
01100 C BETA=INVERSE OF THE TIME CONSTANT TC1
01200 C S=COMPLEX FREQUENCY
01300 C ALR=COEFF.OF ALPHA OF REAL EQUATION
01400 C ALI=COEFF. OF ALPHA OF IMAGINARY EQUATION
01500 C BTR=COEFF. OF BETA OF REAL EQUATION
01600 C BTI=COEFF. OF BETA OF IMAGINARY EQUATION
01700 C COEFR=CONSTANT TERM IN REAL EQUATION
01800 C COEPI=CONSTANT TERM IN IMAGINARY EQUATION

```

SIMULATION PROGRAMS

```

01900 C      *****
02000      COMPLEX S,F1,F2,SF1,SF2,F3,F4,SF3,SF4
02100      F1(S)=AK1*(1+(S*TC1))*CH*(S+B/AJ)*TM/RA
02200      F2(S)=S*TC1*(1.+(1.+S*TA)*(S+B/AJ)*TM)
02300      F3(S)=F1(S)*AKB*HW*CEXP(-S*T2)/AJ
02400      F4(S)=(F2(S)+F1(S)*R*CEXP(-S*T1))*(S+B/AJ)
02500      OPEN(UNIT=1,FILE='ST2.DAT')
02600      READ (1,*) CH,R,TM,B,AJ,RA,TA,T1,T2,AK1,TC1,AKB,HW
02700      DO 800 I=1,10
02800      SIGMA=I-1.0
02900      PRINT 28, SIGMA
03000 28      FORMAT ('1','SIGMA=',F6.4)
03100      PRINT 6, CH,R,TM,B,AJ,RA,TA,T1,T2,AK1,TC1,AKB,HW
03200 6      FORMAT(5X,'CH=',F7.5,5X,'R=',F7.5,5X,'TM=',F
03300      17.5,5X,'B=',F7.5,5X,'AJ=',F7.5,5X,'RA=',F7.5,
03400      25X,'TA=',F7.5,5X,'T1=',F7.5,5X,'T2=',F7.5,5X,
03500      3'AK1=',F10.5,5X,'TC1=',F7.5,'AKB=',F7.5,5X,'HW=',F7.5)
03600      OMEGA=0.0
03700 20      S=CMPLX(-SIGMA,OMEGA)
03800      SF2=S*F2(S)
03900      SF1=S*F1(S)
04000      SF4=S*F4(S)
04100      SF3=S*F3(S)
04200      ALR=REAL(SF4)
04300      ALI=AIMAG(SF4)
04400      BTR=REAL(F3(S))
04500      BTI=AIMAG(F3(S))
04600      COEFR=REAL(SF3)
04700      COEFI=AIMAG(SF3)
04800      DEN=BTI*ALR-BTR*ALI
04900      ANUM=BTR*COEFI-BTI*COEFR
05000      BNUM=ALI*COEFR-ALR*COEFI
05100      IF (DEN.NE.0.) GO TO 10
05200      IF (ANUM.NE.0.) GO TO 200
05300      GO TO 200
05400 10      ALPHA=ANUM/DEN
05500      BETA=BNUM/DEN

```

SIMULATION PROGRAMS

```

05600      PRINT *,S,ALPHA,BETA,ANUM,BNUM,DEN,OMEGA
05700      IF(OMEGA.GE.200.0) GO TO 800
05800 200   OMEGA=OMEGA+2.0
05900      GO TO 20
06000 800   CONTINUE
06100      END
00100 C     PROGRAM NO 7
00200 C     ****
00300 C     DETERMINATION OF THE REGION OF RELATIVE STABILITY
00400 C     OF SPEED LOOP IN THE PLANE OF TWO PARAMETERS
00500 C     ALPHA AND BETA WITH THE VARIATION IN ZHI
00600 C     USING D-DECOMPOSITION METHOD
00700 C     ****
00800 C     VARIABLES USED
00900 C     ****
01000 C     ALPHA=INVERSE OF GAIN K1
01100 C     BETA=INVERSE OF THE TIME CONSTANT TC1
01200 C     S=COMPLEX FREQUENCY
01300 C     ALR=COEFF.OF ALPHA OF REAL EQUATION
01400 C     ALI=COEFF. OF ALPHA OF IMAGINARY EQUATION
01500 C     BTR=COEFF. OF BETA OF REAL EQUATION
01600 C     BTI=COEFF. OF BETA OF IMAGINARY EQUATION
01700 C     COEFR=CONSTANT TERM IN REAL EQUATION
01800 C     COEFI=CONSTANT TERM IN IMAGINARY EQUATION
01900 C     ****
02000      COMPLEX S,F1,F2,SF1,SF2,F3,F4,SF3,SF4
02100      F1(S)=AK1*(1+(S*TC1))*CH*(S+B/AJ)*TM/RA
02200      F2(S)=S*TC1*(1+(1+S*TA)*(S+B/AJ)*TM)
02300      F3(S)=F1(S)*AKB*HW*CEXP(-S*T2)/AJ
02400      F4(S)=(F2(S)+F1(S)*R*CEXP(-S*T1))*(S+B/AJ)
02500      OPEN(UNIT=1,FILE='ST2.DAT')
02600      READ (1,*) CH,R,TM,B,AJ,RA,TA,T1,T2,AK1,TC1,AKB,HW
02700      DO 800 I=1,7
02800      ZHI=(I-1.0)/10
02900      PRINT 28, ZHI
03000 28     FORMAT ('1','ZHI=',F6.4)
03100      PRINT 6, CH,R,TM,B,AJ,RA,TA,T1,T2,AK1,TC1,AKB,HW

```


SIMULATION PROGRAMS

```

03200 6      FORMAT(5X,'CH=',F7.5,5X,'R=',F7.5,5X,'TM=',F
03300      17.5,5X,'B=',F7.5,5X,'AJ=',F7.5,5X,'RA=',F7.5,
03400      25X,'TA=',F7.5,5X,'T1=',F7.5,5X,'T2=',F7.5,5X,
03500      3'AK1=',F10.5,5X,'TC1=',F7.5,'AKB=',F7.5,5X,'HW=',F7.5)
03600      OMEGA=0.0
03700 20     RR=-OMEGA*ZHI
03800      AA=OMEGA*SQRT(1.-ZHI**2)
03900      S=CMPLX(RR,AA)
04000      SF2=S*F2(S)
04100      SF1=S*F1(S)
04200      SF4=S*F4(S)
04300      SF3=S*F3(S)
04400      ALR=REAL(SF4)
04500      ALI=AIMAG(SF4)
04600      BTR=REAL(F3(S))
04700      BTI=AIMAG(F3(S))
04800      COEFR=REAL(SF3)
04900      COEFI=AIMAG(SF3)
05000      DEN=BTI*ALR-BTR*ALI
05100      ANUM=BTR*COEFI-BTI*COEFR
05200      BNUM=ALI*COEFR-ALR*COEFI
05300      IF (DEN.NE.0.) GO TO 10
05400      IF (ANUM.NE.0.) GO TO 200
05500      GO TO 200
05600 10     ALPHA=ANUM/DEN
05700      BETA=BNUM/DEN
05800      PRINT *,S,ALPHA,BETA,ANUM,BNUM,DEN,OMEGA
05900      IF(OMEGA.GE.200.0) GO TO 800
06000 200    OMEGA=OMEGA+2.0
06100      GO TO 20
06200 800    CONTINUE
06300      END
00100 C     PROGRAM NO 8
00200 C     *****
00300 C     FREQUENCY SCANNING TECHNIQUE FOR SPEED LOOP WITH
00400 C     THE VARIATION IN SIGMA
00500 C     *****

```

SIMULATION PROGRAMS

```

500      COMPLEX S,F1,F2,SF1,SF2,F3,F4,SF3,SF4,D
700      F1(S)=AK1*(1+(S*TC1))*CH*(S+B/AJ)*TM/RA
300      F2(S)=S*TC1*(1.+(1.+S*TA)*(S+B/AJ)*TM)
300      F3(S)=F1(S)*AKB*HW*CEXP(-S*T2)/AJ
000      F4(S)=(F2(S)+F1(S)*R*CEXP(-S*T1))*(S+B/AJ)
100      OPEN(UNIT=1,FILE='ST2.DAT')
200      READ(1,*)CH,R,TM,B,AJ,RA,TA,T1,T2,AK1,TC1,AKB,HW
400      PRINT *,CH,R,TM,B,AJ,RA,TA,T1,T2,AK1,TC1,AKB,HW
500      SIGMA=-0.1
500      ALPHA=10.
700      BETA=100
300      PRINT*,ALPHA,BETA,SIGMA
300      OMEGA=0.0
000      PRINT140
.00 140    FORMAT(/,16X,'OMEGA=',19X,'D',/)
200      DO 150 I=1,300
300      S=CMPLX(SIGMA,OMEGA)
400      D=ALPHA*S*F4(S)+BETA*F3(S)+S*F3(S)
500      PRINT 160 ,OMEGA,D
500 160    FORMAT(5X,E21.5,15X,2E13.5)
700 150    OMEGA=OMEGA+0.2
300      STOP
300      END
100 C      PROGRAM NO 9
200 C      *****
300 C      FREQUENCY SCANNING TECHNIQUE FOR SPEED LOOP WITH
400 C      THE VARIATION IN ZHI
500 C      *****
500      COMPLEX S,F1,F2,SF1,SF2,F3,F4,SF3,SF4,D
700      F1(S)=AK1*(1+(S*TC1))*CH*(S+B/AJ)*TM/RA
300      F2(S)=S*TC1*(1.+(1.+S*TA)*(S+B/AJ)*TM)
300      F3(S)=F1(S)*AKB*HW*CEXP(-S*T2)/AJ
000      F4(S)=(F2(S)+F1(S)*R*CEXP(-S*T1))*(S+B/AJ)
100      OPEN(UNIT=1,FILE='ST2.DAT')
200      READ(1,*)CH,R,TM,B,AJ,RA,TA,T1,T2,AK1,TC1,AKB,HW
300      PRINT *,CH,R,TM,B,AJ,RA,TA,T1,T2,AK1,TC1,AKB,HW
400      ZHI=0.1

```

SIMULATION PROGRAMS

```

01500      ALPHA=10.
01600      BETA=40
01700      PRINT*,ALPHA,BETA,ZHI
01800      OMEGA=0.0
01900      PRINT140
02000 140   FORMAT(/,16X,'OMEGA=',19X,'D',/)
02100      DO 150 I=1,200
02200      RR=-OMEGA*ZHI
02300      AA=OMEGA*SQRT(1,-ZHI**2)
02400      S=CMPLX(RR,AA)
02500      D=ALPHA*S*F4(S)+BETA*F3(S)+S*F3(S)
02600      PRINT 160 ,OMEGA,D
02700 160   FORMAT(5X,E21.5,15X,2E13.5)
02800 150   OMEGA=OMEGA+0.2
02900      STOP
03000      END
00100 C     PROGRAM NO 10
00200 C     *****
00300 C     TRANSIENT RESPONSE OF SPEED LOOP WITH A STEP REFERENE
00400 C     INPUT FOR DIFFERENT VALUES OF SPEED CONTROLLER GAIN AND
00500 C     TIME CONSTANT
00600 C     *****
00700 C     VARIABLES USED
00800 C     *****
00900 C     T=INDEPENDENT VARIABLE (TIME)
01000 C     DT = DESIRED TIME STEP FOR NUMERICAL INTEGRATION
01100 C     NEQ=NUMBER OF FIRST ORDER DIFFERENTIAL EQUATIONS
01200      DIMENSION TIME(200),X(200,4),XX(4),F(4),YI(4),YJ(4),
01300      1YK(4),YL(4),UU(4)
01400      COMMON T1,T2,CF,SF
01500      OPEN (UNIT=1,FILE='SA1.DAT')
01600      XX(1)=0.0,XX(2)=0.0,XX(3)=0.0,XX(4)=0.0
01700      NEQ=4;NSTEP=200;DT=0.06;T1=0.0;T2=0.0
01800      CF=0.0;SF=0.0;T=0.0
01900      DO 40 I=1,NSTEP
02000          CALL RUNGE(T,DT,NEQ,XX,F,YI,YJ,YK,YL,UU)
02100      TIME(I)=T

```

SIMULATION PROGRAMS

```

02200      DO 20J=1,NEQ
02300 20    X(I,J)=XX(J)
02400      WRITE (1,111) (TIME(I),X(I,4),X(I,3))
02500 111   FORMAT(5X,3(F10.5,5X))
02600 40    CONTINUE
02700      END
02800 C     *****
02900      SUBROUTINE RUNGE(T,DT,NEQ,XX,F,YI,YJ,YK,YL,UU)
03000 C     *****
03100      DIMENSION YI(NEQ),YJ(NEQ),YK(NEQ),YL(NEQ),XX(NEQ),F(NEQ),UU(NEQ)
03200      COMMON T1,T2,CF,SF
03300      DO10 I=1,NEQ
03400 10     UU(I)=XX(I)
03500      CALL FTN(XX,F,NEQ,T)
03600      DO 50I=1,NEQ
03700      YI(I)=F(I)*DT
03800 50     XX(I)=UU(I)+YI(I)/2.0
03900      T=T+DT/2.0
04000      CALL FTN(XX,F,NEQ,T)
04100      DO 30I=1,NEQ
04200      YJ(I)=F(I)*DT
04300 30     XX(I)=UU(I)+YJ(I)/2.0
04400      CALL FTN(XX,F,NEQ,T)
04500      DO 80I=1,NEQ
04600      YK(I)=F(I)*DT
04700 80     XX(I)=UU(I)+YK(I)
04800      T=T+DT/2.0
04900      CALL FTN(XX,F,NEQ,T)
05000      DO90 I=1,NEQ
05100      YL(I)=F(I)*DT
05200 90     XX(I)=UU(I)+(YI(I)+2.0*YJ(I)+2.0*YK(I)+YL(I))/6.0
05300      RETURN
05400      END
05500 C     *****
05600      SUBROUTINE FTN(XX,F,NEQ,T)
05700 C     *****
05800      DIMENSION XX(NEQ),F(NEQ)

```

SIMULATION PROGRAMS

```

05900      COMMON T1,T2,CF,SF
06000      OPEN(UNIT=2,DEVICE='DSK',FILE='SX2.DAT')
06100      READ (2,*) AK1,TC1,RR,CH,AL,RA,AJ,B,AKB,HW,AK2,TC2
06200      VR=200.0
06300      IF((T-T1).GE.0.01) GOTO 10
06400      GO TO 20
06500 10    CF=RR*XX(3)
06600      T1=T
06700 20    IF((T-T2).GE.0.245) GO TO 30
06800      GO TO 40
06900 30    SF=HW*XX(4)
07000      T2=T
07100 40    EC1=VR-SF
07200      VC1=XX(1)+AK1*(EC1)
07300      IF (VC1.GE.5.) VC1=5.0
07400      IF(VC1.LE.0.5) VC1=0.5
07500      EC2=VC1-CF
07600
07700      F(1)=AK1/TC1*(EC1)
07800      F(2)=EC2*AK2/TC2
07900      VC2=XX(2)+EC2*AK2
08000      EA=VC2*CH
08100      IF (EA.GE.185) EA=185
08200      IF (EA.LE.30.0)EA=30.0
08300      EC3=(EA-AKB*XX(4))
08400      F(3)=(EC3-XX(3)*RA)/AL
08500      F(4)=(AKB*XX(3)-B*XX(4))/AJ
08600      RETURN
08700      END
00100      PROGRAM NO 11
00200      *****
00300      PROGRAM FOR PLOTTING THE TIME RESPONSE
00400      *****:
00500      DIMENSION CURENT(302),TIME(302)
00600      OPEN(UNIT=1,DIALOG)
00700      CALL PLOTS(0.,0.,5)
00800      TIME(301)=0.;TIME(301)=0.10

```

SIMULATION PROGRAMS

```
00900      CURENT(301)=0.0;CURENT(302)=0.2
01000      DO 30 LM=1,4
01100      CALL AXIS(0.,0.,'TIME(SEC)',-9,15.,0.,TIME(301),TIME(302))
01200      CALL AXIS(0.,0.,'CURRENT(AMPS)',13,10.,90.,CURENT(301),
01300      1CURENT(302))
01400 30    CONTINUE
01500      DO 99 J = 1, 300
01600      READ(1,*)TIME(J),CURENT(J)
01700 99    CONTINUE
01800      DO 40 J=1,2
01900      CALL LINE(TIME,CURENT,300,1,0,0)
02000 40    CONTINUE
02100      CALL PLOT(0.,0.,-999)
02200      STOP
02300      END
```